From Half Metal To Spintronics (從半金屬到自旋電子學)

Jauyn Grace Lin

Cener for Condensed Matter sciences
National Taiwan Univsersity

2009/12/10

Context

Chapter One *Half Metal*

Chapter Two *Colossal Magnetoresistance*

Chapter Three *Experiments for Spintronics*

Chapter One

Half Metal

半金屬

Outline

1. *Definition of half metal*
2. *Material classification*
3. *Polarization measurement*
4. *Applications*

New Class of Materials: Half-Metallic Ferromagnets

R. A. de Groot and F. M. Mueller
Research Institute for Materials, Faculty of Science, Toernooiveld, 6525 ED Nijmegen, The Netherlands

and

P. G. van Engen and K. H. J. Buschow
Philips Research Laboratories, 5600 JA Eindhoven, The Netherlands

(Received 21 March 1983)

The band structure of Mn-based Heusler alloys of the $C1_b$ crystal structure (MgAgAs type) has been calculated with the augmented-spherical-wave method. Some of these magnetic compounds show unusual electronic properties. The majority-spin electrons are metallic, whereas the minority-spin electrons are semiconducting.

Compound	$N(E)\uparrow$	$N(E)\downarrow$	$n_{3d}^{\mathrm{Mn}\uparrow}$	$n_{3d}^{\mathrm{Mn}\downarrow}$	$\mu_{\mathrm{tot}}^{\mathrm{cacl}}$	$\mu_{\mathrm{tot}}^{\mathrm{exp}}$
NiMnSb	9.90	0	4.51	0.87	4.00	3.85
PtMnSb	10.05	0	4.57	0.79	4.00	3.97
PdMnSb	9.04	2.97	4.58	0.71	4.05	3.95
PtMnSn	9.78	19.31	4.40	0.78	3.60	3.42

Half metals are the extreme case of strong ferromagnet, where not only 3d electrons are fully polarized, but also other (sp) down-spin bands do not cross the Fermi level.
(examples: NiMnSb, PtMnSb--- Hesuler phases.)

Augmented-spherical-wave method

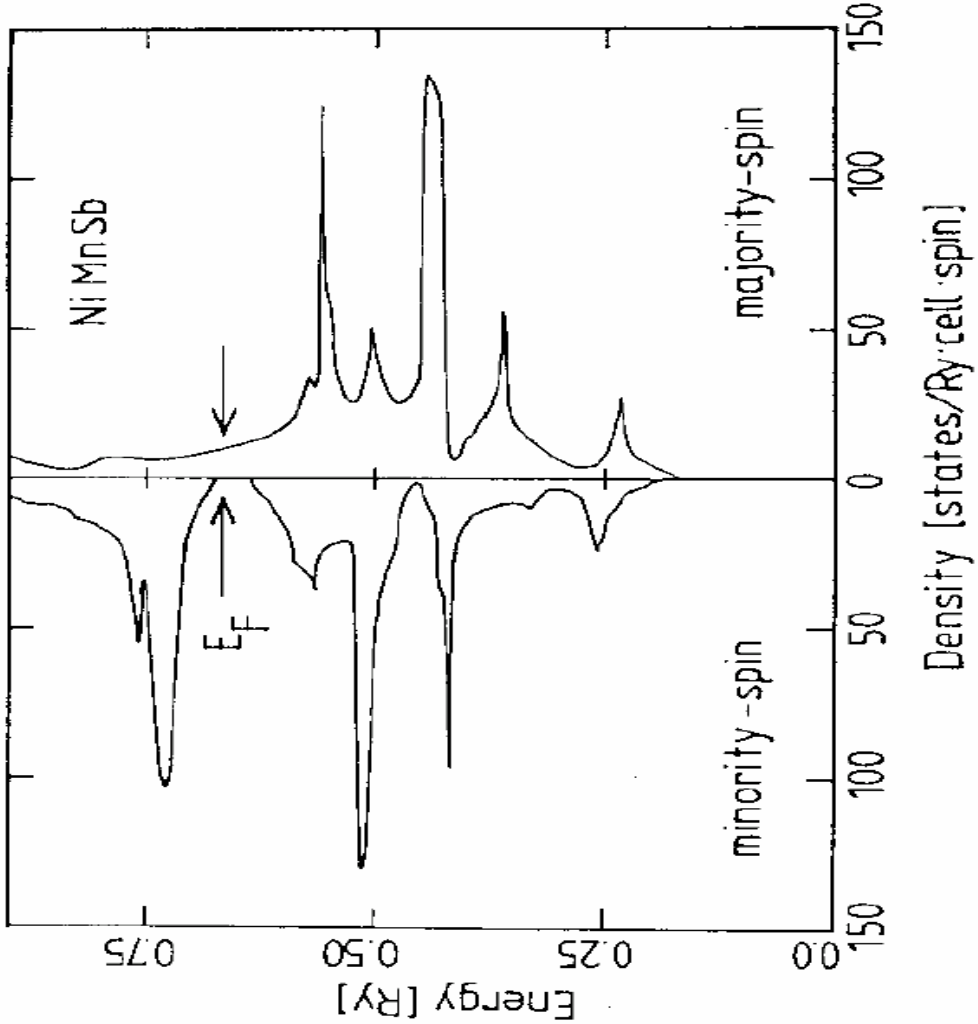

Fig.1. Band structure for NiMnSb [1].

JOURNAL OF APPLIED PHYSICS VOLUME 91 (2002)

Half-metallic ferromagnetism: Example of CrO_2 (invited)

J. M. D. Coey and M. Venkatesan

Physics Department, Trinity College, Dublin 2, Ireland

A **half metal** is a solid with an unusual electronic structure. For electrons of one spin it is a metal with a Fermi surface, but for the opposite spin there is a gap in the spin-polarized density of states, like a semiconductor or insulator. This definition presupposes a magnetically ordered state to define the spin quantization axis. The responses of a half metal to electric and magnetic field at zero temperature are quite different. There is electric conductivity, but no high-field magnetic susceptibility.

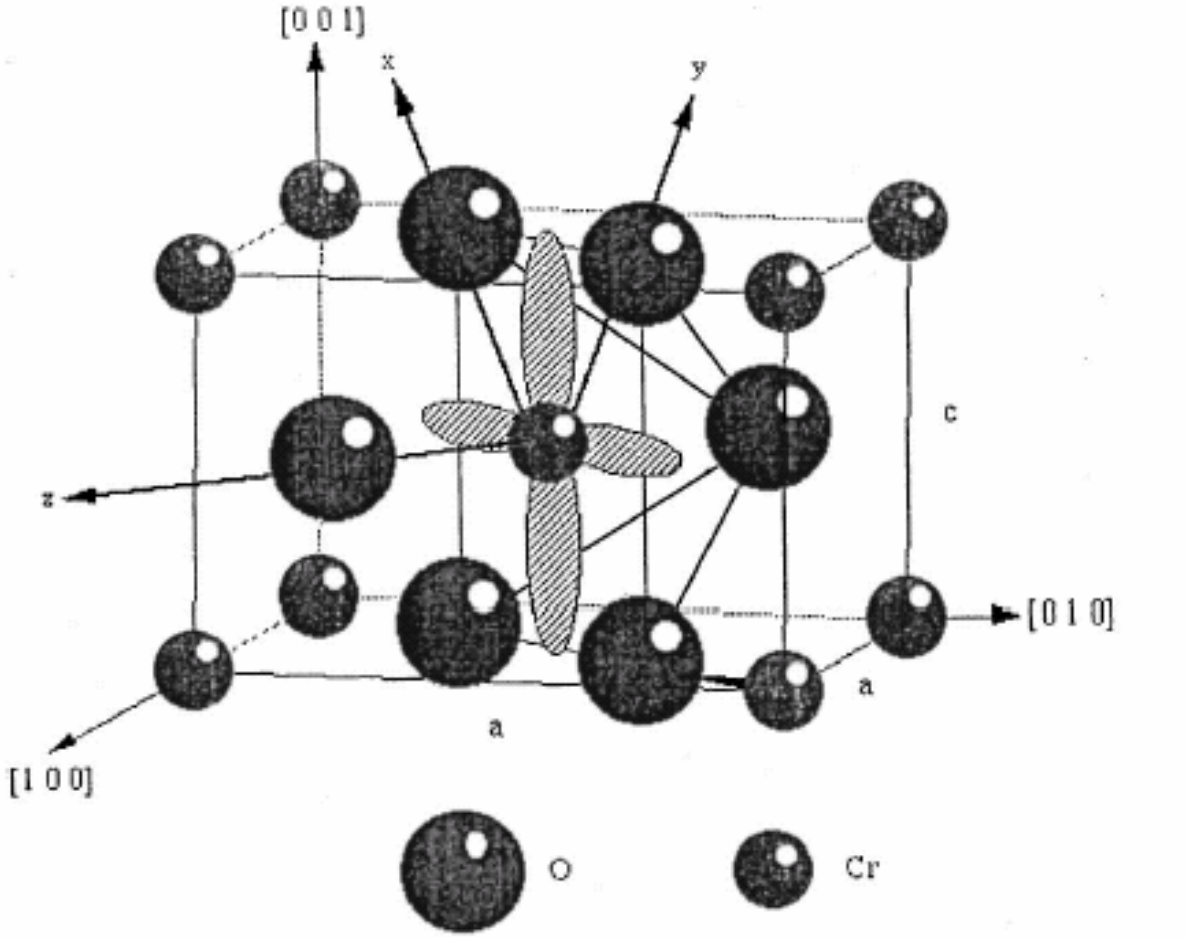

FIG. 4. The rutile structure of CrO_2 . The local axis frame for the t_{2g} orbitals is shown.

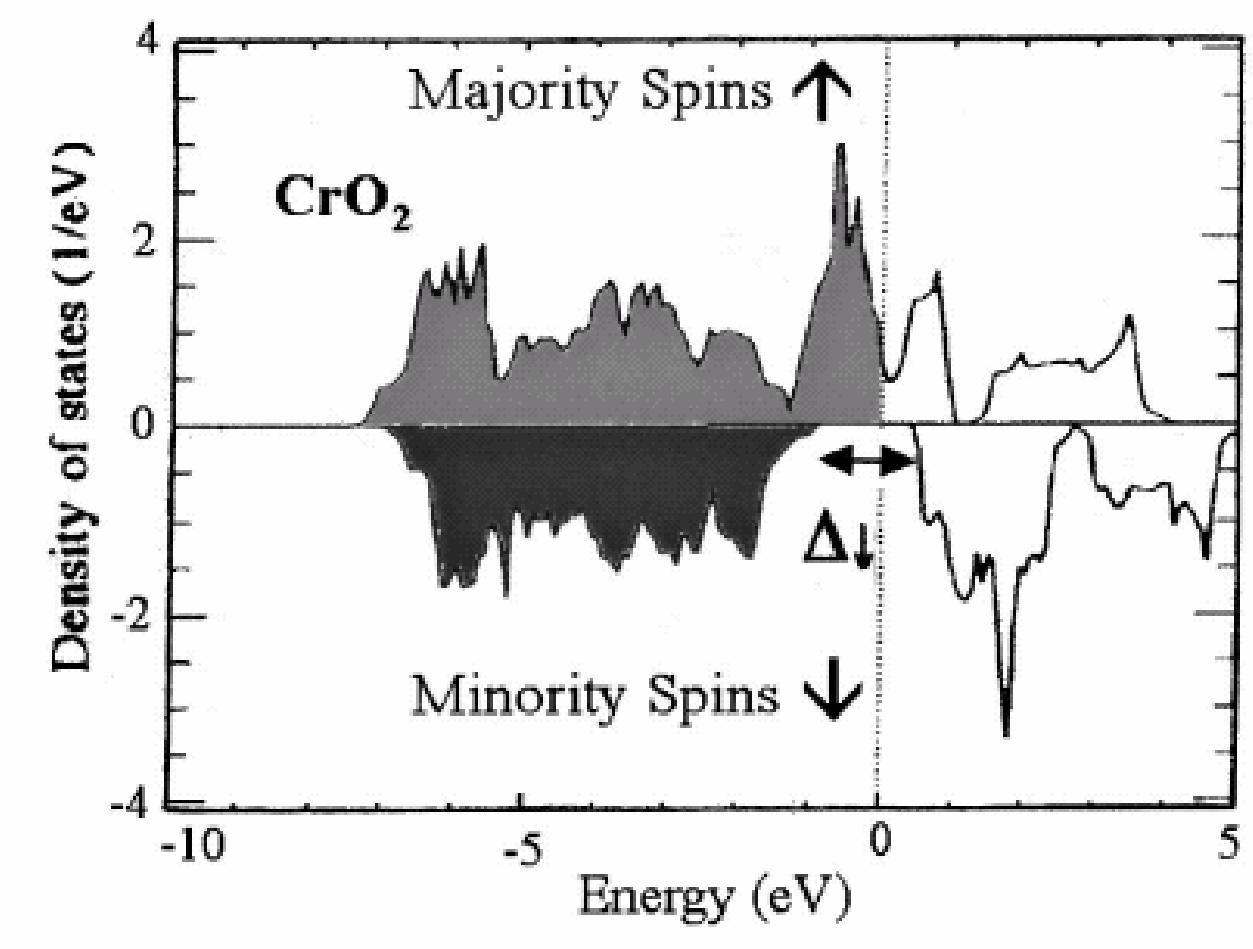

FIG. 5. Spin polarization of the density of states of CrO_2.

TABLE III. Some electronic structure calculation on CrO_2.

Author		$\Delta_\downarrow$ (eV)	Δ_{sf} (eV)	$N_\uparrow$ eV^{-1} $f.u^{-1}$
Schwarz	Ref. 26 LSDA–ASW	1.3	0.3	0.8
Lewis *et al.*	Ref. 2 LSDA–PWPP	1.4	0.3	0.69
Korotin *et al.*	Ref. 27 LSDA+U(3 eV)	2.4	1.7	0.4
Mazin *et al.*	Ref. 31 LSDA/GGA	1.3	0.2–0.7	0.95
Brener *et al.*	Ref. 32 LSDA–LCGO	1.3	0.2	1.16
Kuneš *et al.*	Ref. 28 GGA	1.8	0.7	0.3

Δ_{Sf} : spin-flip gap

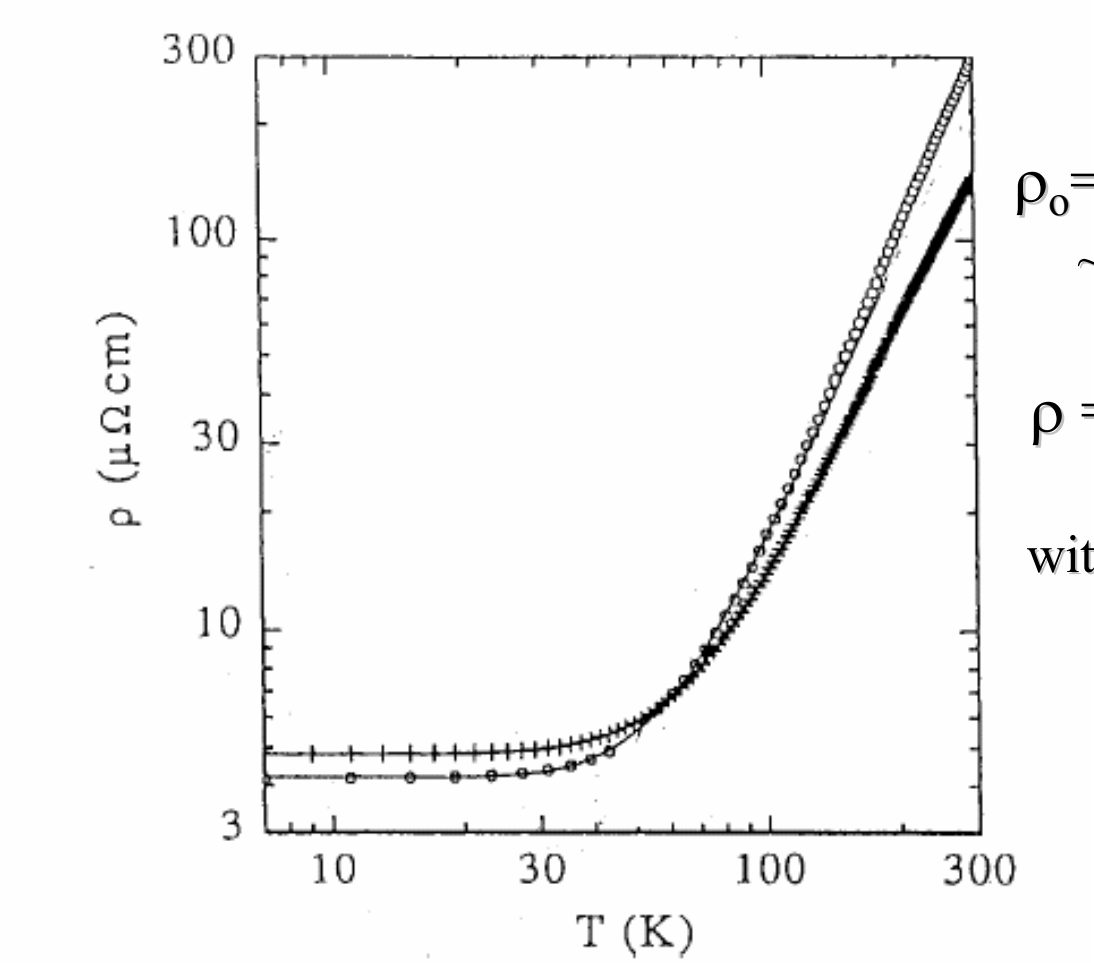

$\rho_o = 4\times10^{-8}$ ohm-m

~ 90 nm mean-free path

$\rho = \rho_o T^2 e^{-\Delta/T}$

with $\Delta \sim 80$K

FIG. 6. Resistivity of CrO_2 thin films.

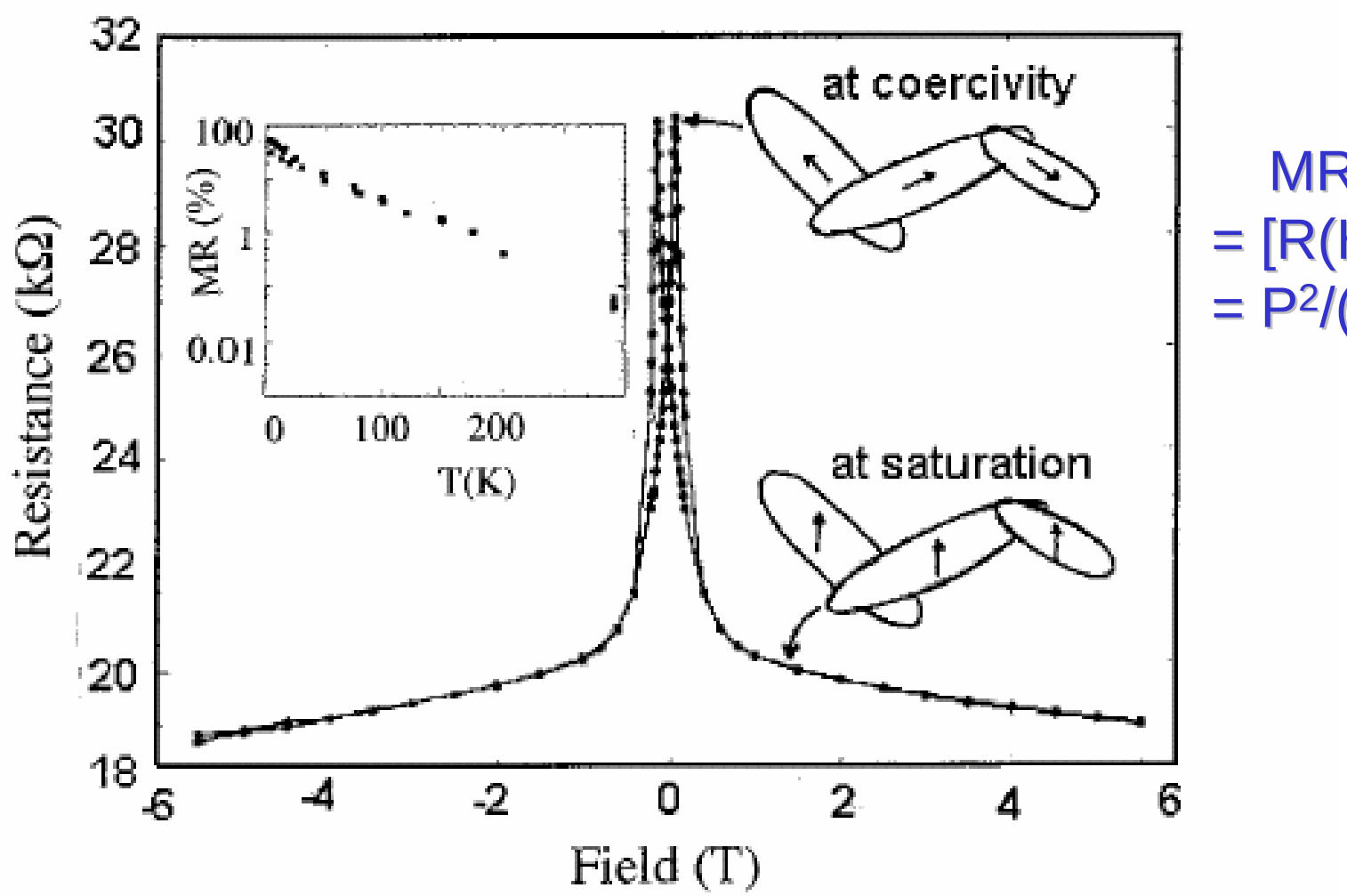

MR
= [R(H)-R(0)]/R(0)
= $P^2/(1+P^2)$

FIG. 7. Magnetoresistance of a CrO_2–Cr_2O_3 pressed powder compact, with temperature dependence shown in the inset.

TABLE I. Summary of the classification of half-metals.

Type	Density of states	Conductivity	↑ electrons at E_F	↓ electrons at E_F
IA	Half-metal	Metallic	Itinerant	None (CrO_2,NiMnSb)
IB	Half-metal	Metallic	None	Itinerant (Sr2FeMoO6)
IIA	Half-metal	Nonmetallic	Localized	None
IIB	Half-metal	Nonmetallic	None	Localized
IIIA	Metal	Metallic	Itinerant	Localized (Magnetite)
IIIB	Metal	Metallic	Localized	Itinerant ($La_{0.7}Sr_{0.3}MnO_6$)
IVA	Semimetal	Metallic	Itinerant	Localized
IVB	Semimetal	Metallic	Localized	Itinerant ($Tl_2Mn_2O_7$)
VA	Semiconductor	Semiconducting	Few, itinerant	None (Doped EuO & EuS)
VB	Semiconductor	Semiconducting	None	Few, itinerant (GaAsMn)

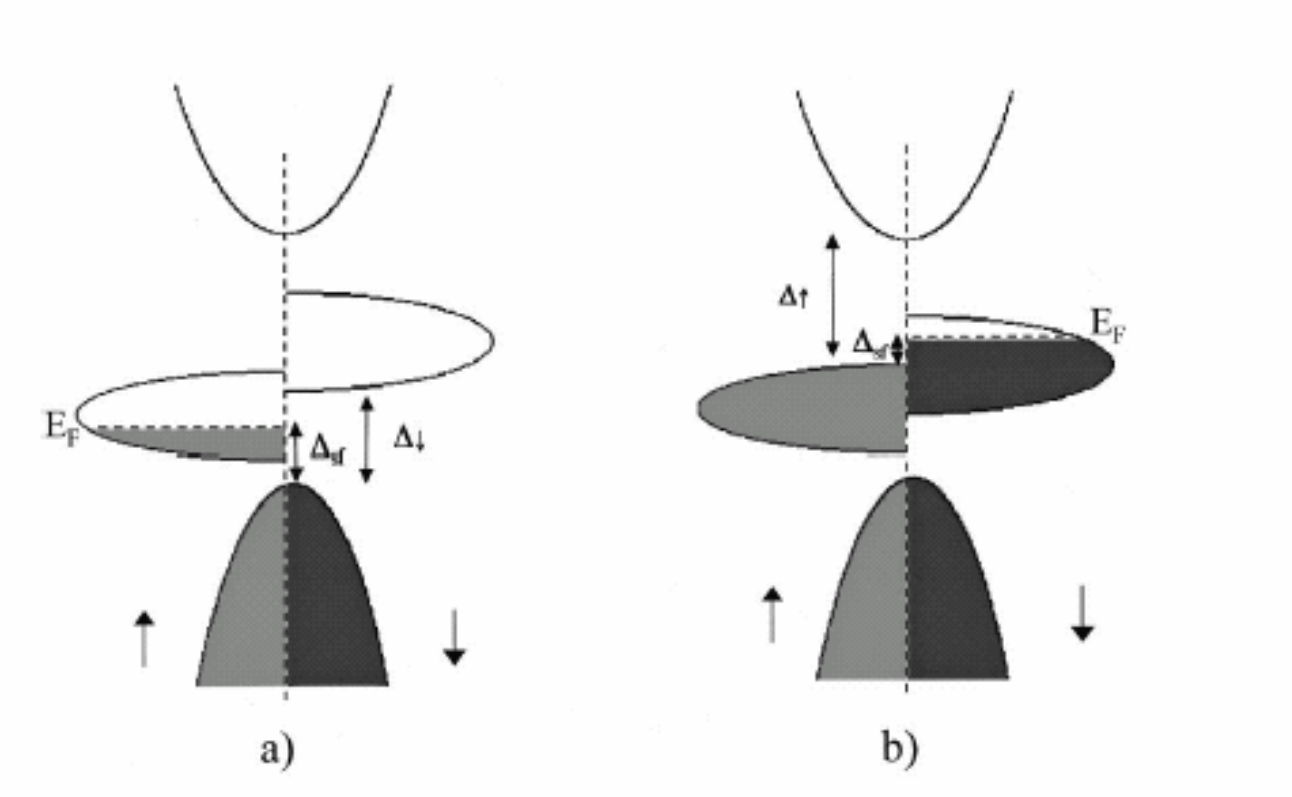

FIG. 1. Schematic density of states for a half metal, (a) Type I_A with only ↑ electrons at E_F and (b) Type I_B with only ↓ electrons at E_F . In narrow d bands, the states at E_F may be localized (type II).

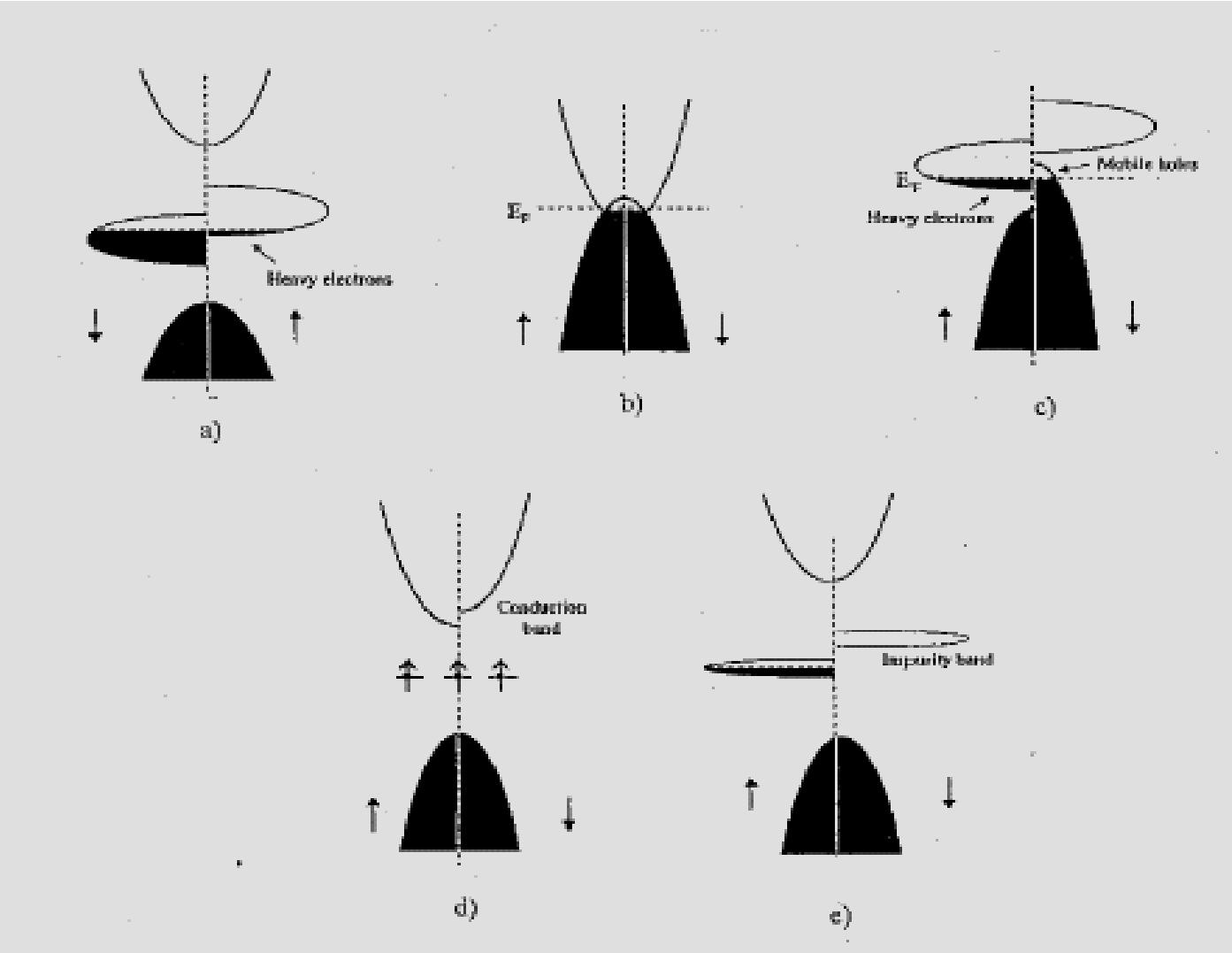

FIG. 2. Schematic density of states for (a) a type III_A half metal, where electrons of one spin direction are itinerant and the others are localized, (b) a semimetal, (c) a type IV_A half metal, and (d), (e) two types of ferromagnetic semiconductor.

Definition of polarization

$$P_0 = (N^{\uparrow} - N^{\downarrow})/(N^{\uparrow} + N^{\downarrow}),$$

--- straightforward

$$P_n = (\langle N^{\uparrow} v^{\uparrow n} \rangle - \langle N^{\downarrow} v^{\downarrow n} \rangle)/(\langle N^{\uparrow} v^{\uparrow n} \rangle + \langle N^{\downarrow} v^{\downarrow n} \rangle).$$

--- real measurement

ν: fermi velocity of electrons

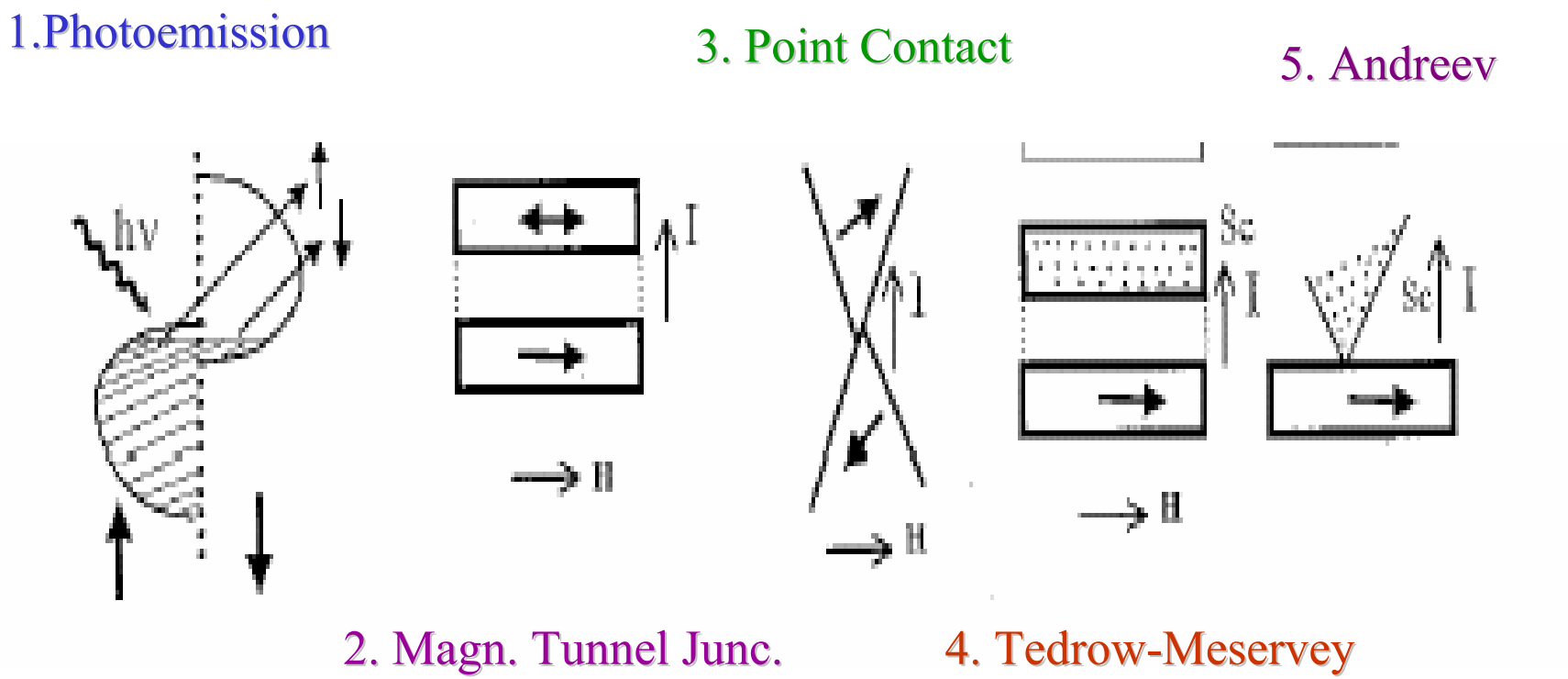

FIG. 3. Comparison of five methods of measuring *P*: Photoemission, tunnel junction, point contact, Tedrow–Meservey experiment, Andreev reflection.

TABLE II. Calculated spin polarization in ferromagnetic oxides.

	CrO_2 (Ref. 2)	$(La_{0.67}Ca_{0.33})MnO_3$ (Ref. 7)	$Tl_2Mn_2O_7$ (Ref. 8)
$N^{\uparrow}$ (eV^{-1} f.u^{-1})	0.69	0.58	1.25
$N^{\downarrow}$ (eV^{-1} f.u^{-1})		0.27	0.24
$V_F^{\uparrow}$ (10^6 ms^{-1})	0.25	0.76	0.06
$V_F^{\downarrow}$ (10^6 ms^{-1})		0.22	0.33
P_0 %	100	36	66
P_1 %	100	76	−5
P_2 %	100	92	−71

Applications of Half metals

a. **Magneto-optical effects**
   Large Kerr rotation in PtMnSb.

b. **Magneto-resistance applications**
   Spin-valve system --- pick-up head, MRAM

c. **Spin electronics**--- Injection of polarized carriers
   i) The spin injection in a normal metal can give information on the spin diffusion length in this metal.
   ii) Spin injection may act as a pair-breaking agent in a super-conductor.
   iii) Half metals can also be used to build a spin transistor
   iv) Another possible application is as polarized tips in STM, in order to visualize the orientation of magnetic domains.

Chapter Two

Colossal Magnetoresistance (CMR)

龐磁阻

Outline

1. *Introduction: Definition of CMR*
2. *Material structure*
3. *Physical Properties & Mechanism*

Introduction ---何為磁性/電子自旋

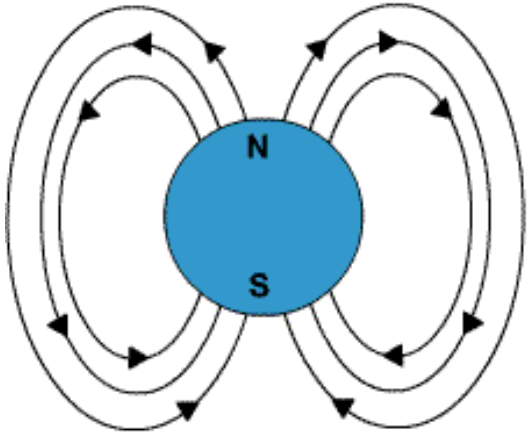

Magnetic moment of electron

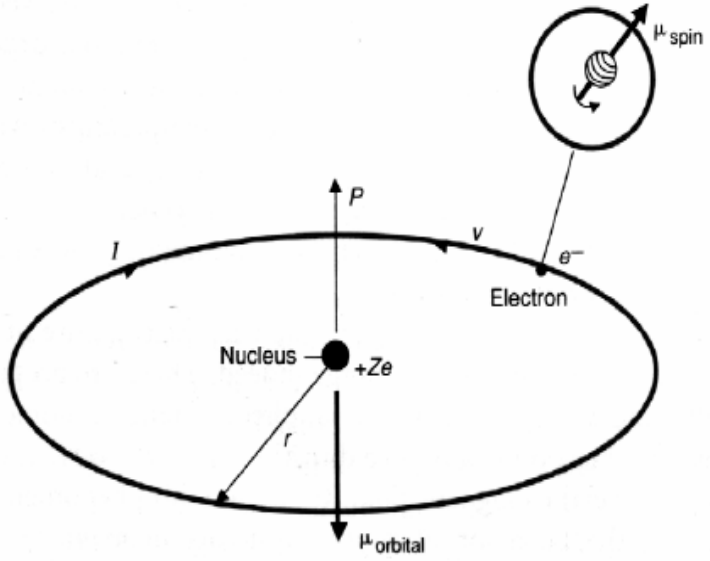

$\mu_{spin} = \mu_B$

Figure M8. Origin of the magnetic moments in atoms due to an electron orbiting the nucleus ($\mu_{orbital}$) and to the electron spin about its axis ($\mu_{spin} = \mu_B$).

Introduction --- Domain structure

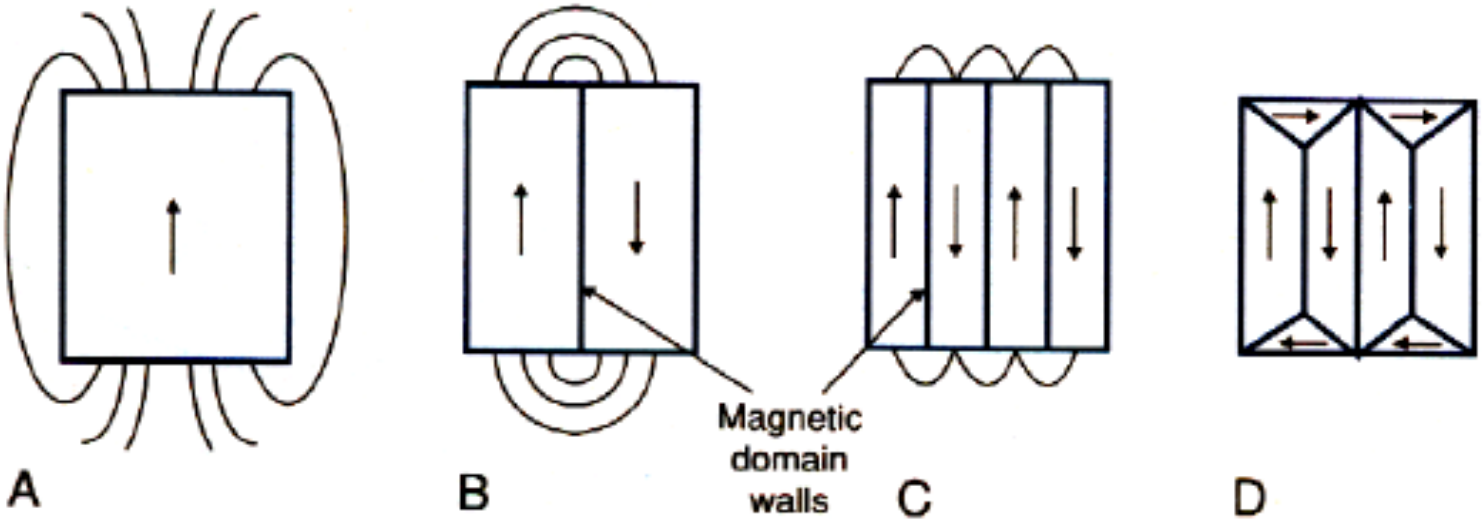

Introduction ---物質的基本磁性

順磁

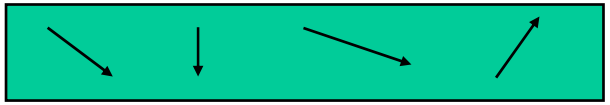

鐵磁

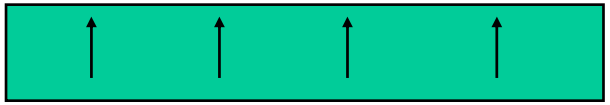

反鐵磁

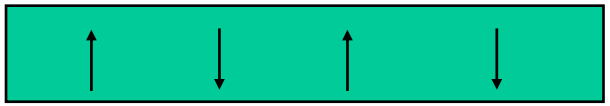

亞鐵磁

斜磁

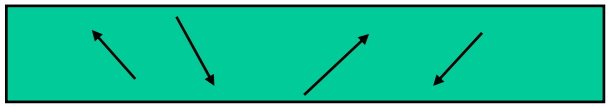

Introduction ---物質的自發磁性

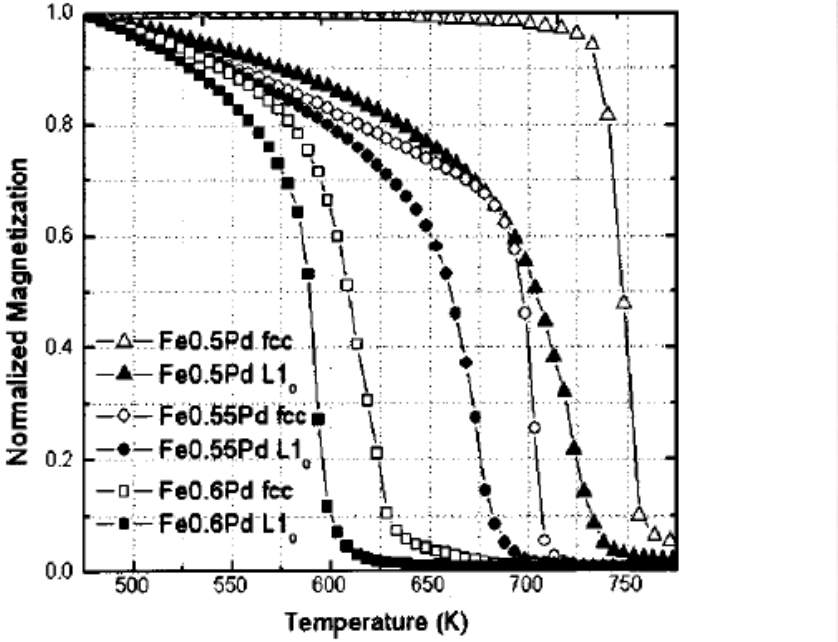

WEISS MOLECULAR-FIELD APPROXIMATION 433

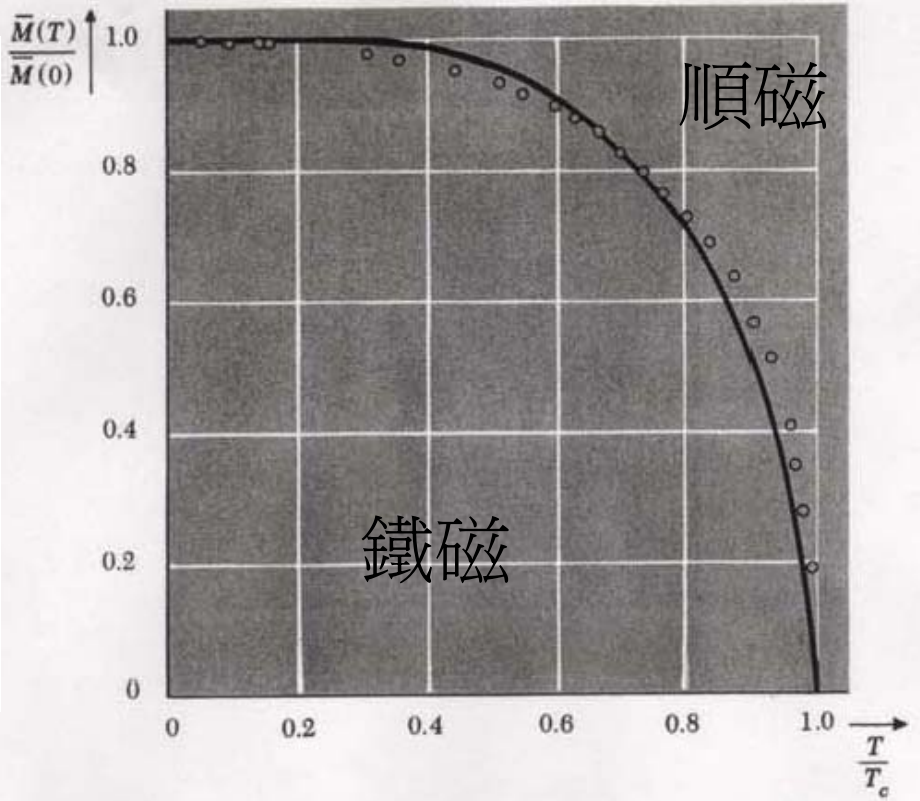

Fig. 10·7·2 Spontaneous magnetization $\bar{M}$ of a ferromagnet as a function of temperature T in zero external magnetic field. The curve is based on the molecular field theory of (10·7·10) and (10·7·9) with $S = \frac{1}{2}$. The points indicate experimental values for nickel (measured by P. Weiss and R. Forrer, Ann. Phys., vol. 5, p. 153 (1926)).

1. Introduction ---何謂電阻(率)

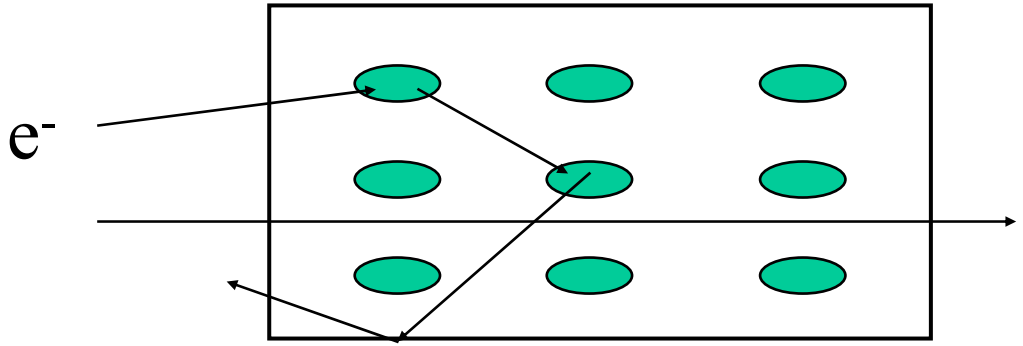

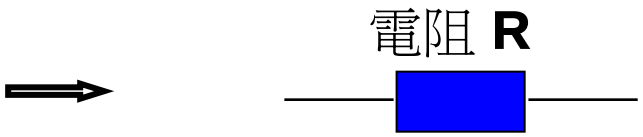

$\rho = R*A/w$

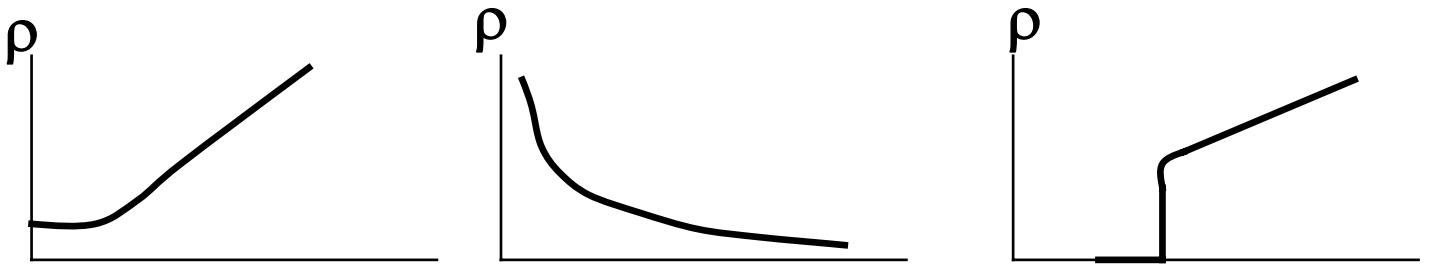

金屬　　半導體　　超導體

Introduction ---何謂磁阻

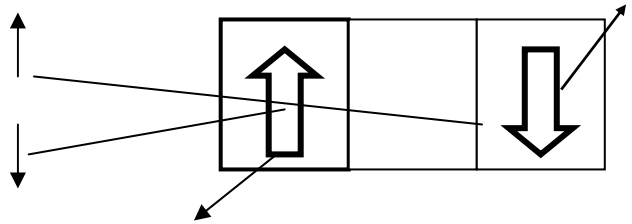

H = 0

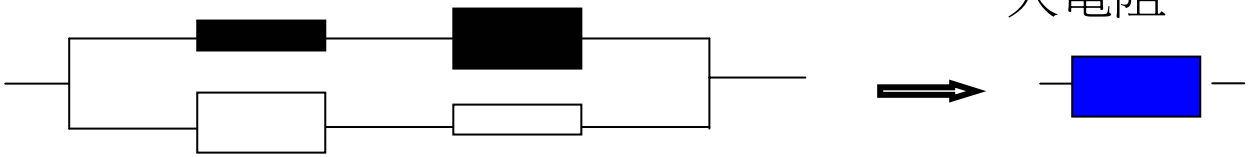

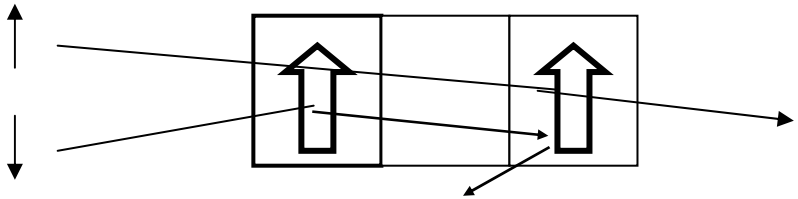

H = Ha

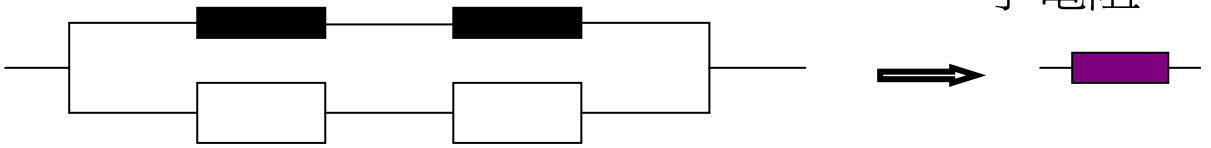

Introduction --- 何謂龐磁阻(CMR)

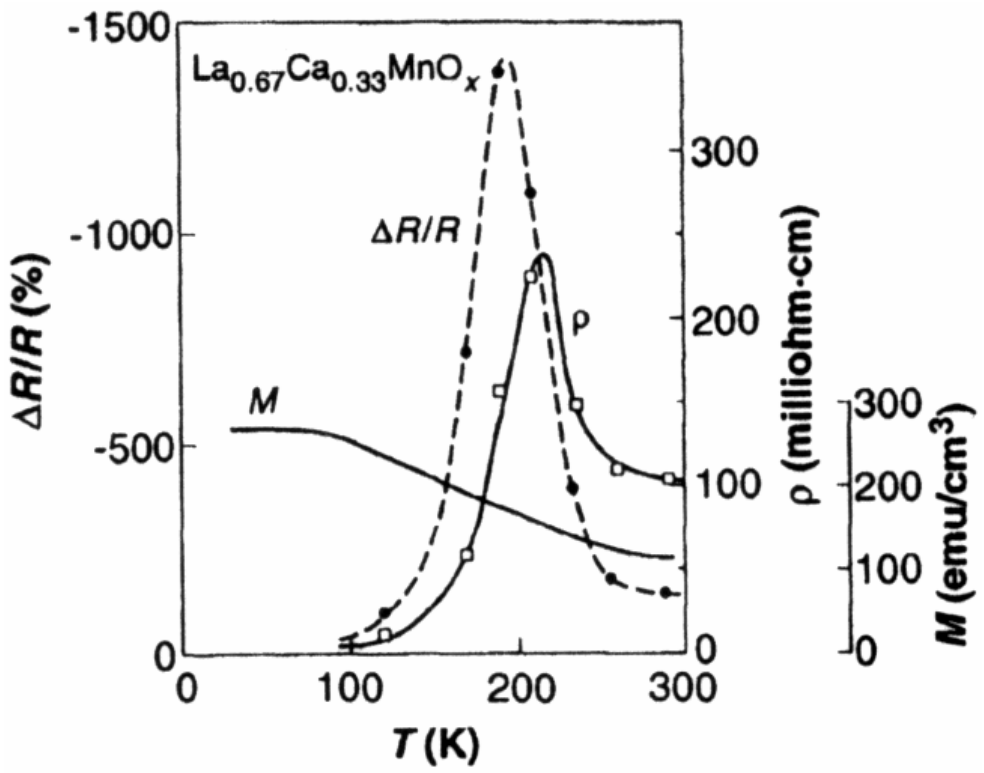

1) Very high magnetoresistance (99% at Tp)
2) Polarization 100% (half metal)
3) M- I (F/AF) transition
4) Phase separation
5) Charge ordering
6) Orbital ordering

MR =[ρ(H)-ρ(0)]/ρ(H=6 tesla)

S. Jin et al. Science 265 (1994)

MR ratio of spintronic materials

Type	MR	Field	Temp.	Sample
OMR	0.01%	~Tesla	RT	Cu,Al
AMR	2 %	10 Oe	RT	Fe,Co,Ni
GMR	10 %	2 Oe	RT	Fe/Cr/Fe
TMR	40 %	10 Oe	RT	Co/AlO/Co
CMR	10 (99)%	~Tesla	RT(LT)	La-Sr-Mn-O

2. Material Perovskite layered structure

$LaMnO_3$: Cubic (insulator, Antiferromagnetic)

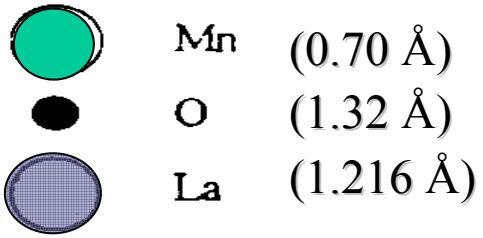

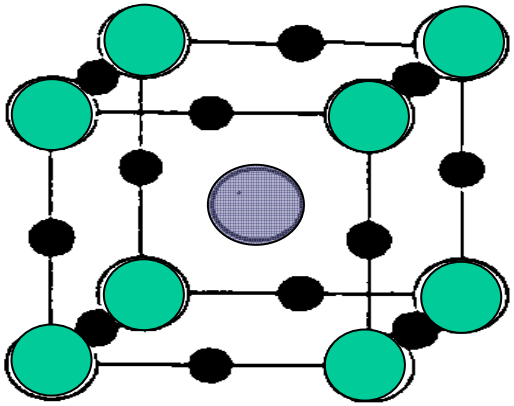

$(La,Sr)MnO_3$: orthorhombic

(Metal, Ferromagnetic)

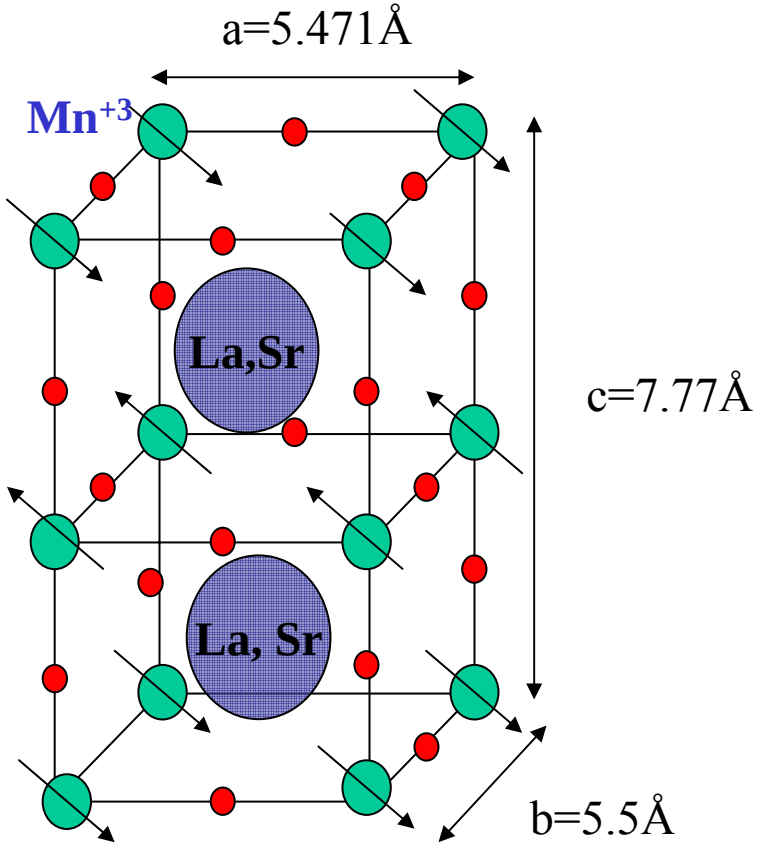

X – ray diffraction pattern

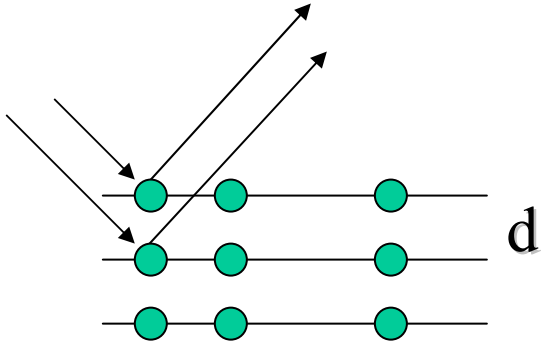

Bragg condition:

$n\lambda = 2d\sin\theta$

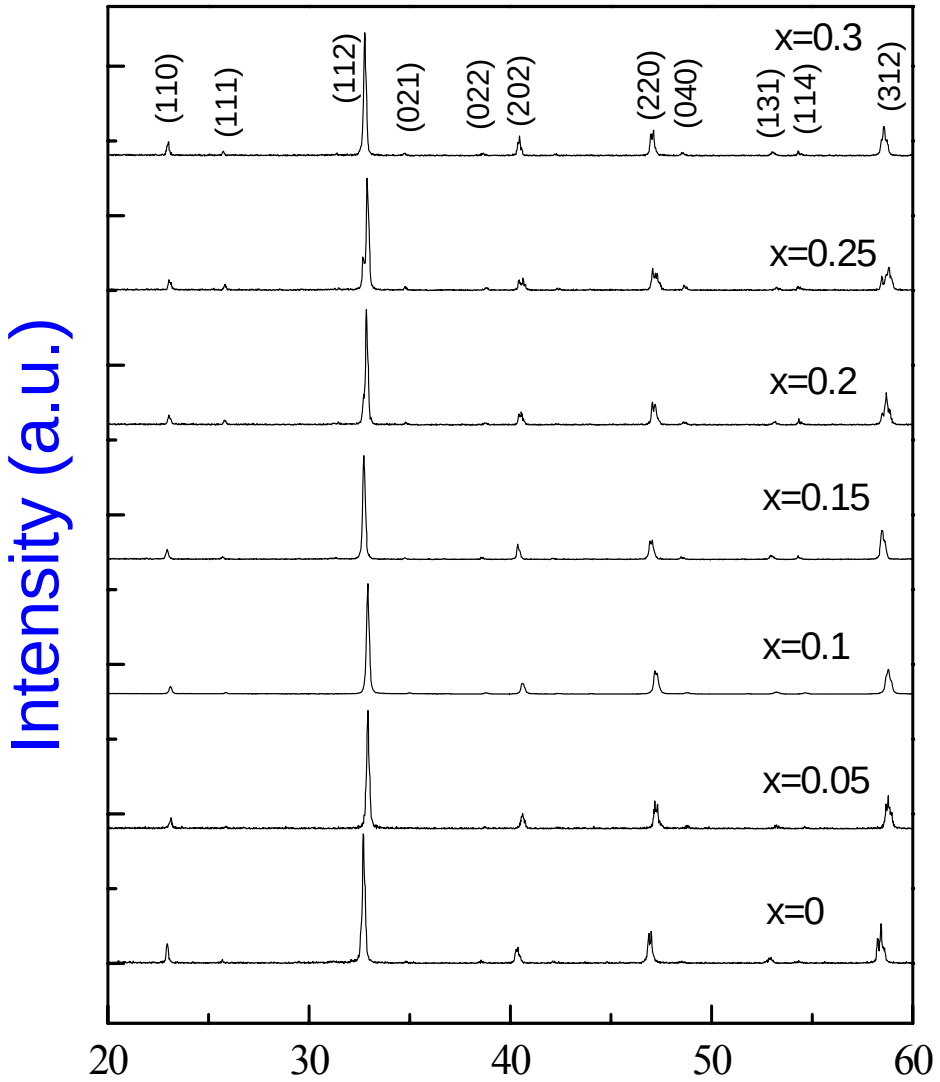

Phase diagrams of $R_{1-x}A_xMnO_3$

degrees of freedom: charge, spin, orbital

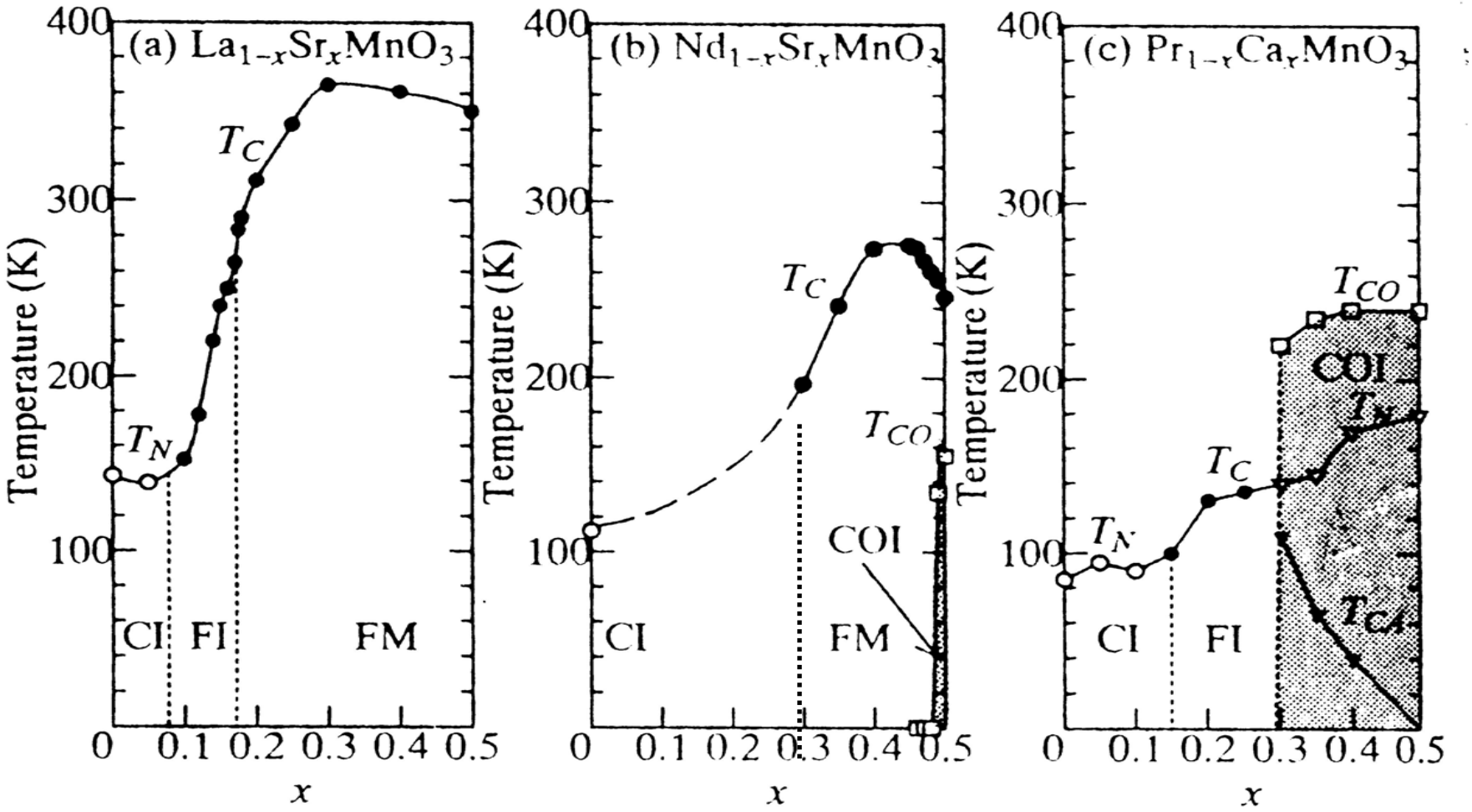

3. Physical properties & mechanism

What’s the new physics

Double exchange (1951, Zener)

$(La,Sr,)MnO_3$

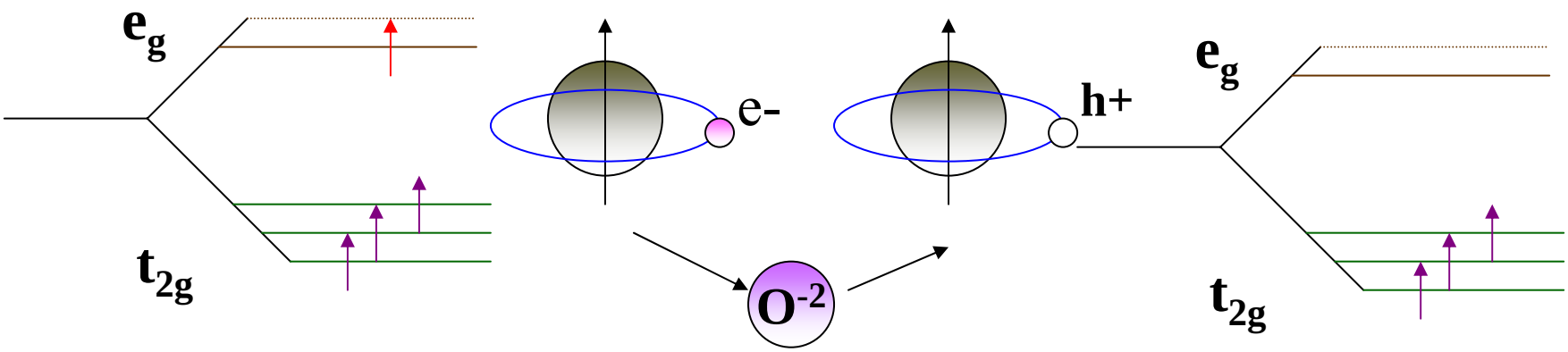

SP

$Mn^{+3}: 3d^4 (t_{2g}^3 e_g^1)$

$Mn^{+4}: 3d^3 (t_{2g}^3 e_g^0)$

Mechanism vs. degree of freedom

- FM/AFM superexchange --- spin
- Charge/orbital ordering --- charge/orbital
- double exchange --- charge/spin
- Lattice distortion --- lattice
  (John-Teller effect)

Physical Review B, Volume 58, Number 17 1 November 1998-I

Phase diagram of manganese oxide

Ryo Maezono, Surnio Ishihara, and Naoto Nagaosa
Department of Applied Physics, University of Tokyo, Bunkyo-ku, Tokyo 113, Japan

$$H = H_K + H_{Hund} + H_{on\,site} + H_S$$

$$H_K = \sum_{\sigma\gamma\gamma'(ij)} t_{ij}^{\gamma\gamma'} d_{i\sigma\gamma}^{+} d_{j\sigma\gamma'}$$ (Kinetic energy of e_g electrons)

$$H_{Hund} = -J_H \sum_i \vec{S}_{t2gi} \cdot \vec{S}_{egi}$$ (Hund coupling between e_g & t_{2g} spins)

$$H_{on\,site} = -\sum_i (\tilde{\beta} T_i^2 + \tilde{\alpha} S_{egi}^2)$$ (Coulomb interaction between e_g-electrons)

$$H_S = J_S \sum_{(ij)} \vec{S}_{t2gi} \cdot \vec{S}_{t2gj}$$ (Super exchange t_{2g} spins)

2D-F

1D-F

(x=0.0) ; spin F

(x=0.3) ; spin F

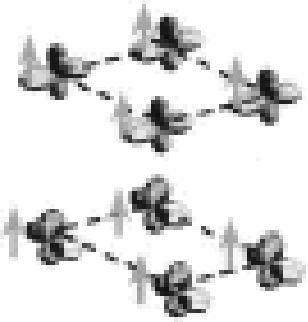

(0.3<x<0.8) ; spin F

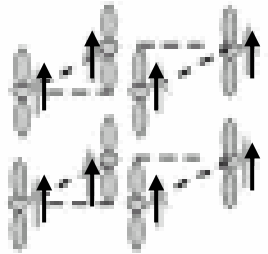

(x=0.8) ; spin F

A

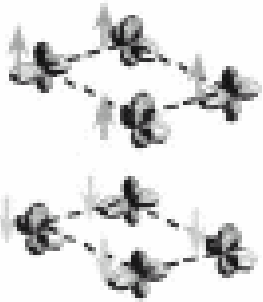

(x=0.0) ; spin A

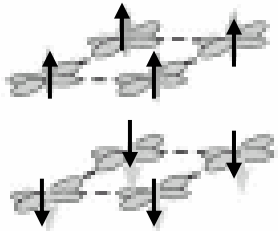

(0.1<x<0.45) ; spin A

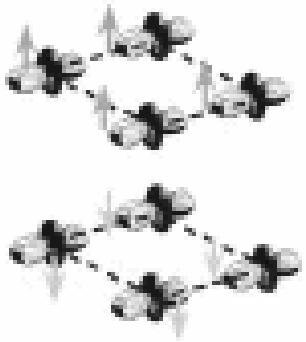

(0.45<x<0.75) ; spin A

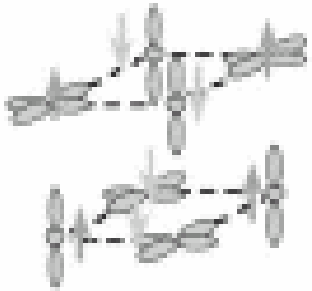

(x=0.0) ; spin C

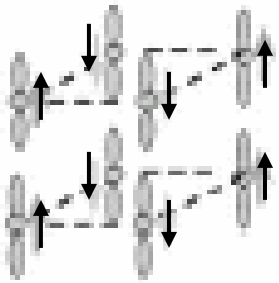

(x＋0.0) ; spin C

G

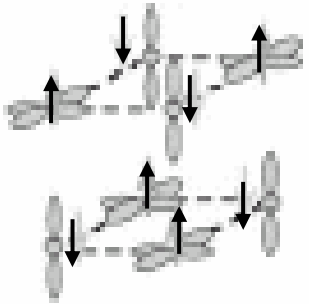

(x=0.0) ; spin G

Charge Ordering (Mn^{+4}/Mn^{+3} = n/8)

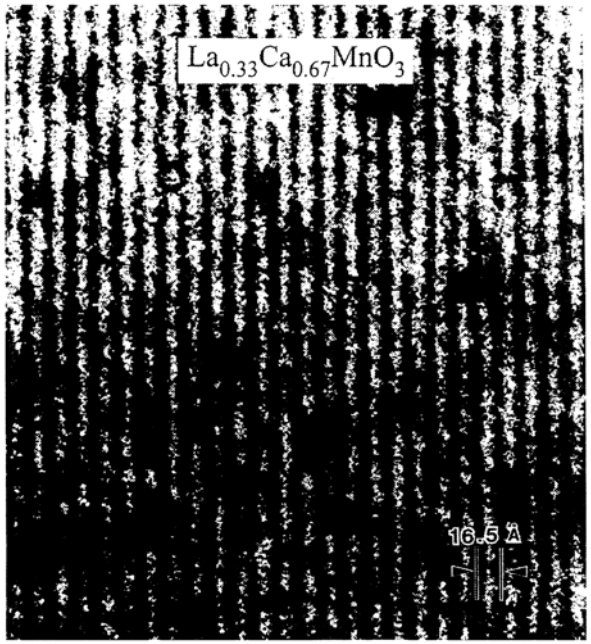

Chen et al., J. Appl. Phys. 81 (1997)

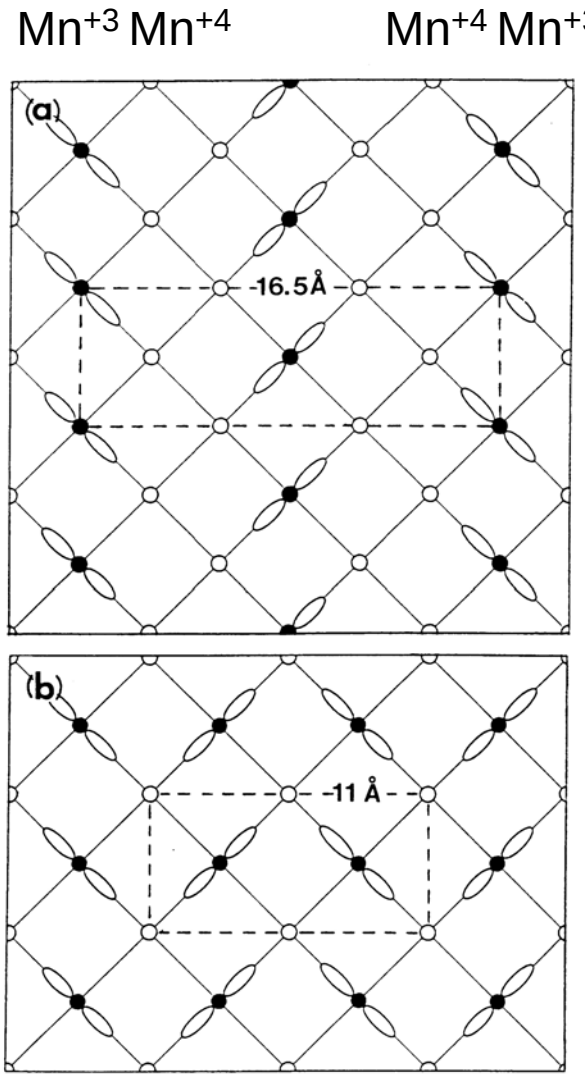

(0.67~5/8)

(0.5=4/8)

Spin/orbital structure

Neutron diffraction
Magnetic Dichroism

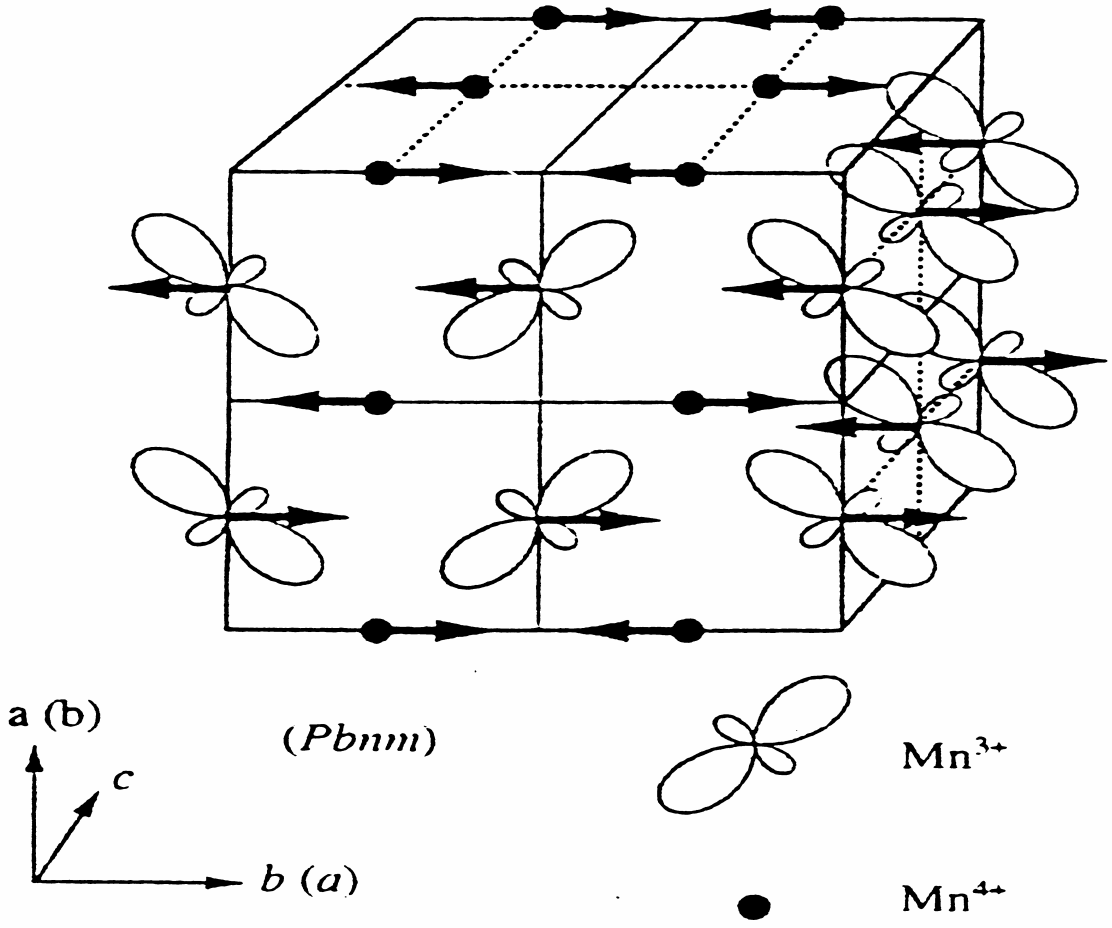

$Nd_{1-x}Sr_xMnO_3$

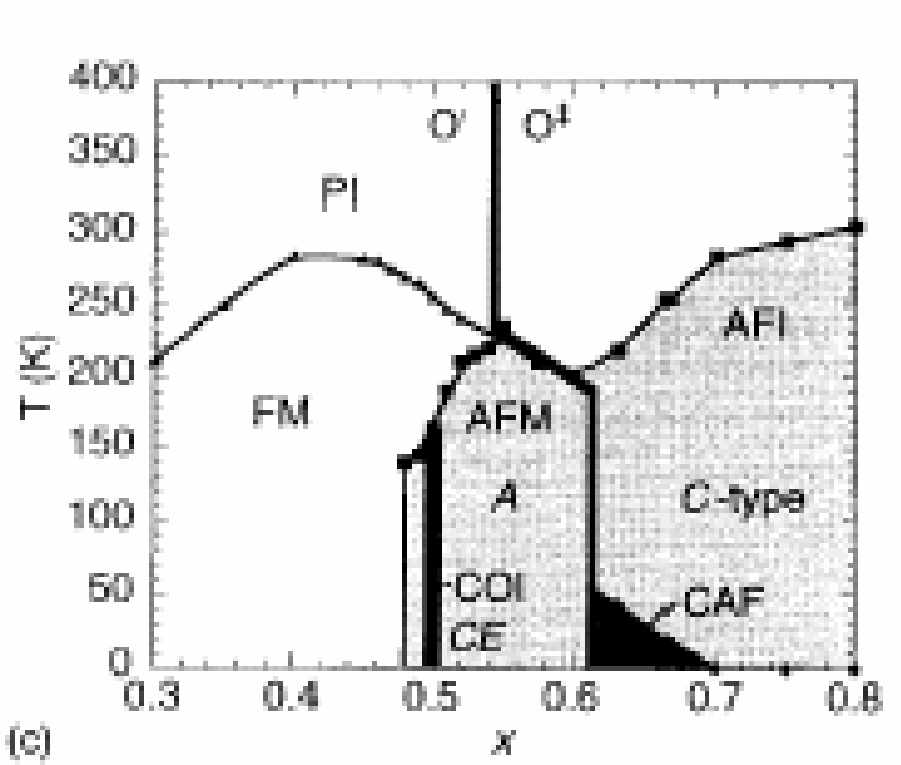

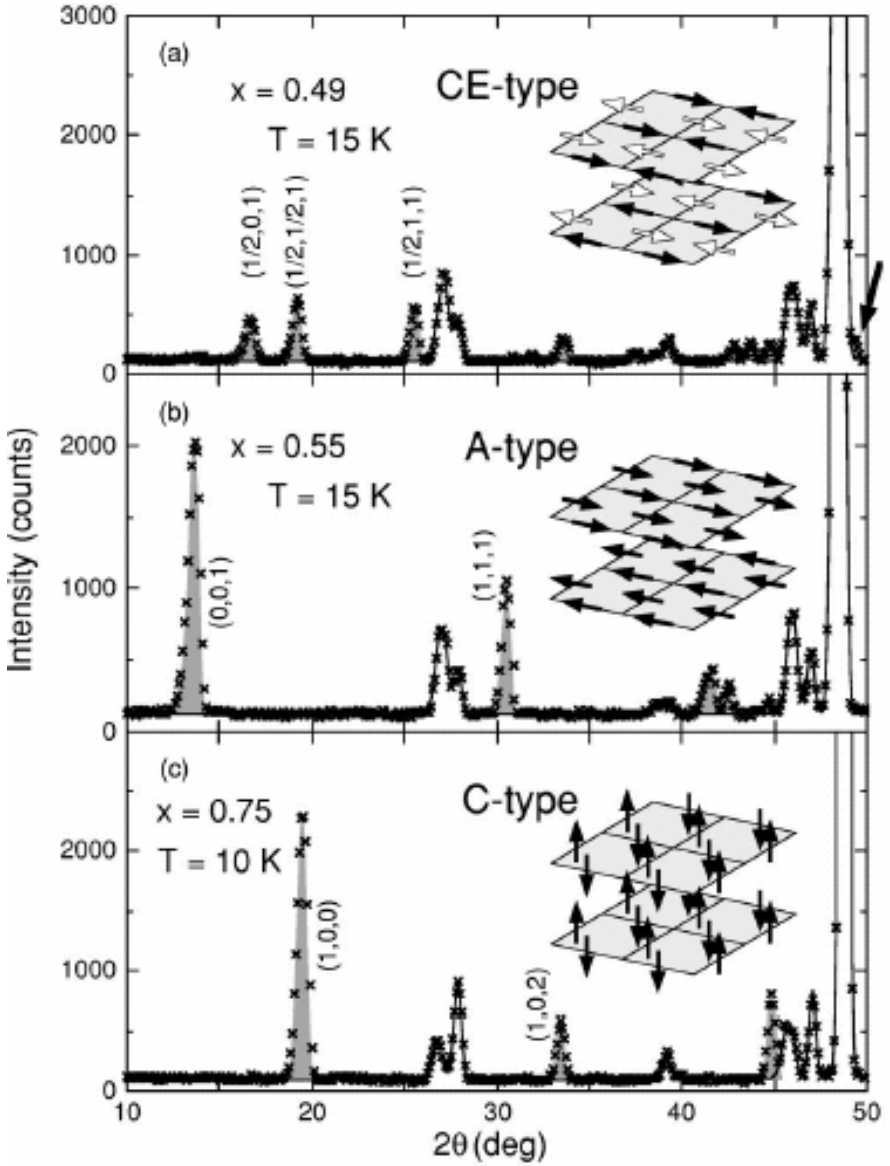

Kajimoto et al., PRB 30, 9506 (1999)

Orbital switching in A-type spin state

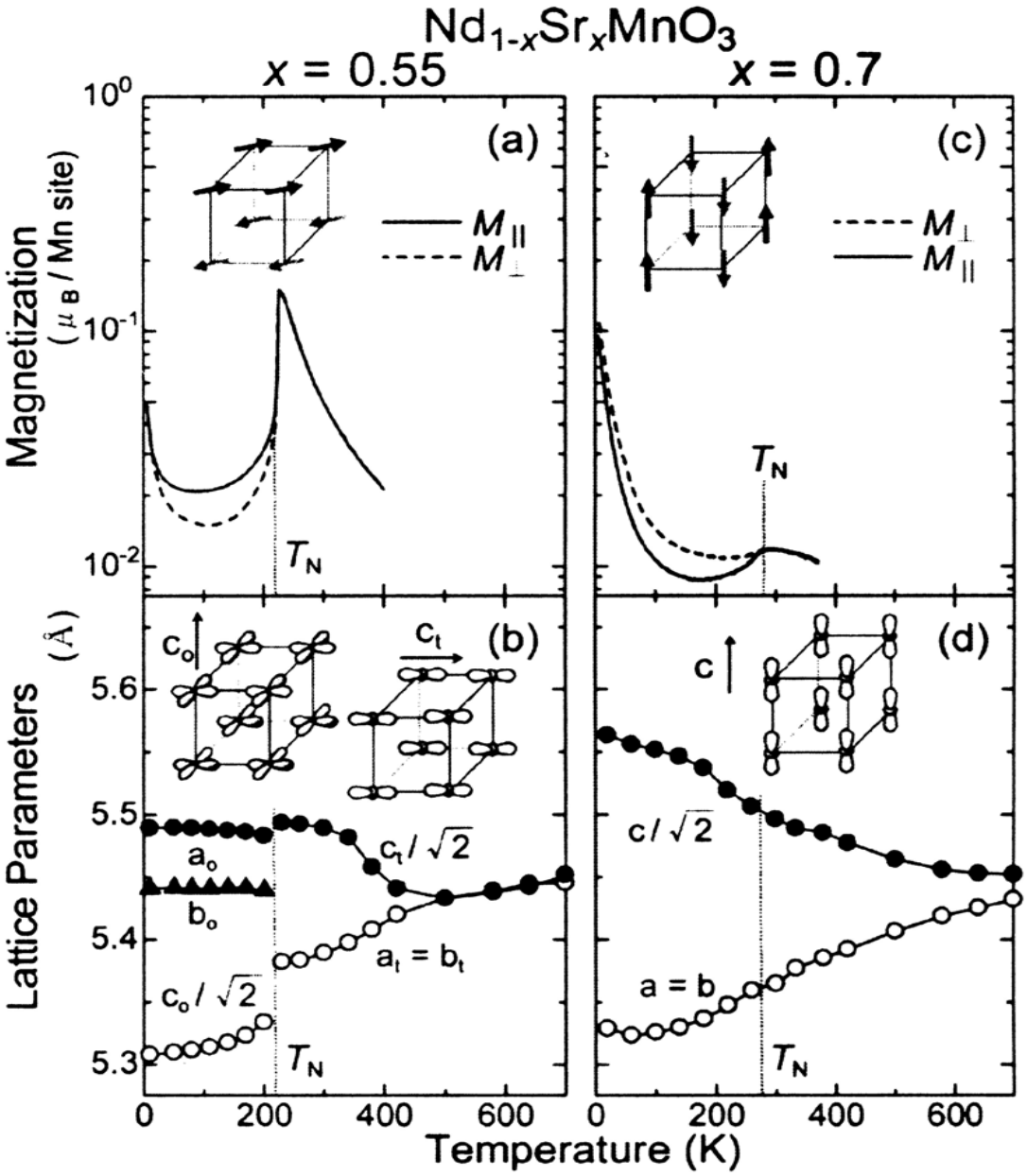

Spin A-Type :

from d_{3z2-r2} to d_{x2-y2}

at T_N ~ 220 K

Spin C-type :

remains d_{3z2-r2}

with T_N ~ 270 K

Tobe, PRB 67, 140402 (2003)

Origin of CMR: Phase separation

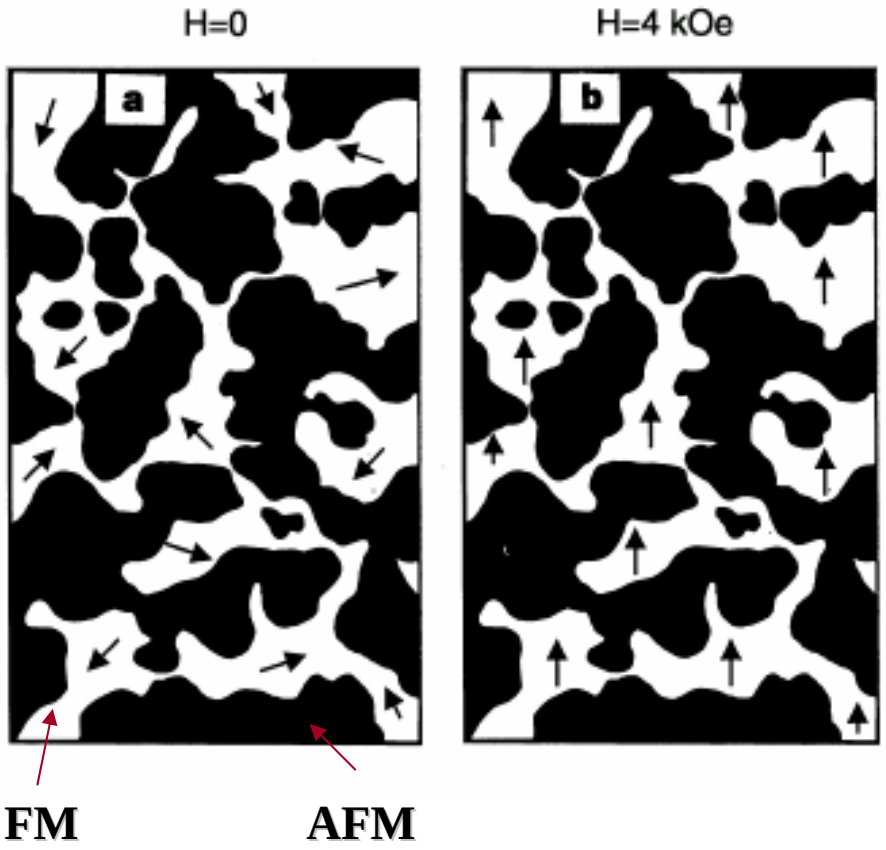

Spin line up (metal)

AFM Melting as H≧1 Tesla (insulator)

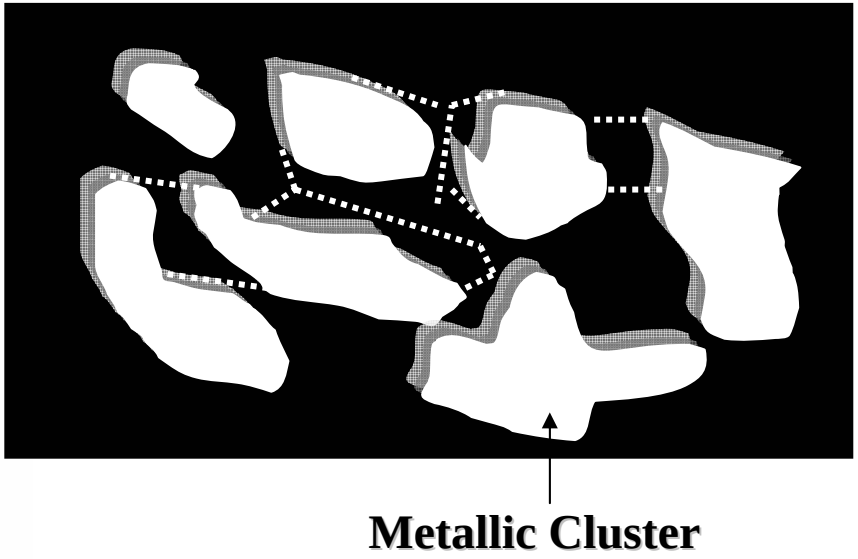

M. Uehara, et all, Nature 399 (1999)

Chapter Three

Experiments for Spintronics

III-1. Bulks

Phase separation

fine tuning the MR value by

Ionic radius size

Key parameters

- hole concentration (charge/orbital/spin)
- radius of A-site (electron/orbital/spin)

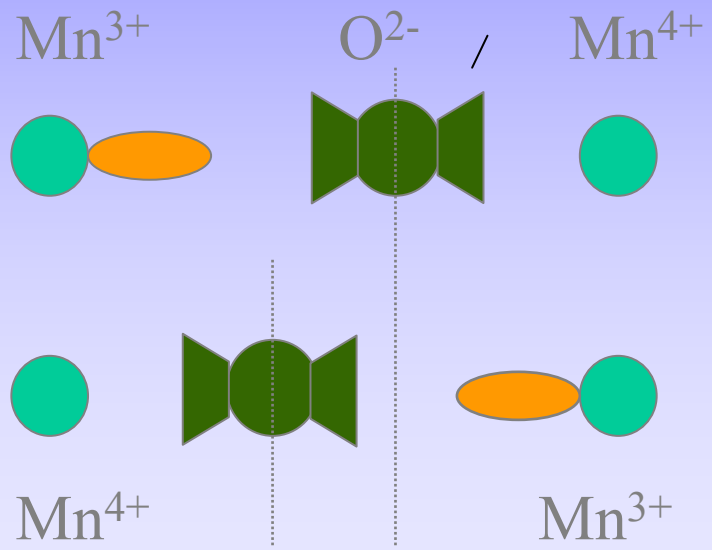

$La_{1-x}Sr_xMnO_3$

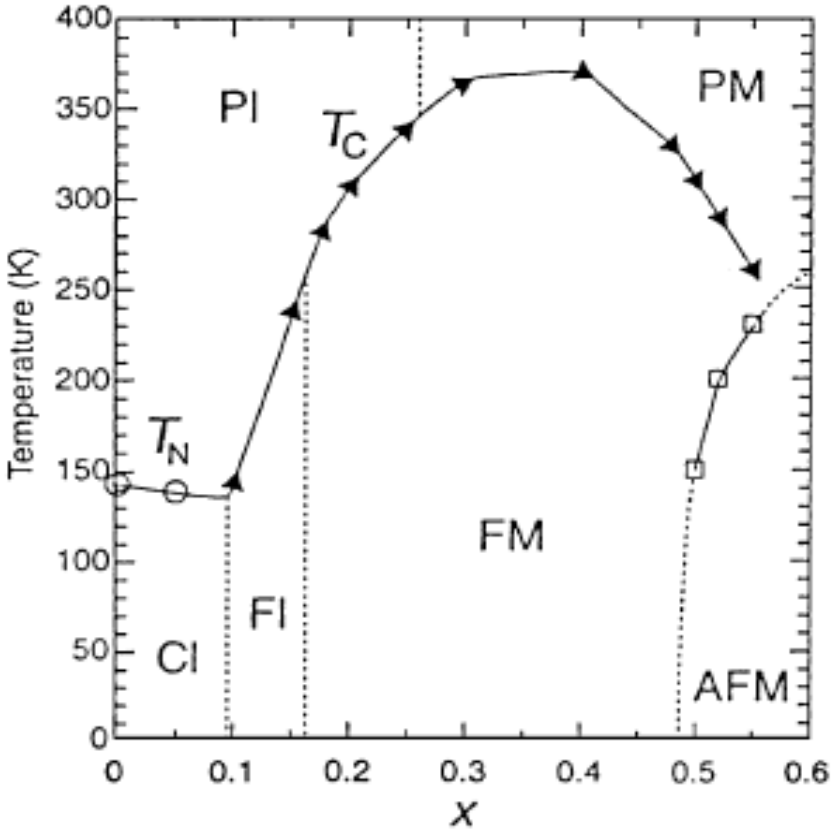

E. Dagotto *et. al*., Physics Reports 344, 1-153 (2001)

$R_{0.7}(Ca,Sr)_{0.3}MnO_3$

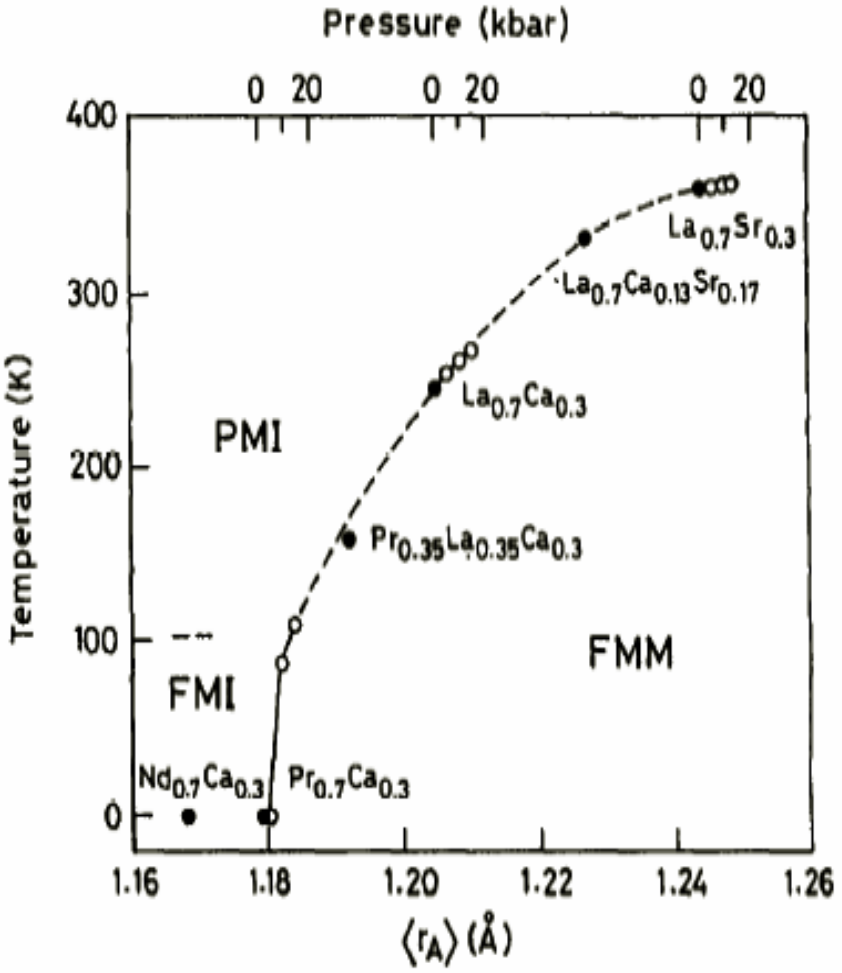

C. N. R. Rao et al. J. Phys. Chem. Solids 59, 487 (1998)

Bulk Making

Step 1 Pre-heating R_2O_3: 900℃/ 3 h .

Step 2 Mix R_2O_3 (R=rare earth ion),$CaCO_3$, $SrCO_3$, $MnCO_3$

Step 3 Reaction: 1200℃/ 24 h

Step 4 Pellet :d = 1 cm, Thickness =3 mm, 3 tons/ cm^{-2}

Step 5 Anneal: 1400℃ /16 h

Physical Property measurement System (PPMS)

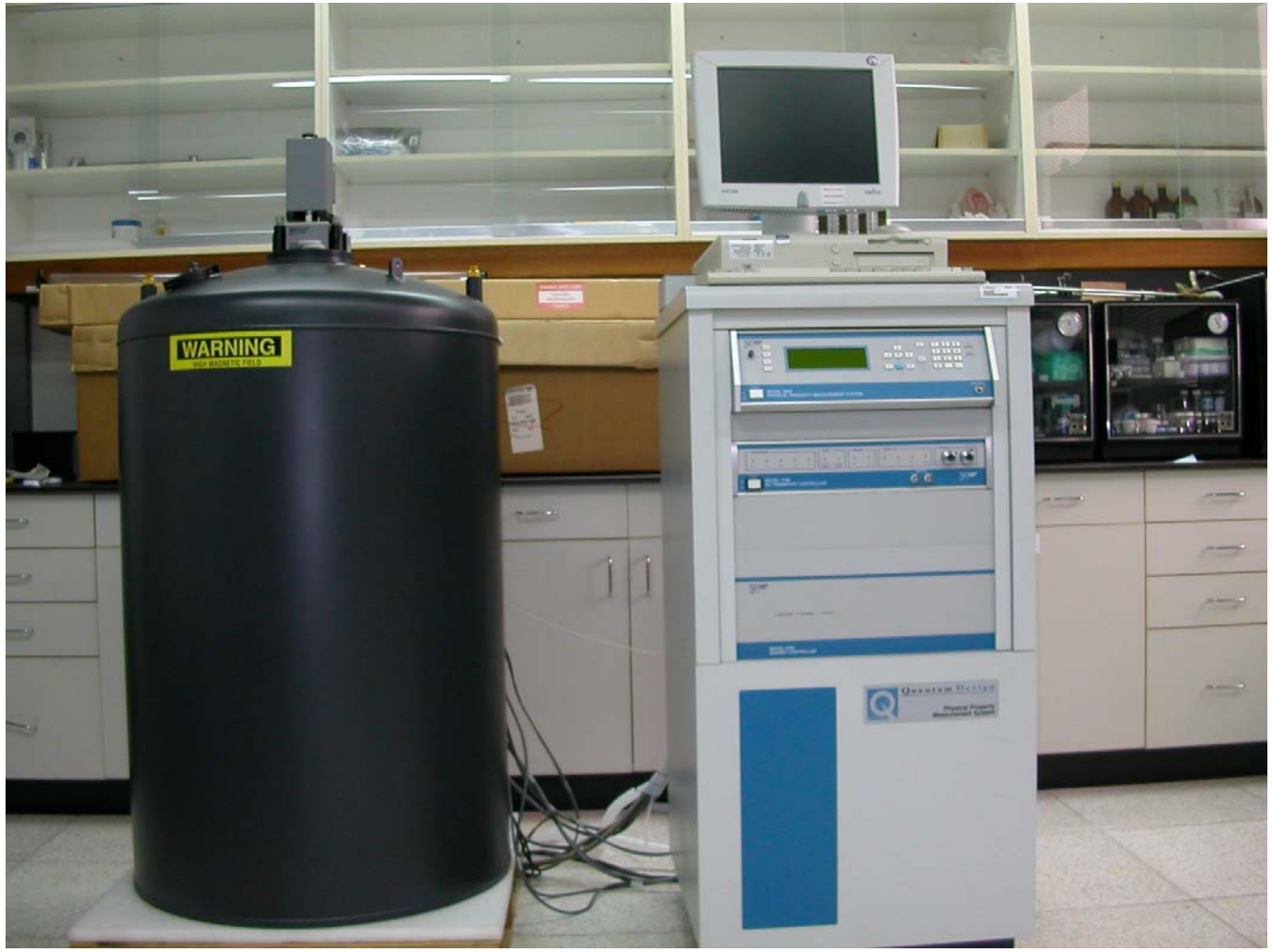

0 – 7 Tesla
1.4 – 400 K
Hall effect
resisitivity
AC susceptibility

Basic M – T curve

Para- to antiferromagnetic

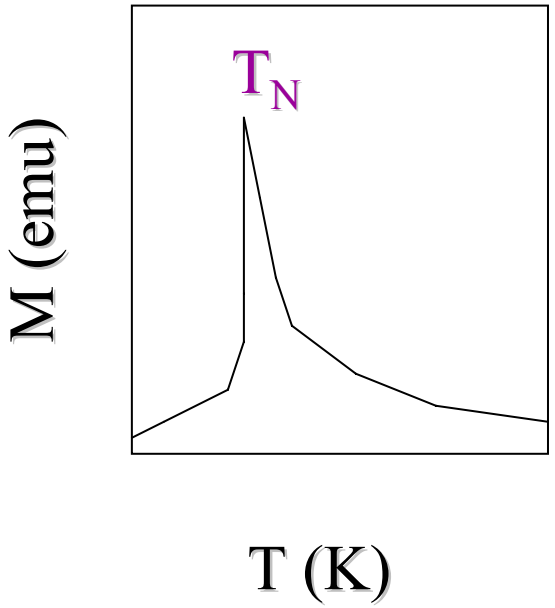

Para- to ferromagnetic

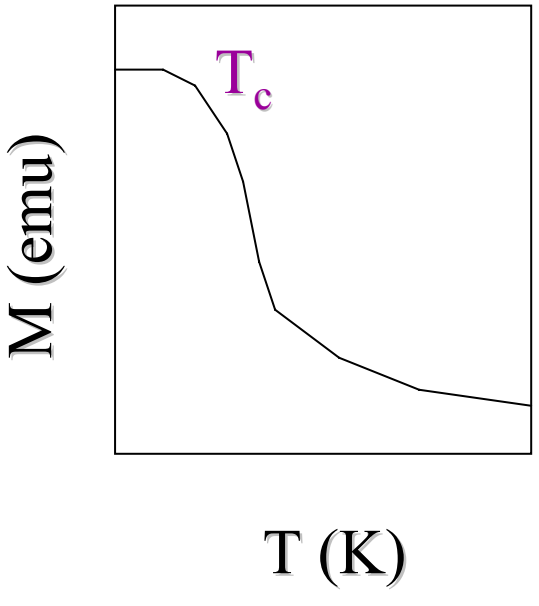

$M \sim C/T$, $C/(T+T_N)$, $C/(T-Tc)$

Basic R – T curve

$\rho = \rho_o + \rho_1 T^{\alpha}$

metal

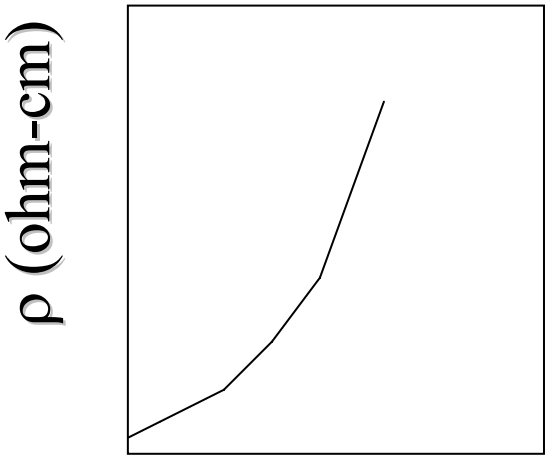

$\rho = \rho_o \exp(C/T^{\beta})$

insulator

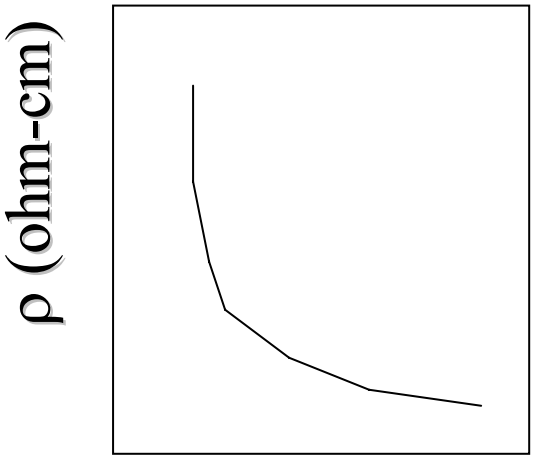

PHYSICAL REVIEW B, VOLUME 65, 024422 (2001)

Thermal and magnetic instability near the percolation threshold of $Nd_{0.5}Ca_{0.5-y}Sr_yMnO_3$

C. W. Chang,* A. K. Debnath,† and J. G. Lin‡
Center for Condensed Matter Science, National Taiwan University, Taipei, Taiwan

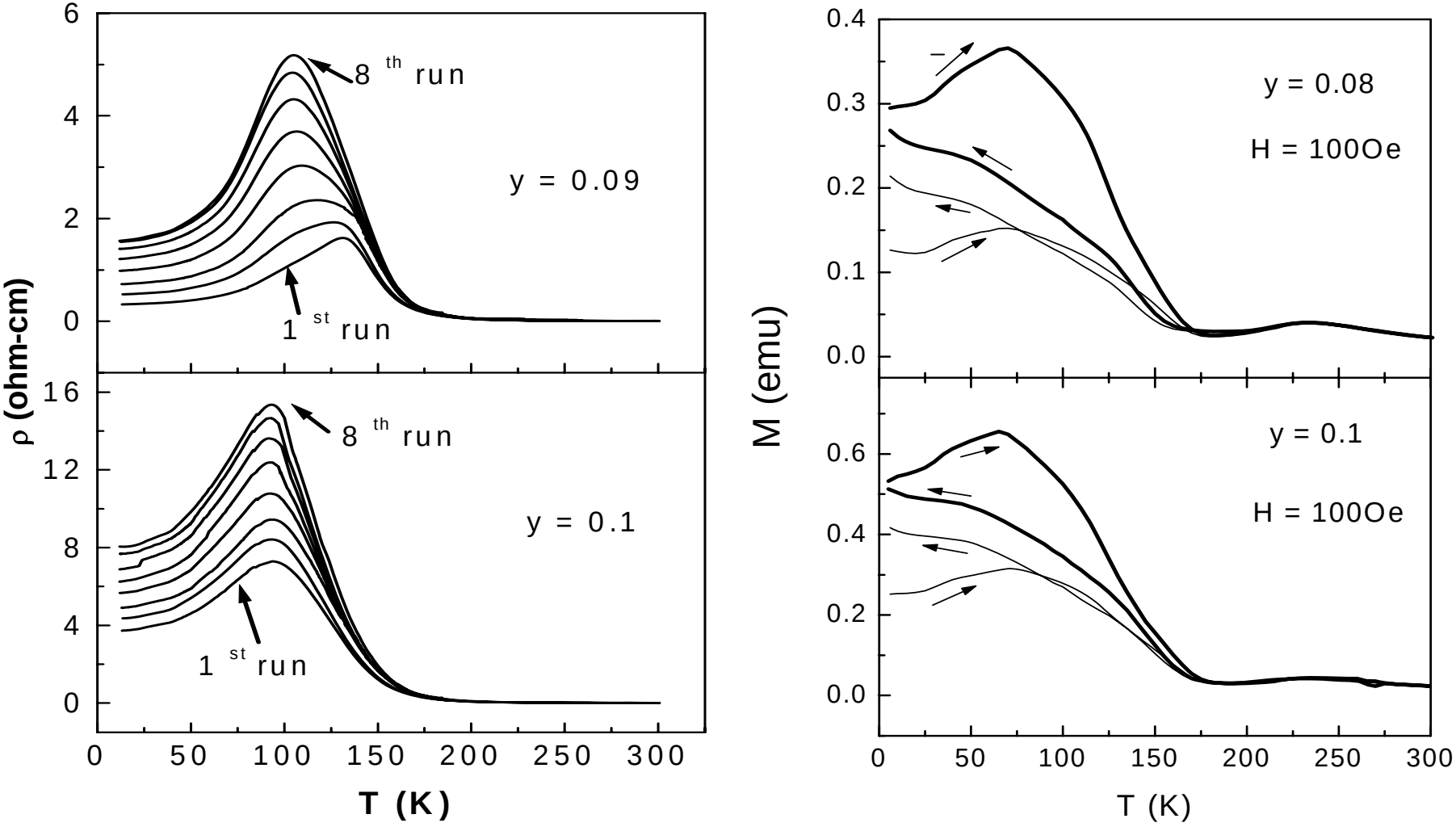

PHYSICAL REVIEW B, VOLUME 65, 024422 (2001)

Termal and magnetic instability near the percolation threshold of $Nd_{0.5}Ca_{0.5-y}Sr_yMnO_3$

C. W. Chang,* A. K. Debnath,† and J. G. Lin‡
Center for Condensed Matter Science, National Taiwan University, Taipei, Taiwan

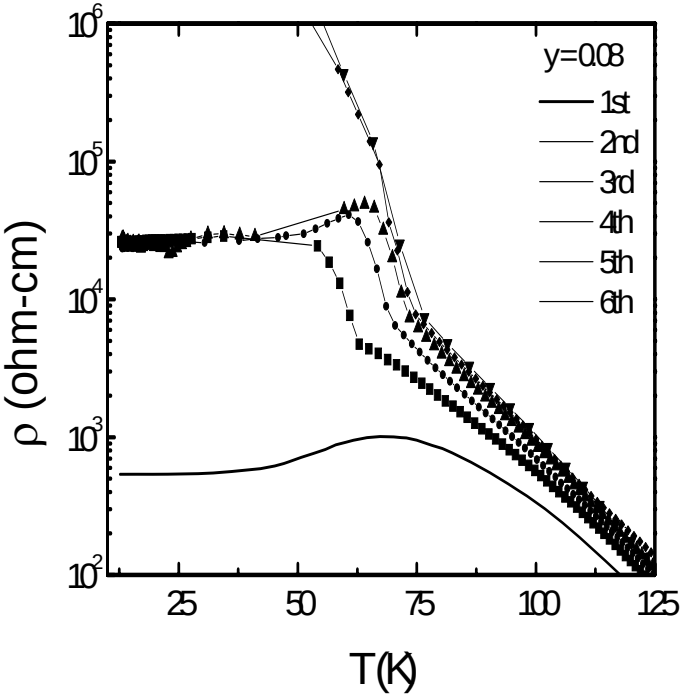

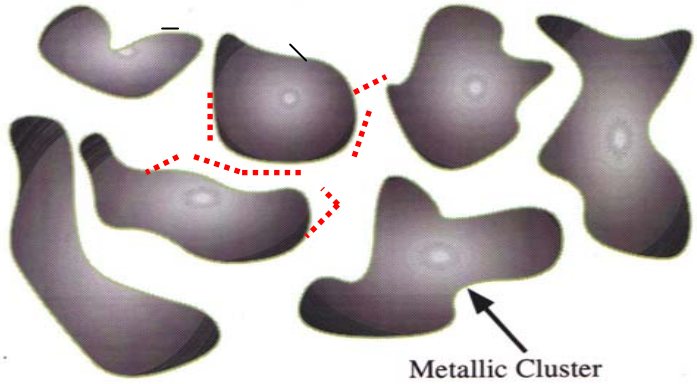

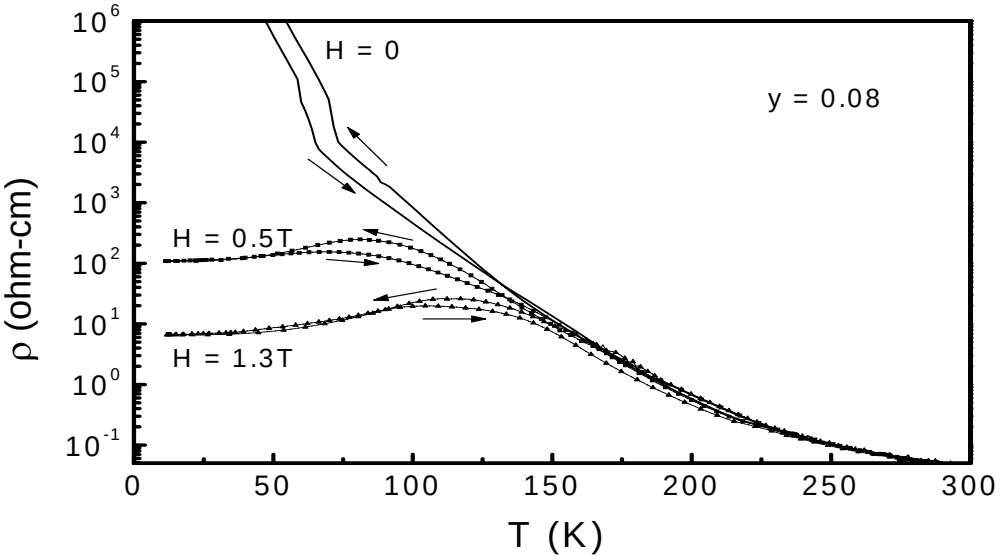

III-2 films & bilayers

(1) Nanocrystalline LSMO films

(2) Nanocrystalline YBCO/LSMO bilayers

(3) Epitaxial YBCO/NCMO bilayers

Experiment Flow Chart

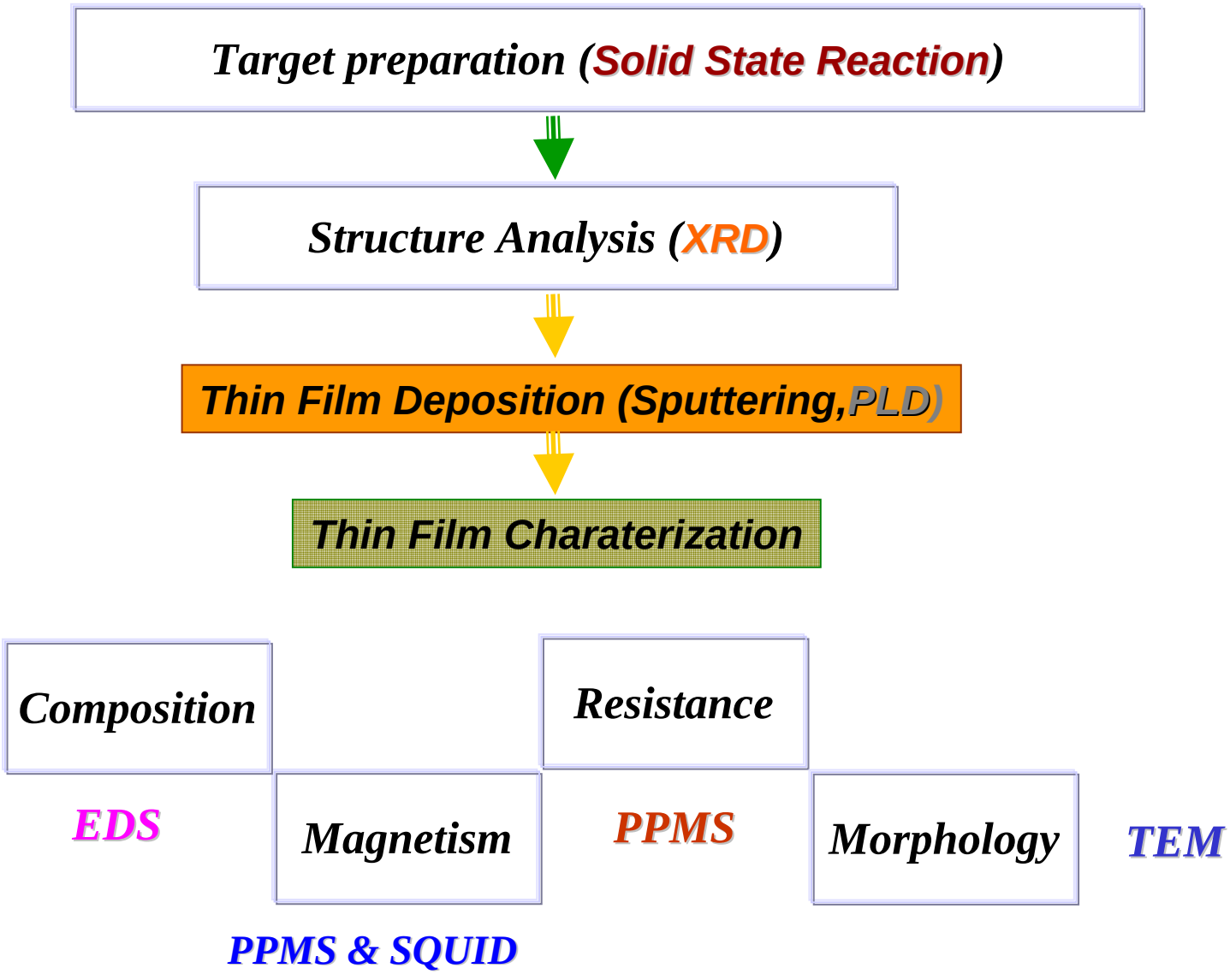

Target preparation

Powders

- $La_{0.7}Sr_{0.3}MnO_3$ (LSMO):

  La_2O_3, $SrCO_3$, $MnCO_3$ Powder
  100˚C (3 hrs.) in air
  1100˚C (24 hrs.) in air

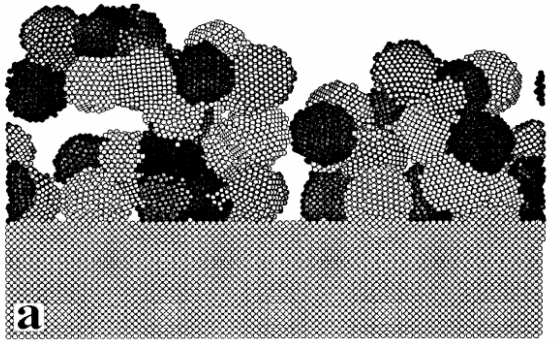

Solid state reaction

- $YBa_2Cu_3O_7$ (YBCO)

  Y_2O_3, $BaCO_3$, CuO_2 Powder
  100˚C (3 hrs.) in air
  1050˚C (36 hrs.) in oxygen
  400˚C (12 hrs.) in oxygen

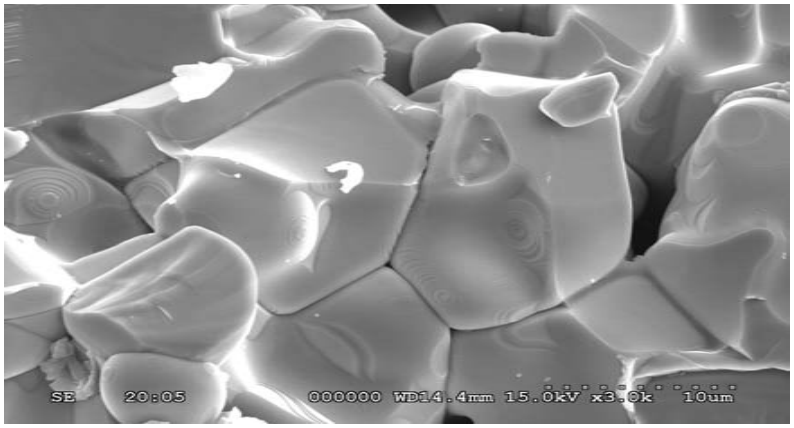

RF sputter system (Millton CVT, 13.6 MHz)

10^{-8} torr
four guns
1000 ˚C

Film making

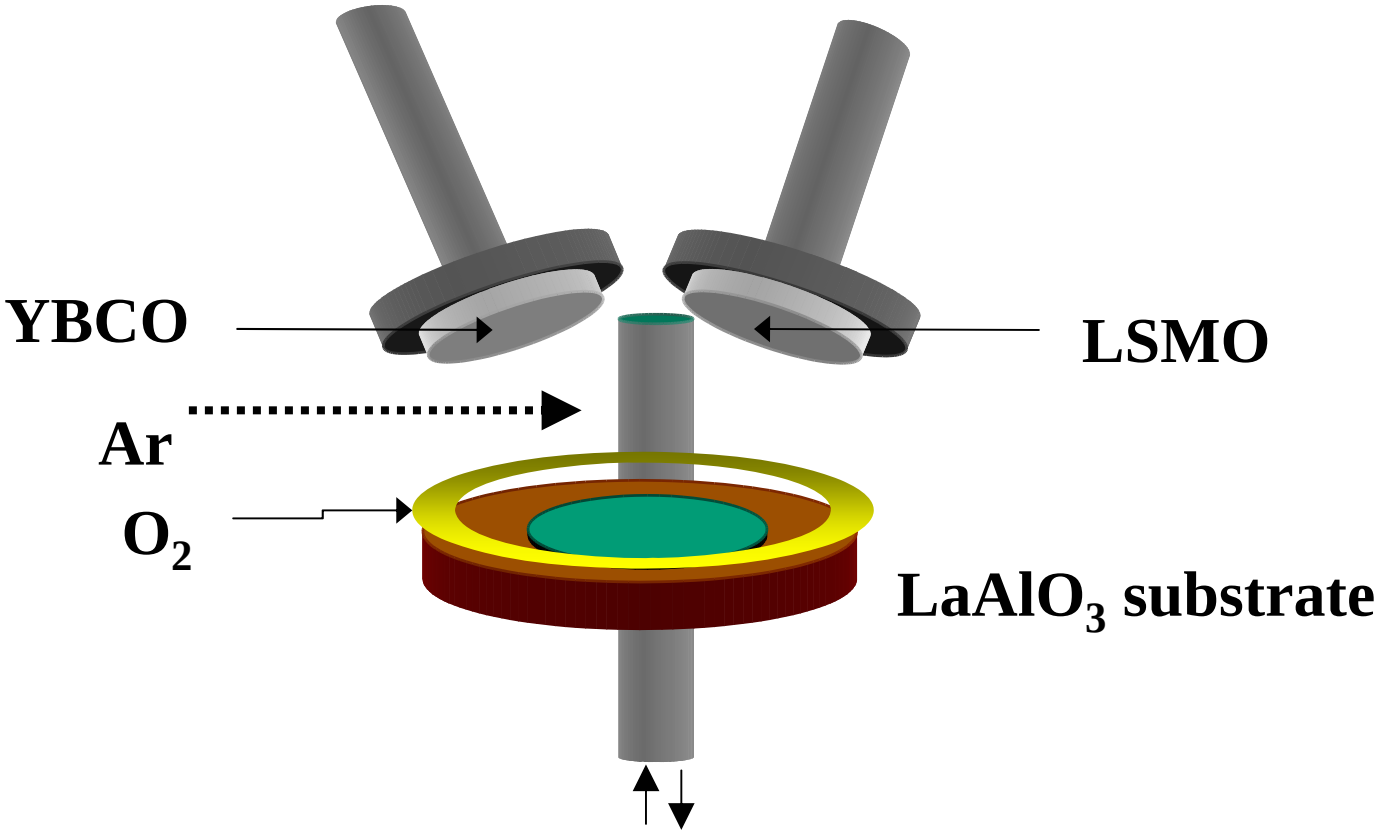

Reactive co-sputtering process

Topic (1): Nanocrystalline LSMO films

--- Low field MR effects

Giant electroresistance

JOURNAL OF APPLIED PHYSICS **98**, 114318 (2005)

Low-field magnetoresistance in nanocrystalline $La_{0.7}Sr_{0.3}MnO_3$ films

S. L. Cheng and J. G. Lin[a)]
Center for Condensed Matter Sciences/Center for Nanostorage Research, National Taiwan University, Taipei 106, Taiwan

(Received 28 March 2005; accepted 1 November 2005; published online 14 December 2005)

Nanocrystalline $La_{0.7}Sr_{0.3}MnO_3$ films with thickness $t=10$-60 nm were grown on $LaAlO_3(100)$ substrates by radio-frequency magnetron sputtering. Their electrical resistivity and low-field magnetoresistance (MR) were measured. Metal-insulator transitions occur above 275 K for films with $t=20$-60 nm, but the electron localization prevails in the 10 nm thick film. Furthermore, only the 10 nm thick film has an MR that depends on the inverse of temperature, consistent with the model of spin-polarized tunneling. This relationship may reflect a critical aspect of the structure of grain/grain-boundaries. Accordingly, the tunneling MR in this film is 27% at 75 K. © *2005 American Institute of Physics*. [DOI: 10.1063/1.2140081]

• Substrate ⇒	Si (100) , $LaAlO_3$(100)
• Target ⇒	LSMO (YBCO)
• RF power ⇒	80 Watt
• Base pressure ⇒	3×10^{-7} torr
• Mixed gas ⇒	Ar:O_2=98:2
• Sputtering pressure	70 mtorr
• Base temperature ⇒	Room temperature
• pre-sputtering ⇒	3 minutes
• Working distance ⇒	10 cm
• Annealing tempert.	800 – 920 ℃ (700 ℃)
• Annealing time ⇒	1 hrs

Structures of LSMO layer

XRD – monoclinic

c-oriented

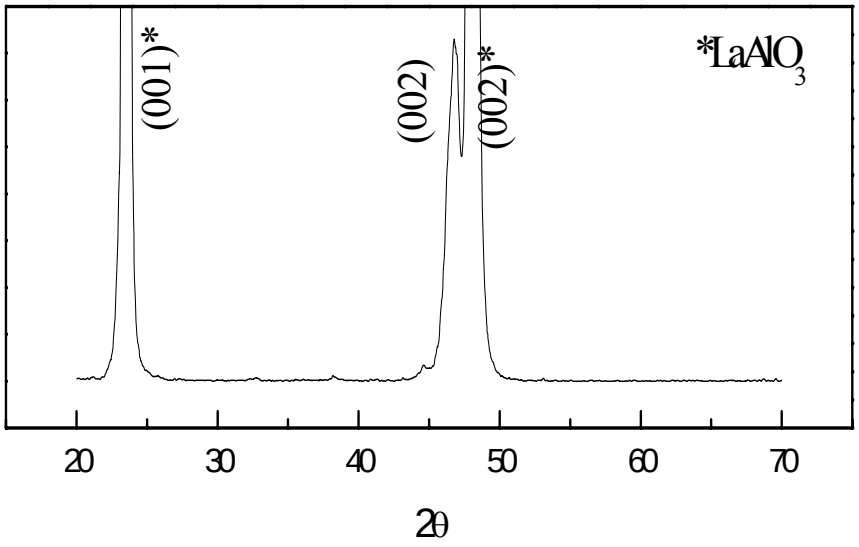

AFM - granular

R_{rms} = 3 nm

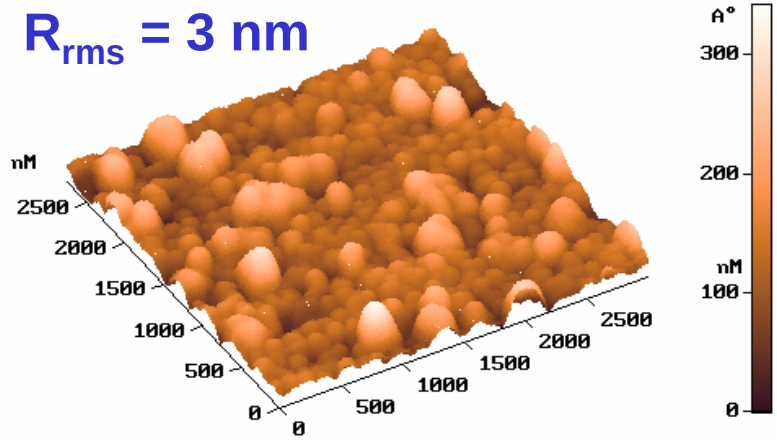

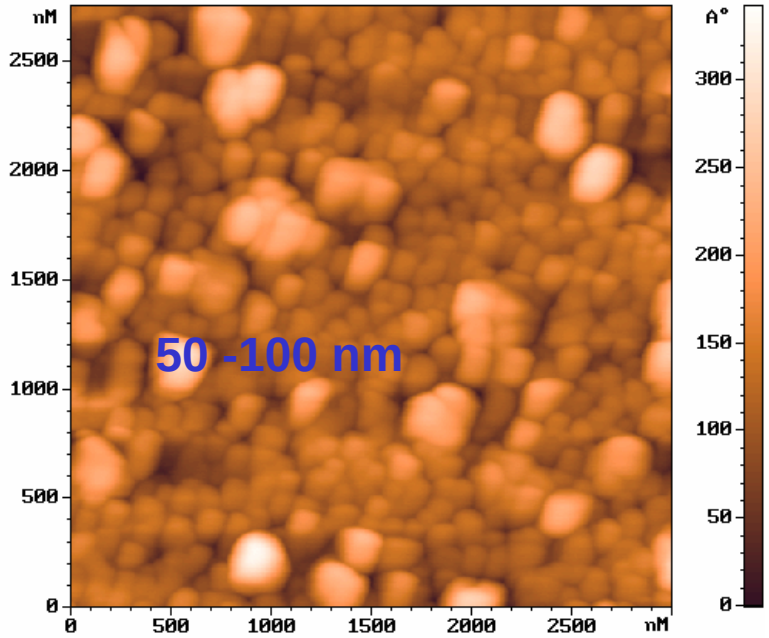

Magnetization for LSMO

H=500 Gauss

ZFC(black line); FC (red line)

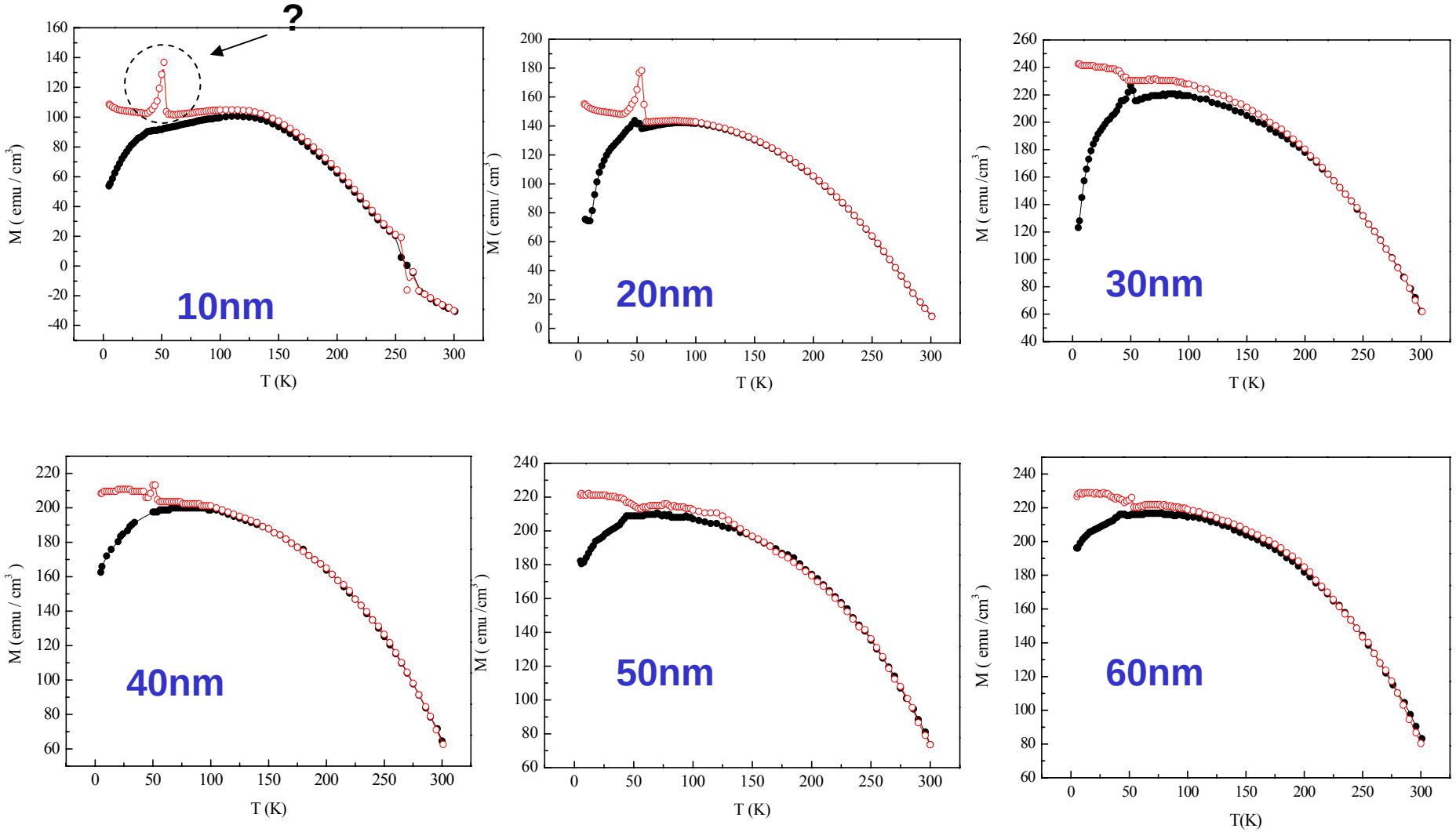

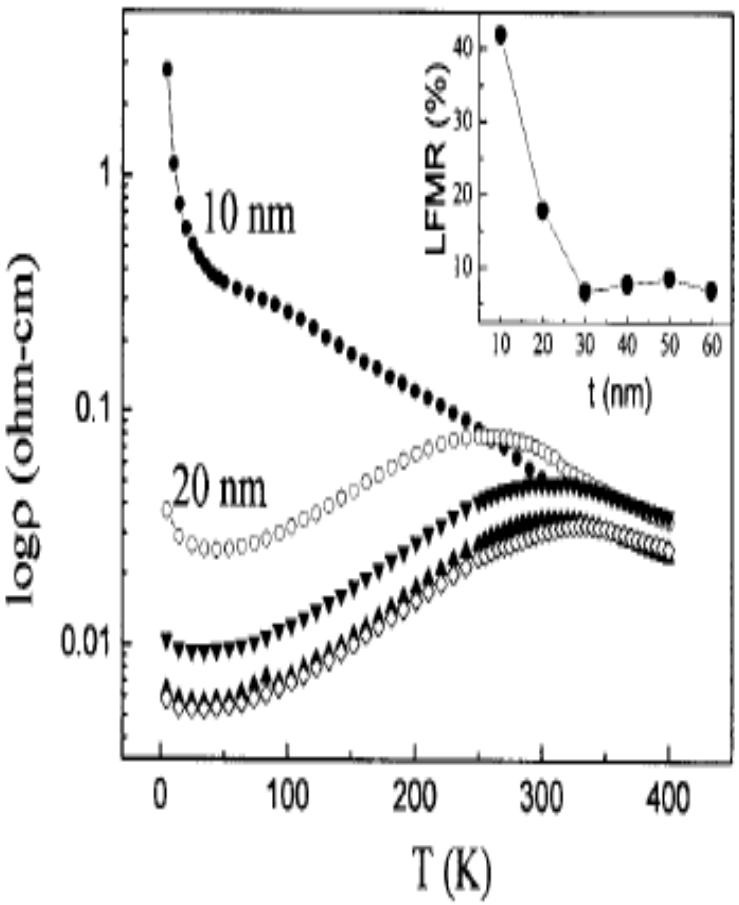
logρ (ohm-cm)
1
0.1
0.01
10 nm
20 nm
LFMR (%)
40
30
20
10
10 20 30 40 50 60
t (nm)
0 100 200 300 400
T (K)

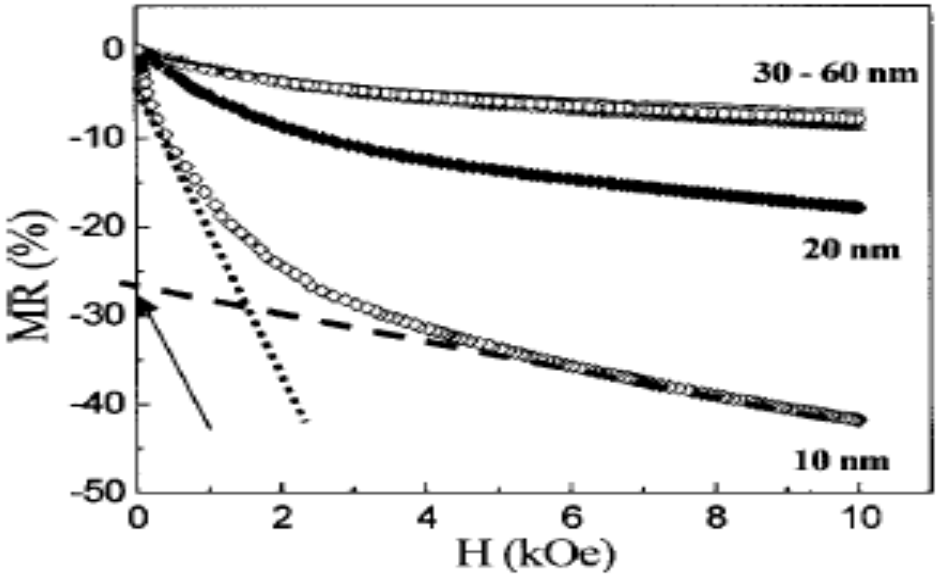
MR (%)
0
-10
-20
-30
-40
-50
30 - 60 nm
20 nm
10 nm
0 2 4 6 8 10
H (kOe)

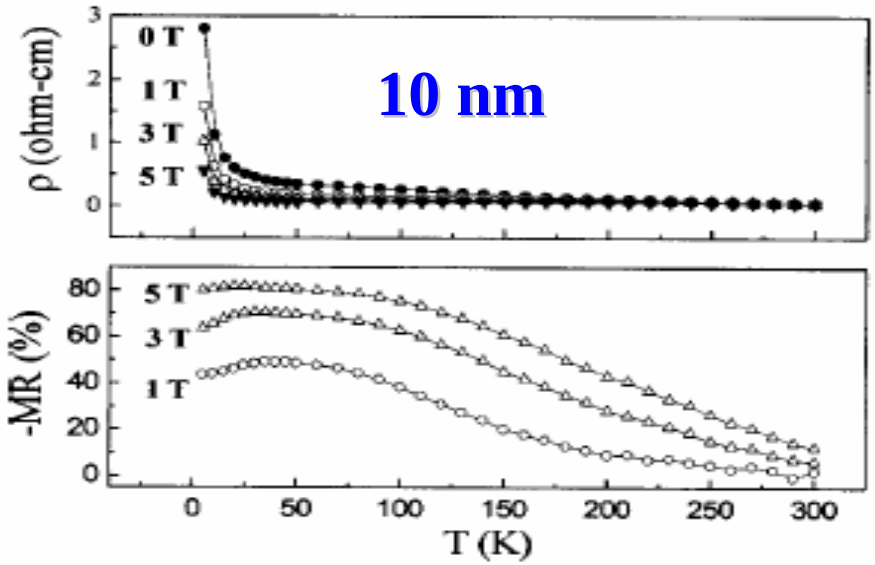
ρ (ohm-cm)
3
2
1
0
0 T
1 T
3 T
5 T
10 nm
-MR (%)
80
60
40
20
0
5 T
3 T
1 T
0 50 100 150 200 250 300
T (K)

PHYSICAL REVIEW B **67**, 064412 (2003)

Current-induced giant electroresistance in La0.7Sr0.3MnO3 thin films

A. K. Debnath* and J. G. Lin†

Center for Condensed Matter Sciences, National Taiwan University, Taipei 10617, Taiwan

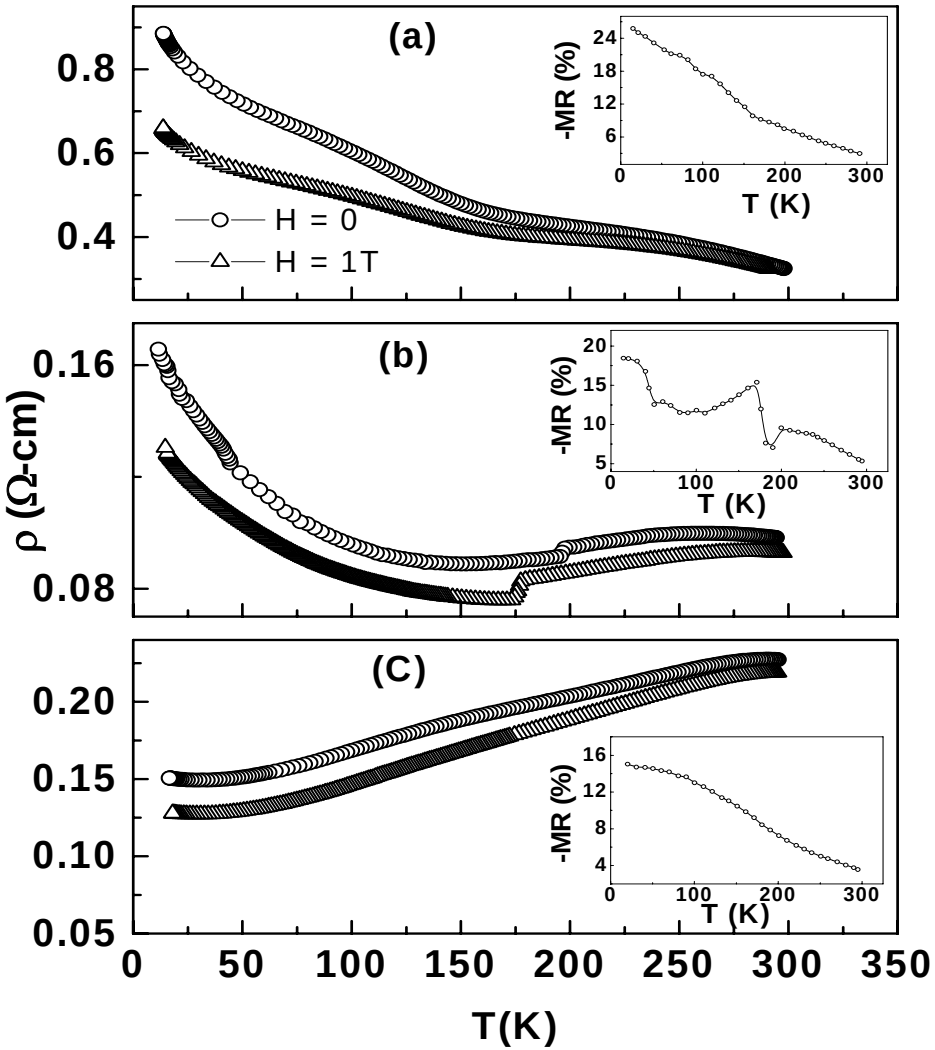

60 nm

80 nm

100 nm

PHYSICAL REVIEW B **67**, 064412 (2003)

Current-induced giant electroresistance in La0.7Sr0.3MnO3 thin films

A. K. Debnath* and J. G. Lin†

Center for Condensed Matter Sciences, National Taiwan University, Taipei 10617, Taiwan

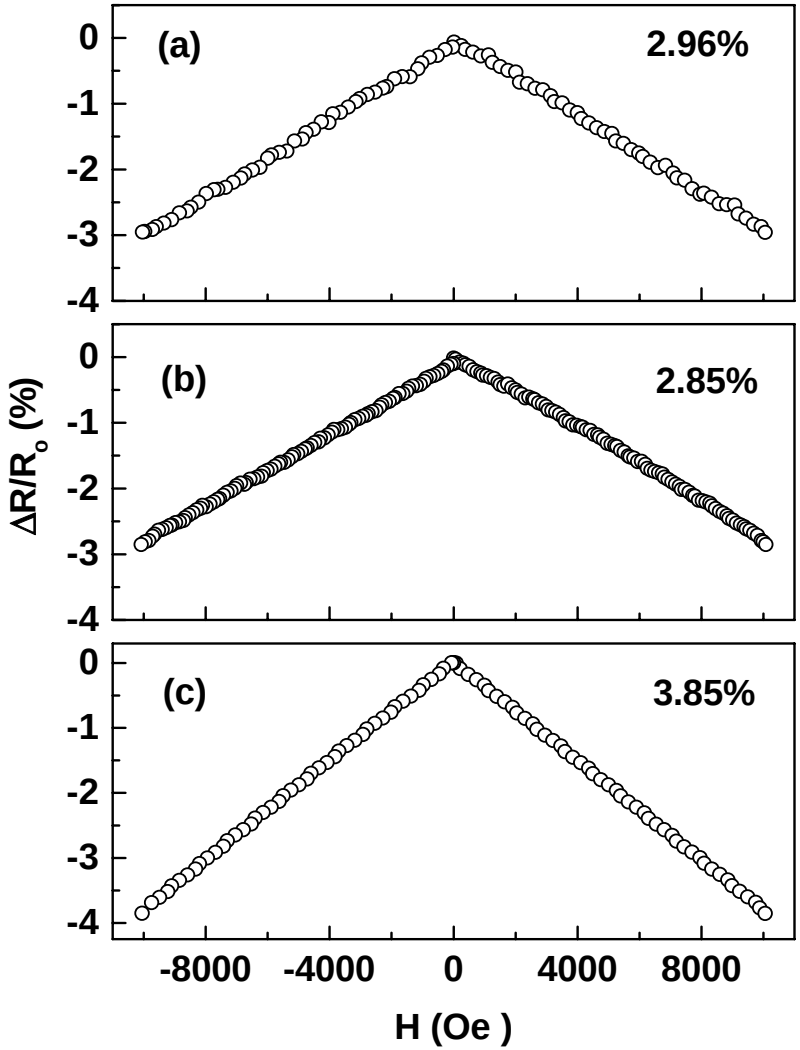

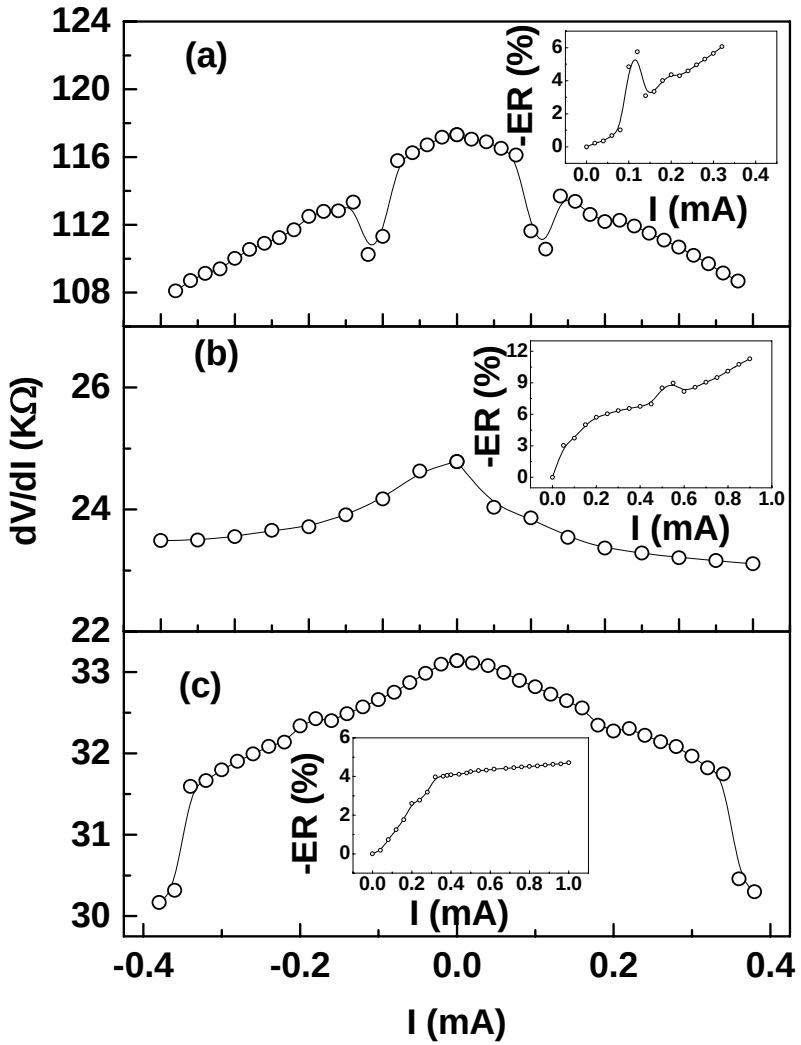

PHYSICAL REVIEW B **67**, 064412 (2003)

Current-induced giant electroresistance in La0.7Sr0.3MnO3 thin films

A. K. Debnath* and J. G. Lin†

Center for Condensed Matter Sciences, National Taiwan University, Taipei 10617, Taiwan

Current in nanowire of LSMO induced magnetic field, and the thermal energy delocalized the electrons.

thickness (nm)	MR_H (%)	MR_I (%)	ratio
60	2.96	5.6 (I = 0.3)	1.9
80	2.85	6.4 (I = 0.3)	2.3
		11.3 (I = 0.9)	4.0
100	3.85	3.5 (I = 0.3)	0.9
		4.6 (I = 0.9)	1.2

Topic (2): Nanocrystalline YBCO/LSMO bilayers

--- Proximity effect, spin injection & vortex pinning

Multilayer spintronic devices

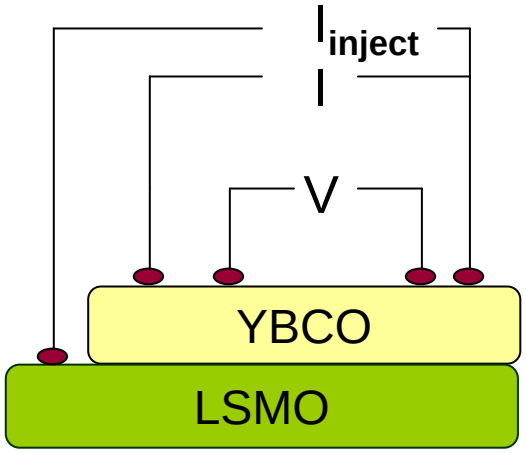

Spin-injection
I_c - depression

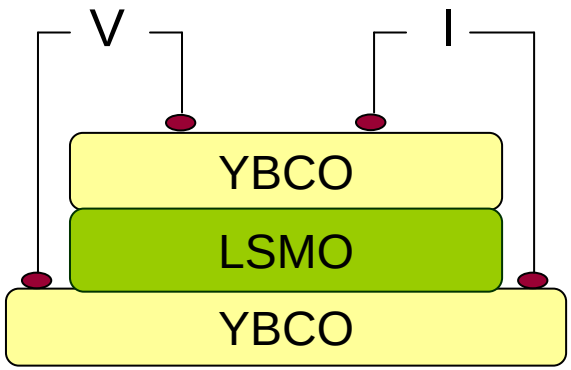

proximity effect
T_c - depression

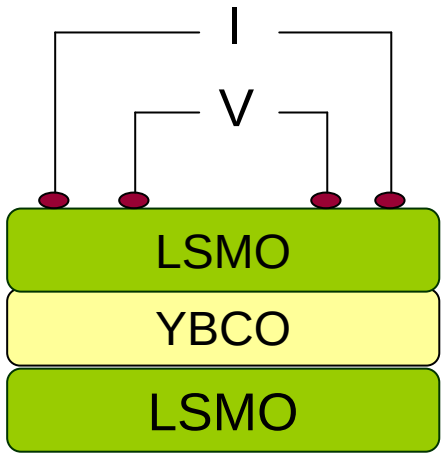

FM/N/FM structure
MR enhancement

Interesting topics on YBCO/LSMO

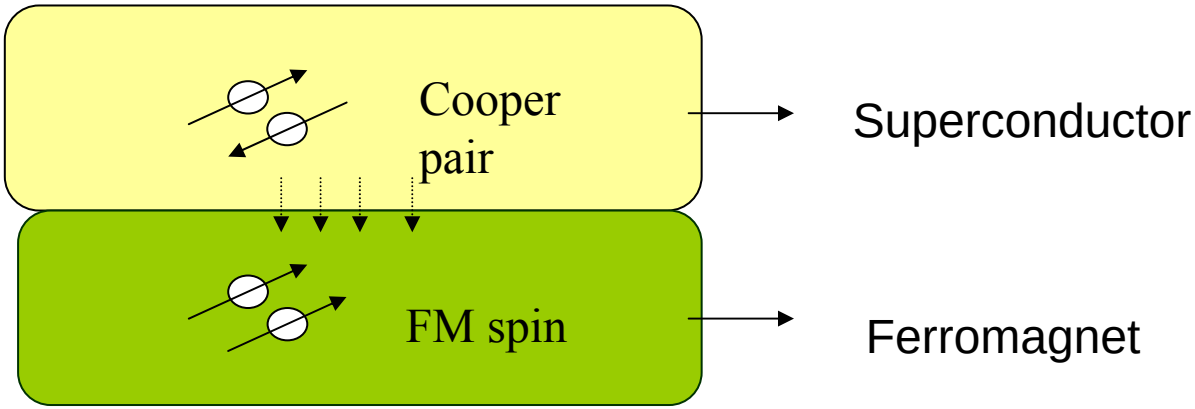

1) **Proximity effects**
2) **Andreev reflection**
3) **Spin injection**
4) **Spin-accumulation**
5) **π –phase shift**

Proximity effect

1) Influence of magnetism on supercond.

Intermixing $\Rightarrow$ effective exchange field

$H_{effect} = H_{ex}\,[d_F/(d_s+d_F)]$, **$T_c$ oscillation**

2) Influence of supercond. on magnetism

Intermixing $\Rightarrow$ reconstruction of magnetic order

T_{curie} oscillation

Spin-injection

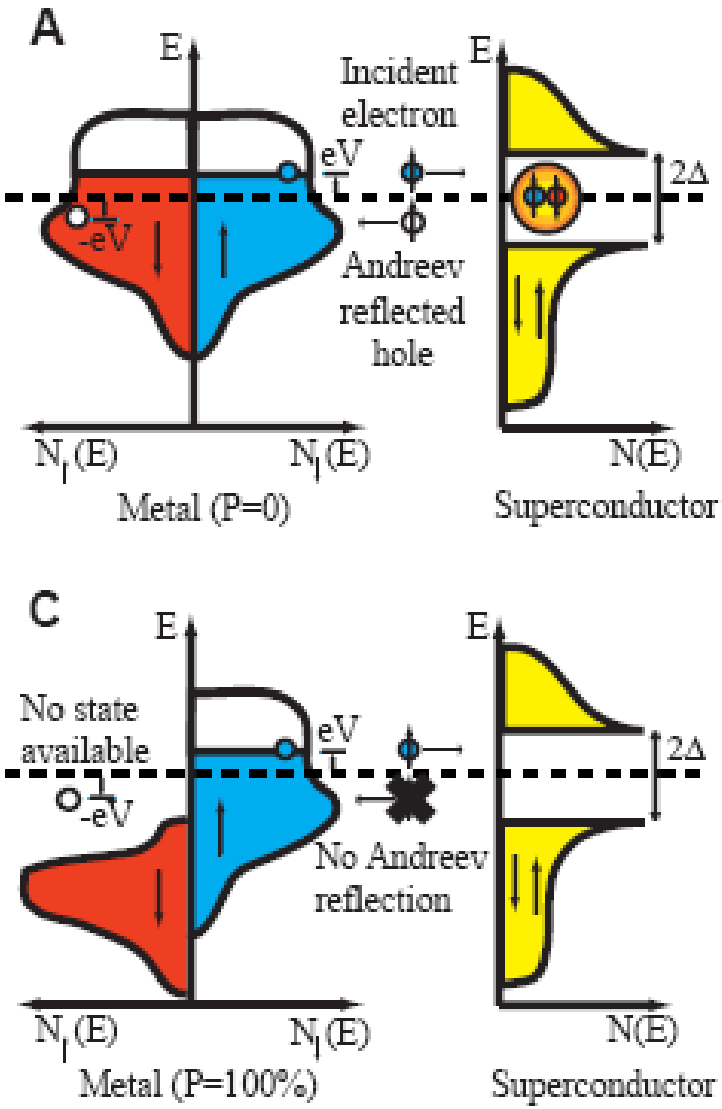

- Normal electron injected to superconductor will be reflected as a hole;
- Polarized electron injected into superconductor will kill a Cooper pair.

SCIENCE VOL 282 2 OCTOBER 1998

Superconductor: $RBa_2Cu_3O_7$, R = Y or rare earth element

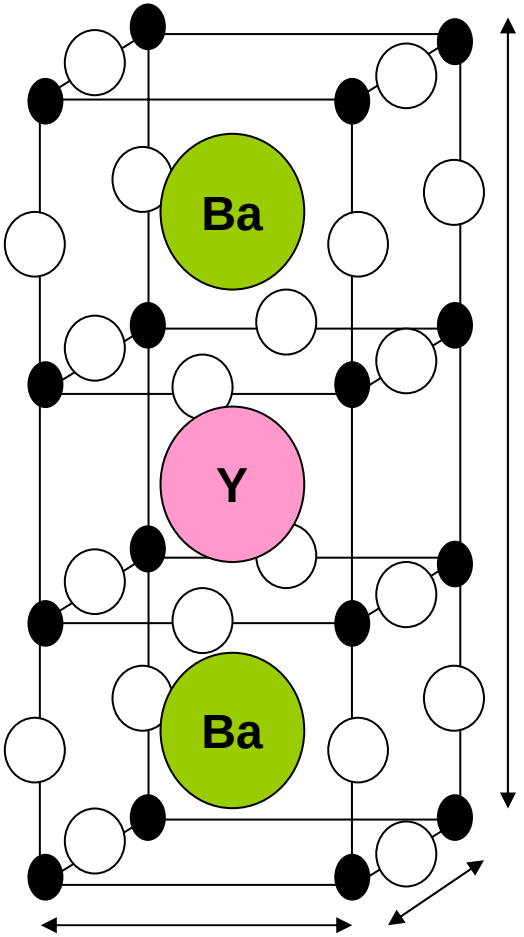

- $YBa_2Cu_3O_7$ ξ_S ~ 3-10 nm
- Critical parameter T_c = 90 K, H_{c2} ~ 165 T
- SQUID, Bolometer, Filter, Resonator…

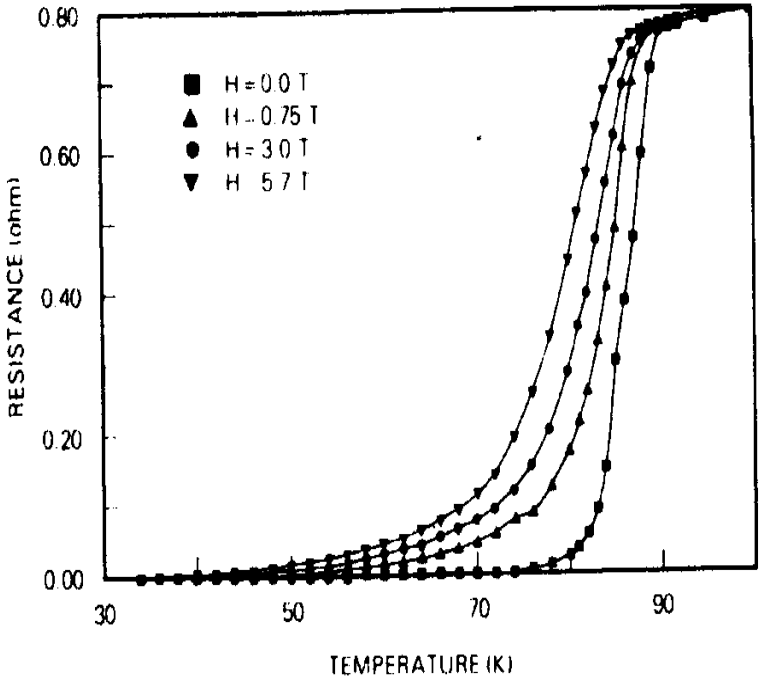

Wu, Chu et al., PRL (1987)

Half metal: $(R,Ca)MnO_3$, R = La, Nd, Pr….

- Ferromagnetic with 90 % polarization for LCMO. ξ_M ~ 10 -15 nm
- Colossal magnetoresistance (CMR)
- Sensor, pick-up head, MRAM

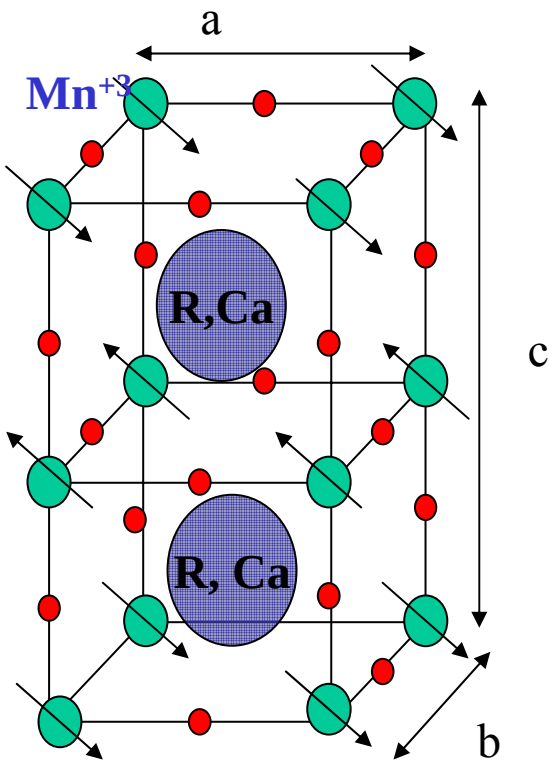

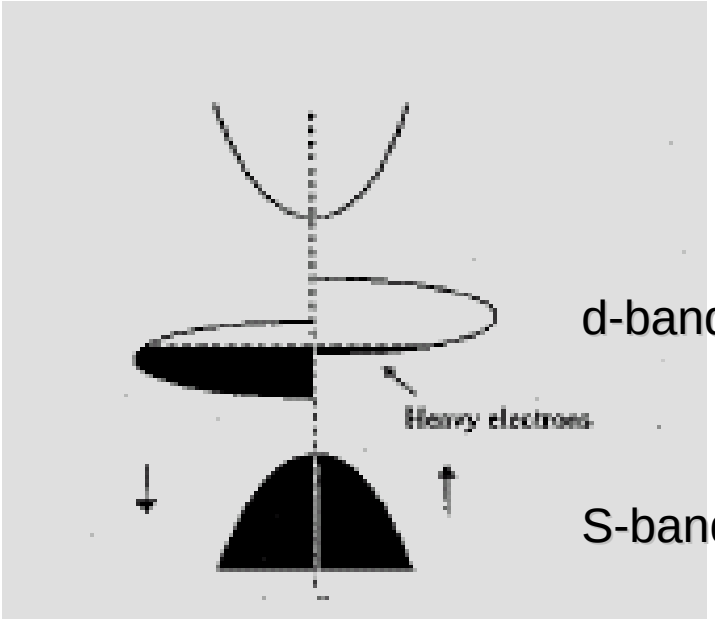

Jin et al, Science (1995)

Vortex pining device

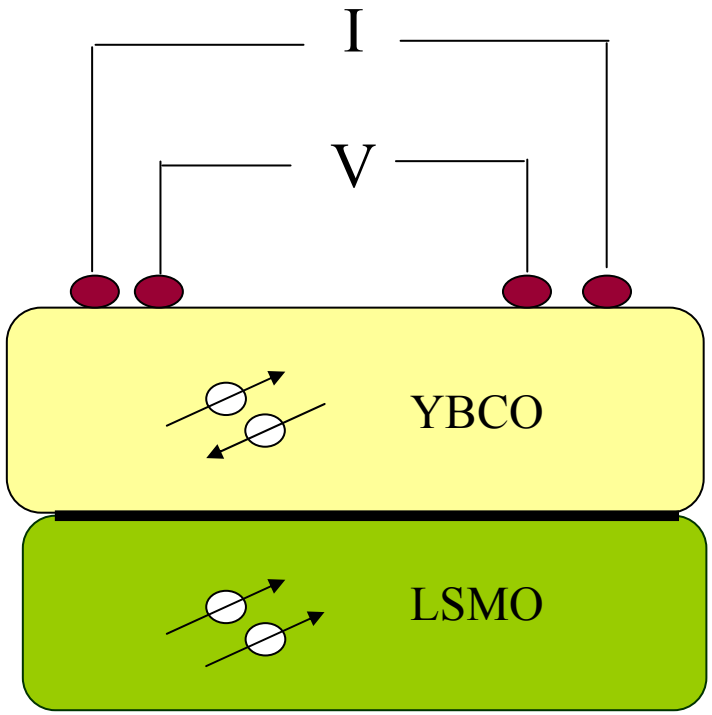

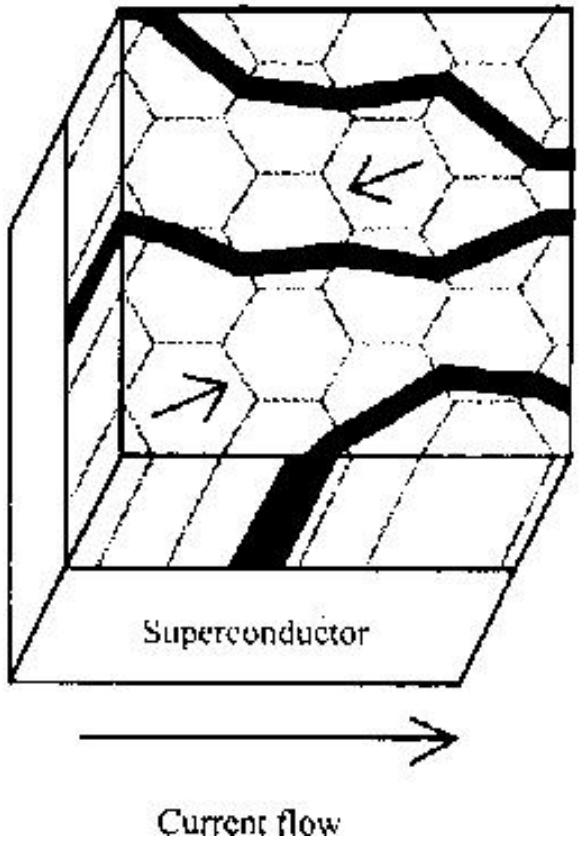

Available online at www.sciencedirect.com
SCIENCE DIRECT®
Physica C 437–438 (2006) 187–189
PHYSICA C
www.elsevier.com/locate/physc

High field pinning-effects in $YBa_2Cu_3O_7/La_{0.7}Sr_{0.3}MnO_3$ nanocrystalline bilayers

J.G. Lin [a,b,*], S.L. Cheng [b]

[a] *Center for Condensed Matter Sciences, National Taiwan University, Taipei 106, Taiwan*
[b] *Center for Nanostorage Research, National Taiwan University, Taipei 106, Taiwan*

Available online 26 January 2006

I-V characteristic

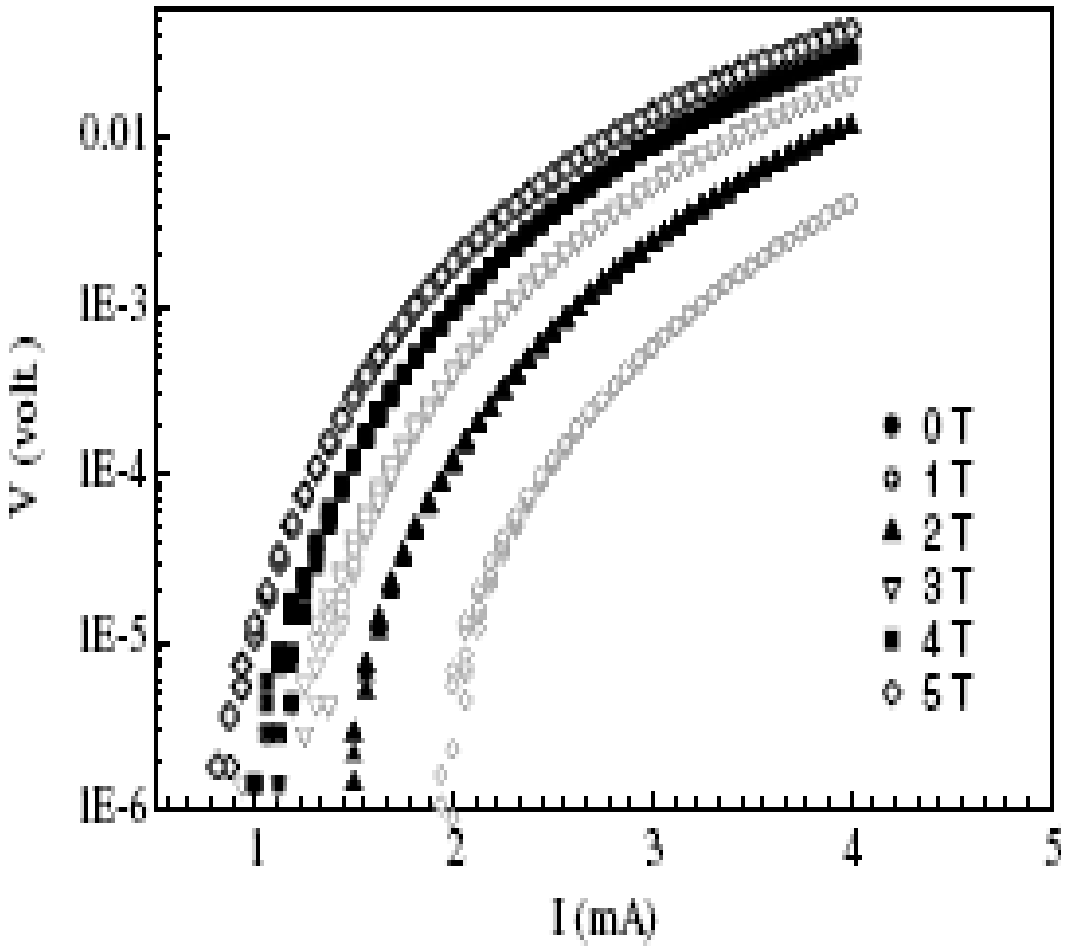

Critical current I_C

Normal state resistance Rn

Energy gap Δ

Ic = I(V=1 μV)

$I_C Rn = \pi \Delta / 2$

$= 3.52 \pi K_B T_C / 4$

I- V Characteristic (1.9 K)

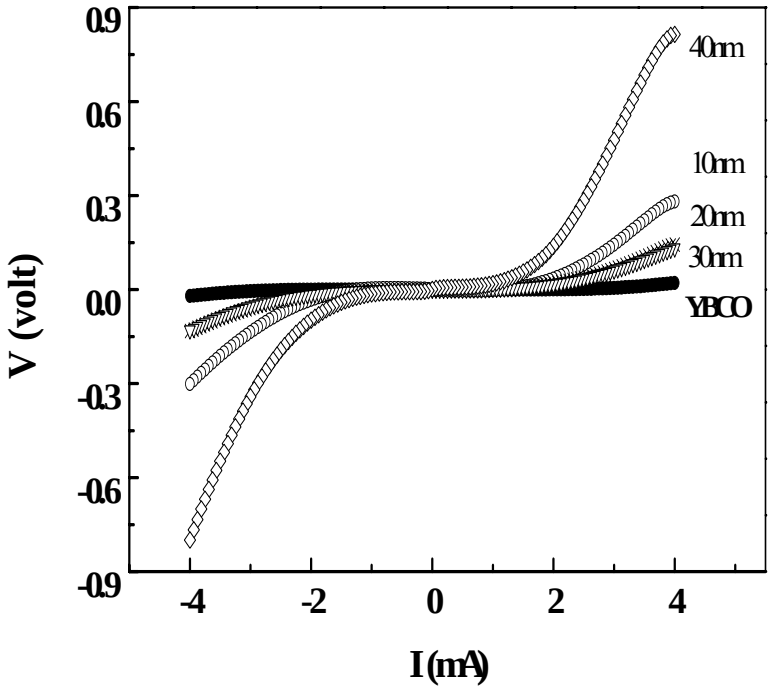

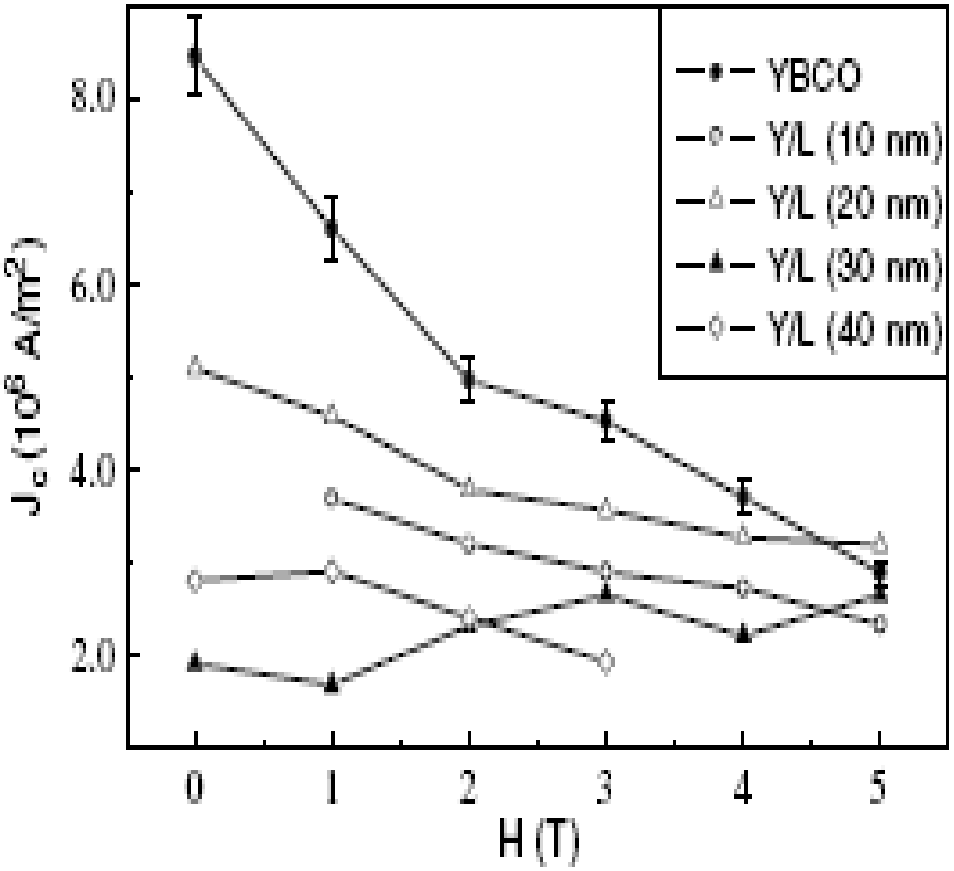

Ic decreases with increasing thickness of LSMO

Subject (3): Epitaxial YBCO/NCMO bilayers

--- **How the superconductivity is affected by weak ferromagnetic insulator ?**

Low-current-induced electrical hysteresis in $Nd_{0.7}Ca_{0.3}MnO_3$

Daniel Hsu
Center for Condensed Matter Science, National Taiwan University, Taipei 106, Taiwan; Center for Nanostorage Research, National Taiwan University, Taipei 106, Taiwan; and Institute of Mechanical Engineering, National Taiwan University, Taipei 106, Taiwan

J. G. Lin[a)]
Center for Condensed Matter Science, National Taiwan University, Taipei 106, Taiwan and Center for Nanostorage Research, National Taiwan University, Taipei 106, Taiwan

W. F. Wu
Institute of Mechanical Engineering, National Taiwan University, Taipei 106, Taiwan

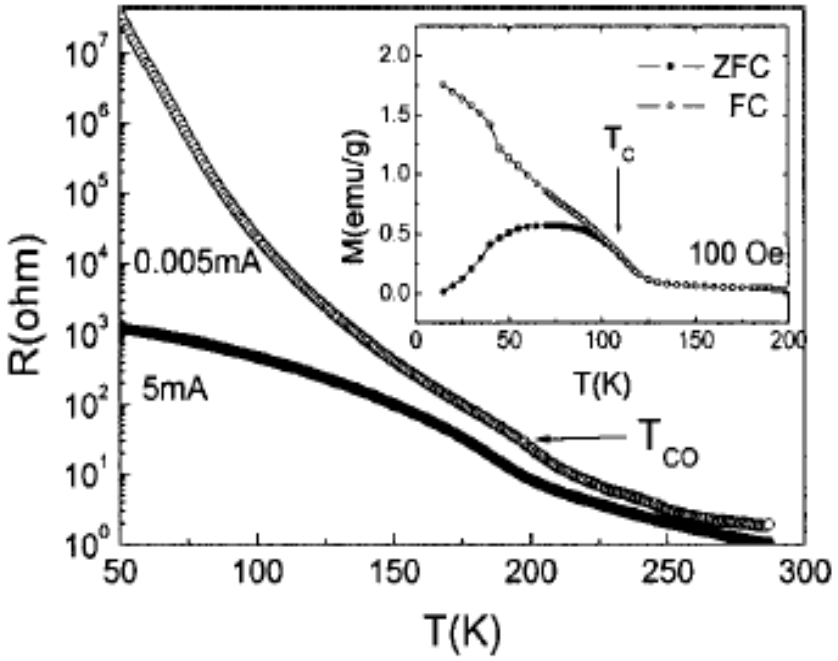

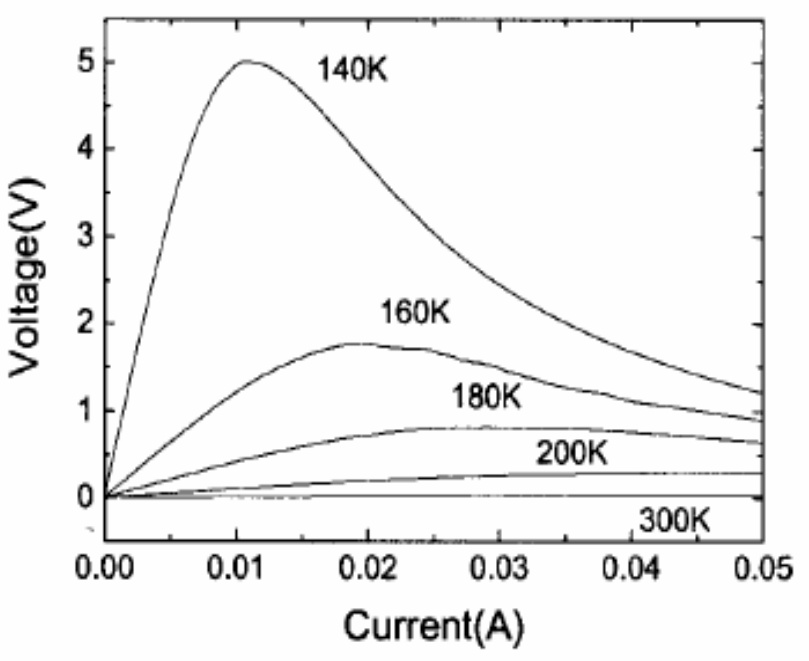

Substrate criteria

1. Atomically flat
2. Chemically comparable
3. Well lattice mismatch

   For YBCO, $LaAlO_3$ (100) is ~ 0.4%;

   $SrTiO_3$(100) is 0.2% for *a*-parameter, 0.3% for *b*-parameter;

   $NdGaO_3$ (110) is 0.7 % for *a*- and *b*-parameters

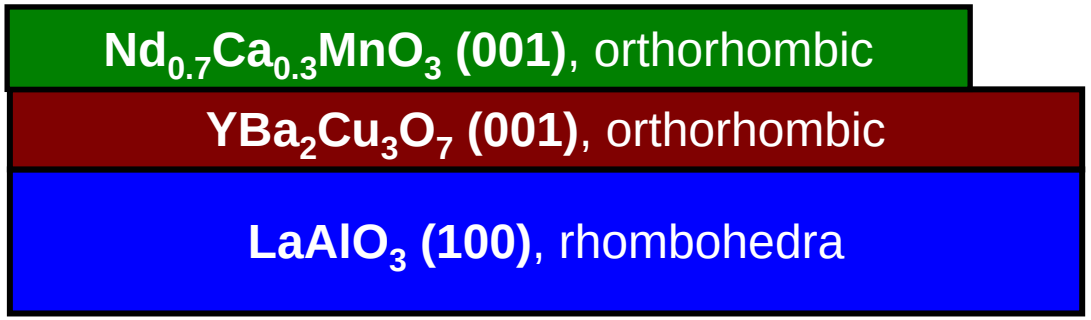

$LaAlO_3$

a=b=c=3.79 Å

α=β=γ=90.12°

o-$YBa_2Cu_3O_7$

a=3.82 Å, b=3.85 Å,

c=11.63 Å; α=β=γ=90°

o-$Nd_{0.7}Ca_{0.3}MnO_3$

a=5.42 Å, b=5.46 Å,

c=7.72 Å;α=β=γ=90o

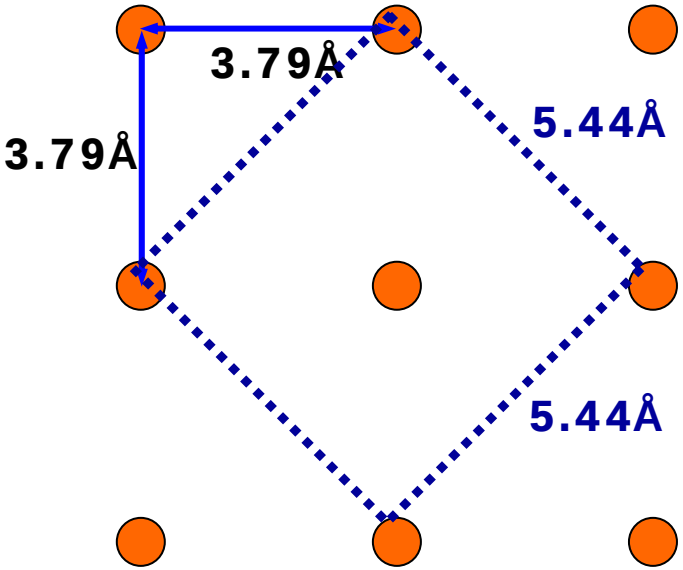

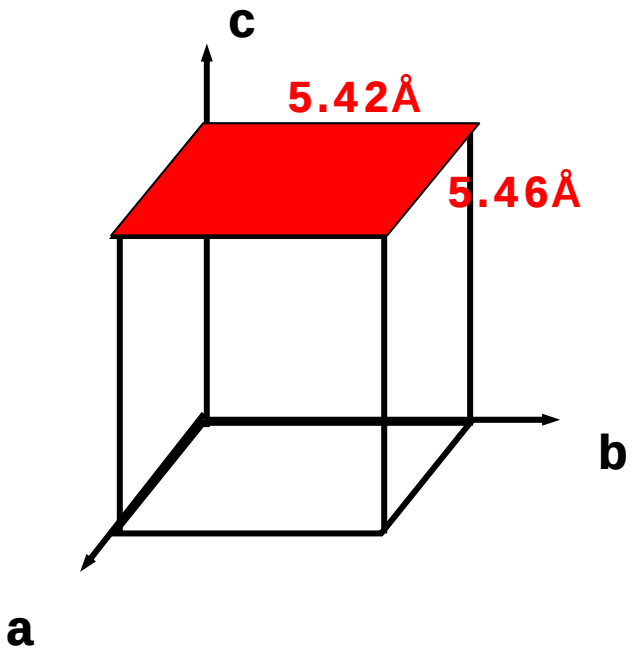

Pulse-Laser-Deposition system –Neocera 180

KrF Laser (248 nm)

Focus Len

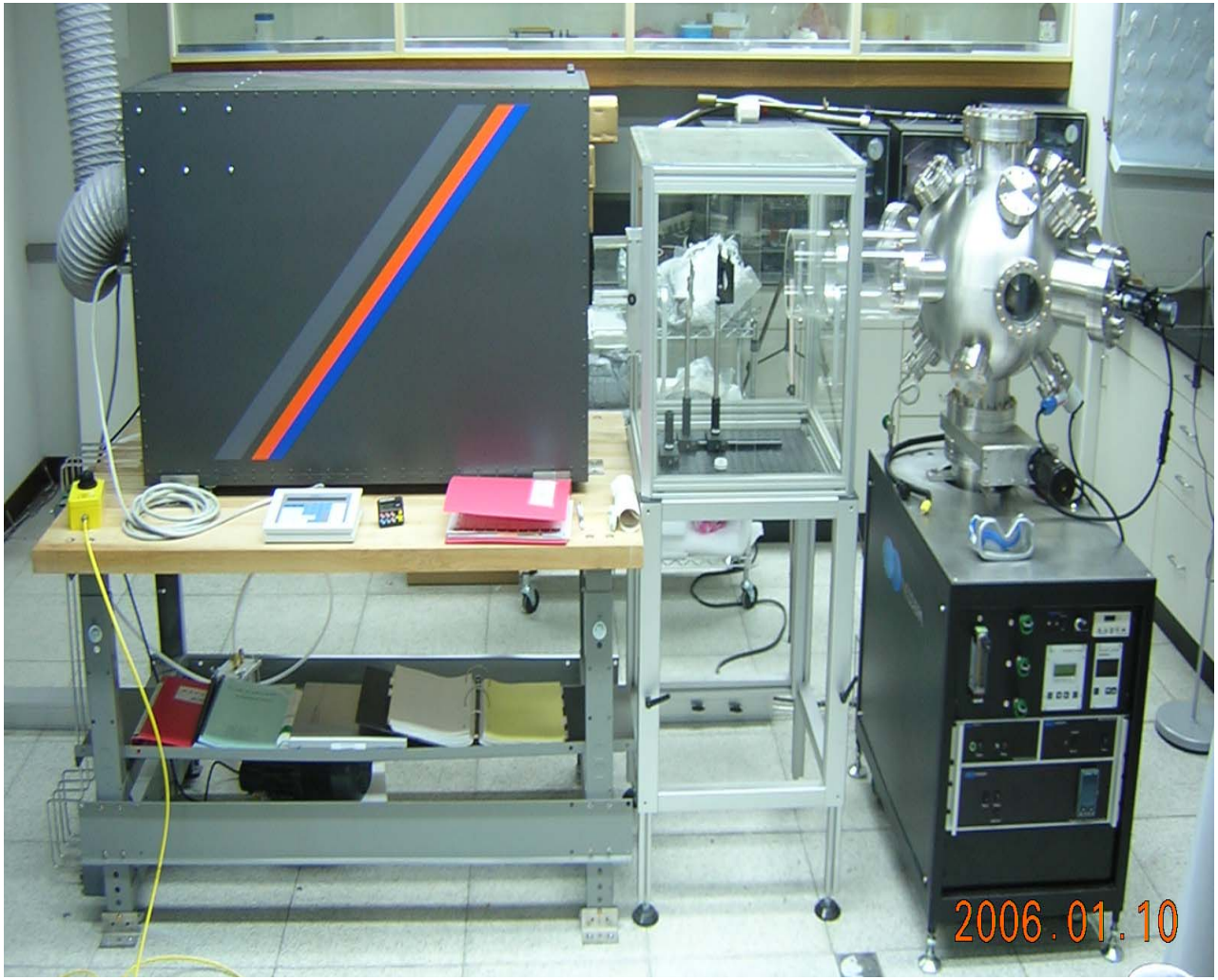

Chamber

10^{-8} torr

Pump
Flow meter
Vacuum gauge

Pulse-Laser Deposition system (II) - Chamber

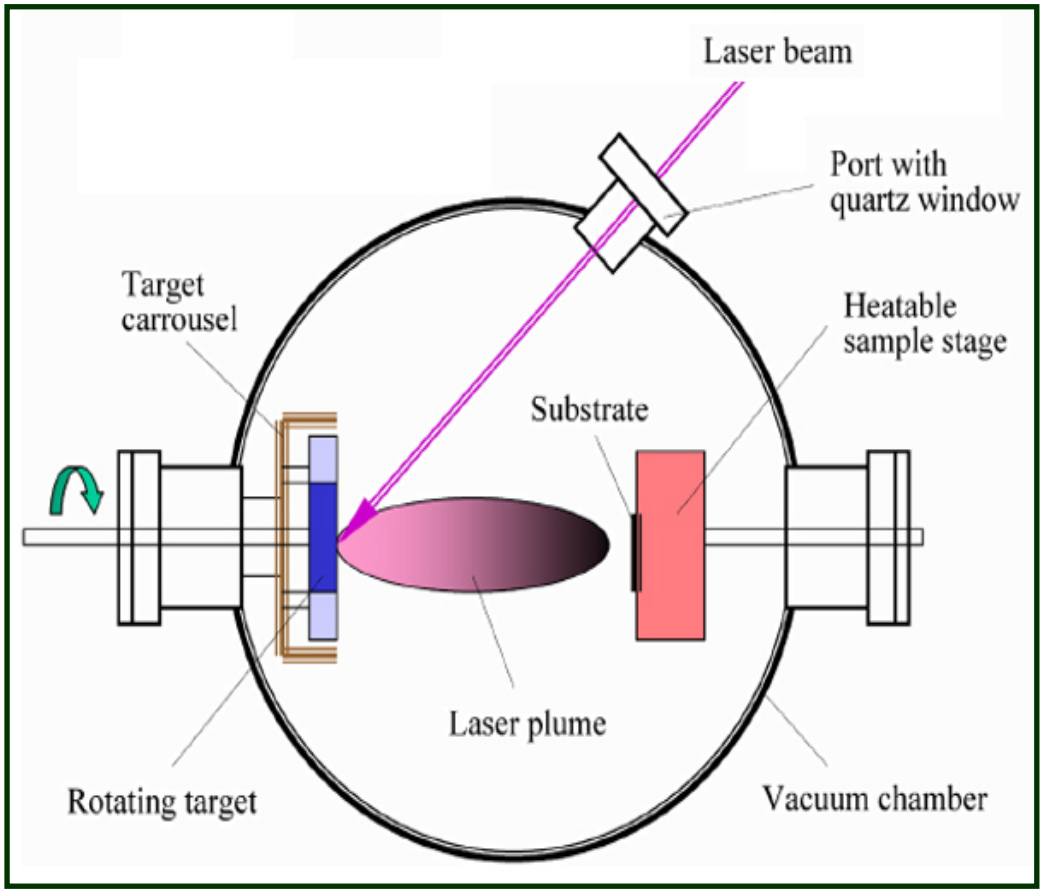

YBCO

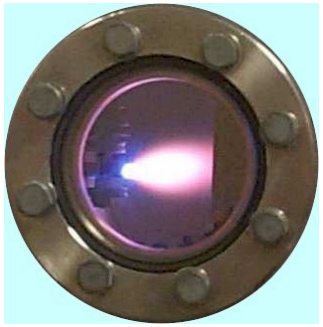

NCMO

NCMO/YBCO heterostructure

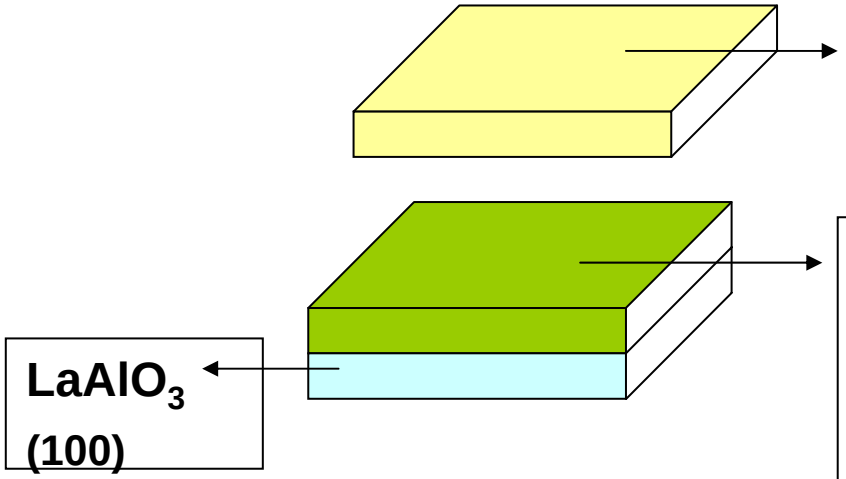

$Nd_{0.7}Ca_{0.3}MnO_3$, (40 -350 nm)

780°C for 1 hour in 50 mtorr O_2

$YBa_2Cu_3O_7$(100-600 nm)

850 °C for 1 hour

400 °C for 6 hours

in 300 mtorr O_2

$LaAlO_3$ (100)

X-ray Diffraction Patterns & TEM image

- Both NCMO & YBCO are with c-axis perpendicular to the film surface

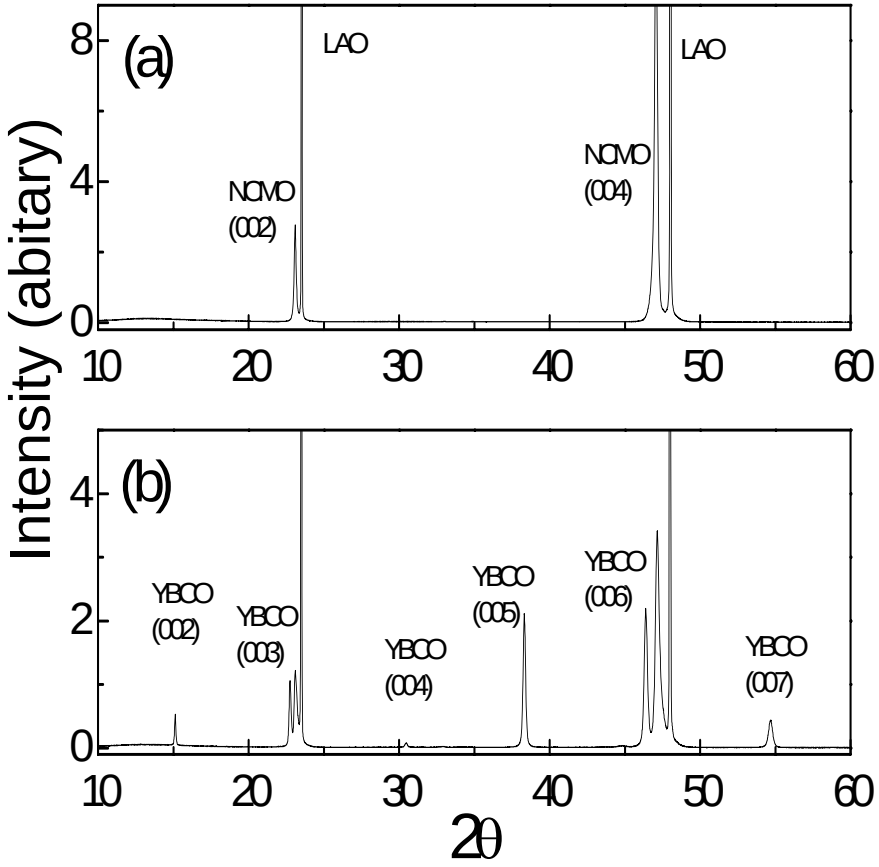

- Epitaxial growth along [001]

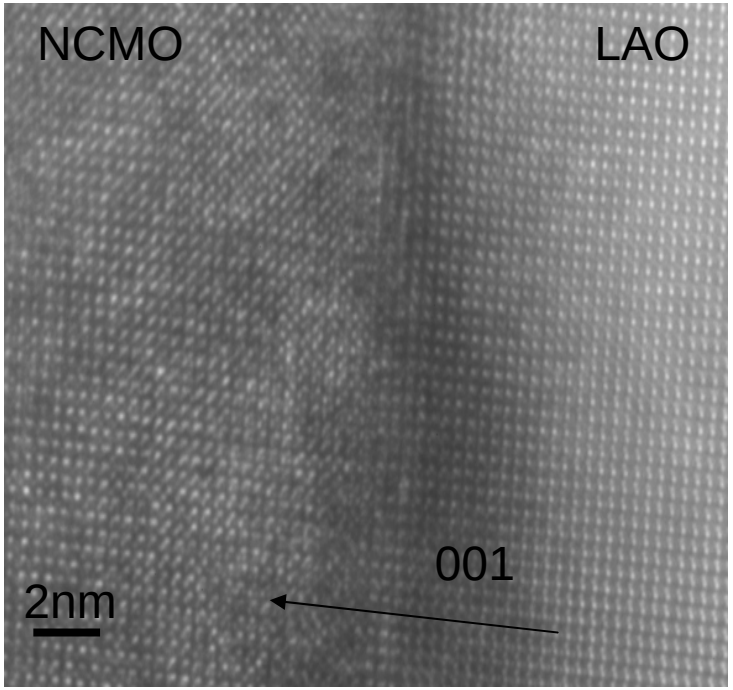

Basic characterization

(High resolution TEM & electron diffractions)

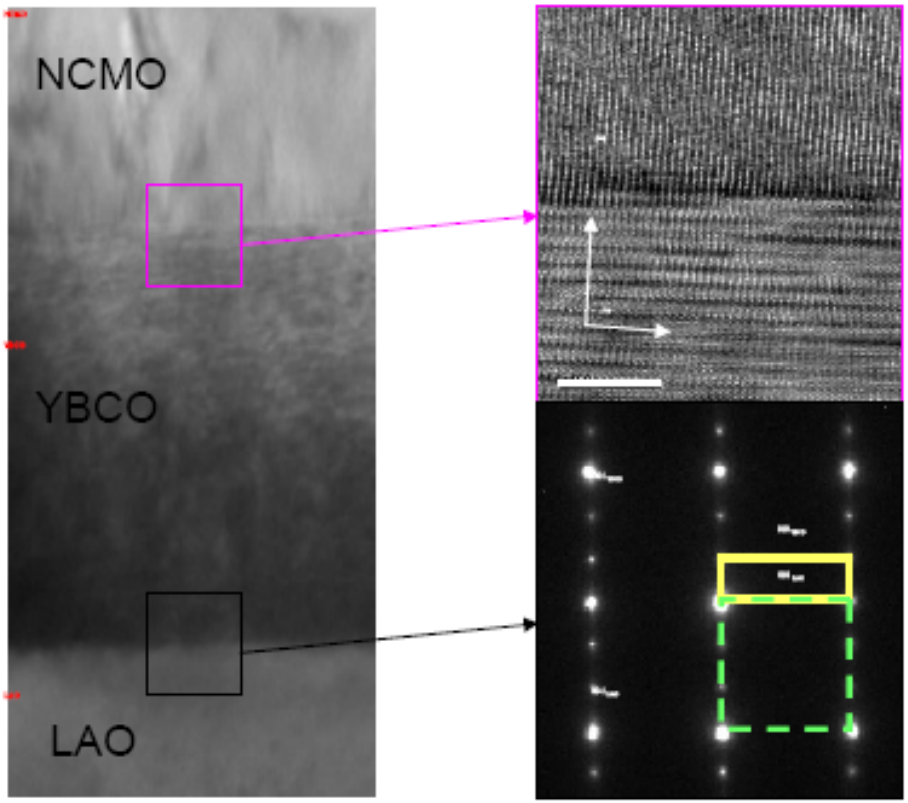

(Scanning EDX)

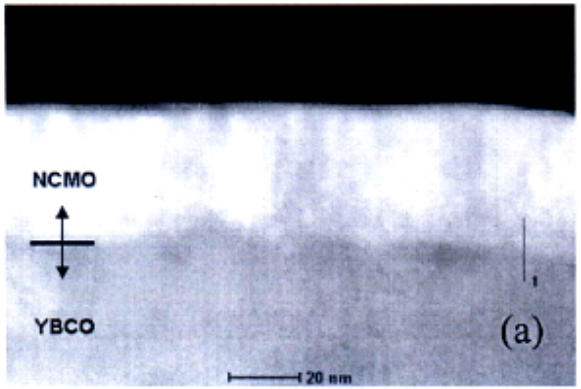

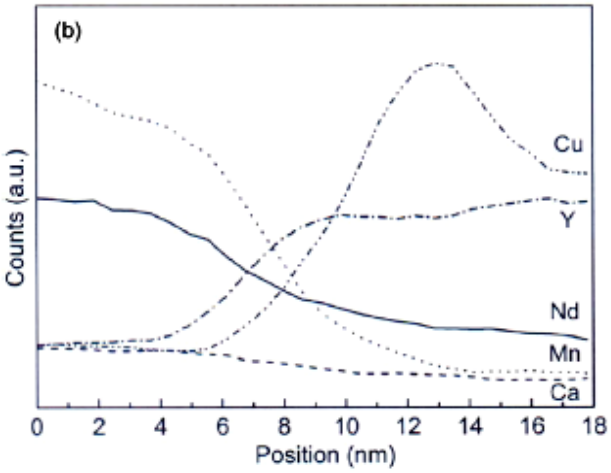

Magnetization(M) vs. Temperature (T) – by SQUID

- T_c is 88 K for YBCO; T_N is ~ 75 K for NCMO; Both transition temperature do not change in NCMO(40nm)/YBCO(160nm).

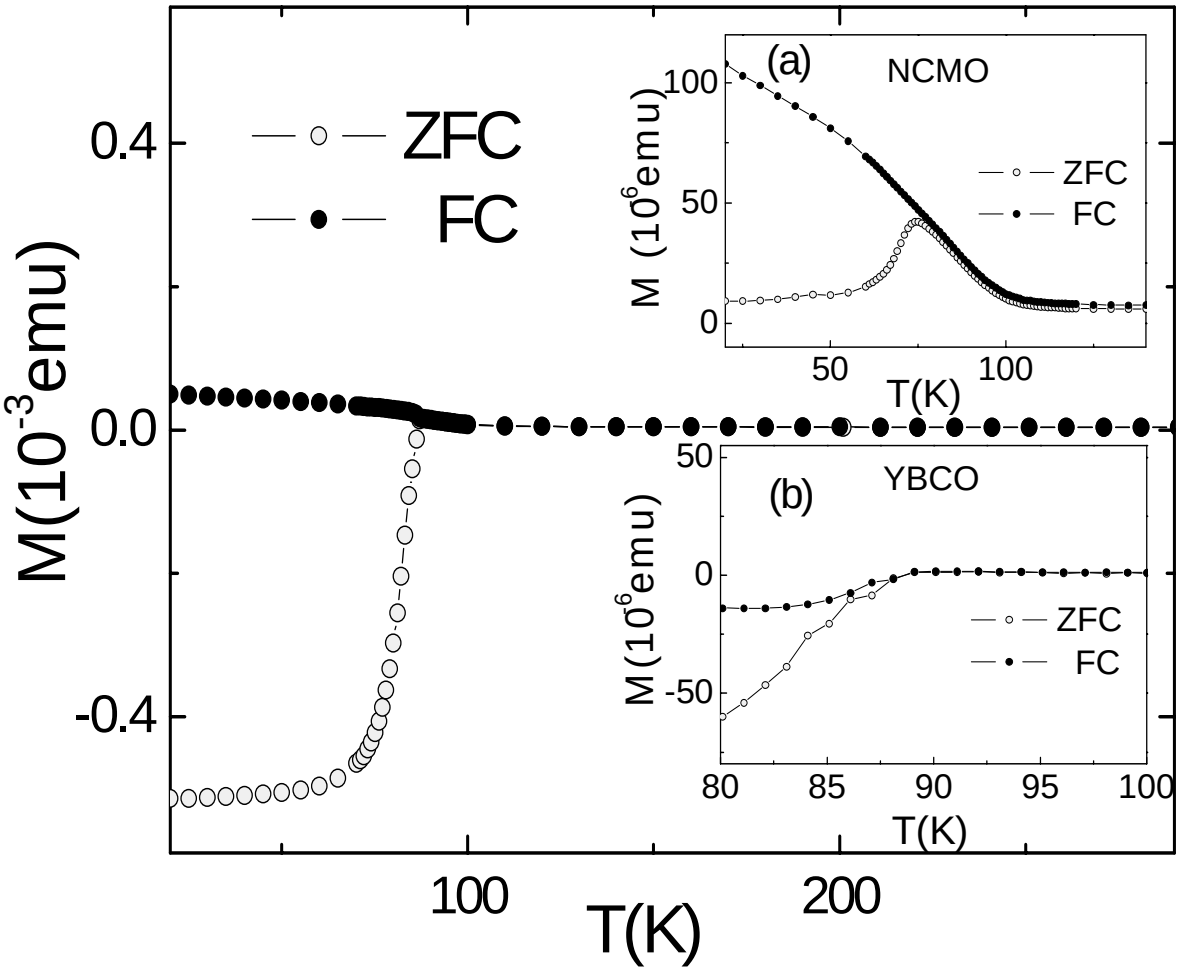

4-Probe method

- YBCO : T_c ~ 88 K & ΔT < 2 K; NCMO: Insulating

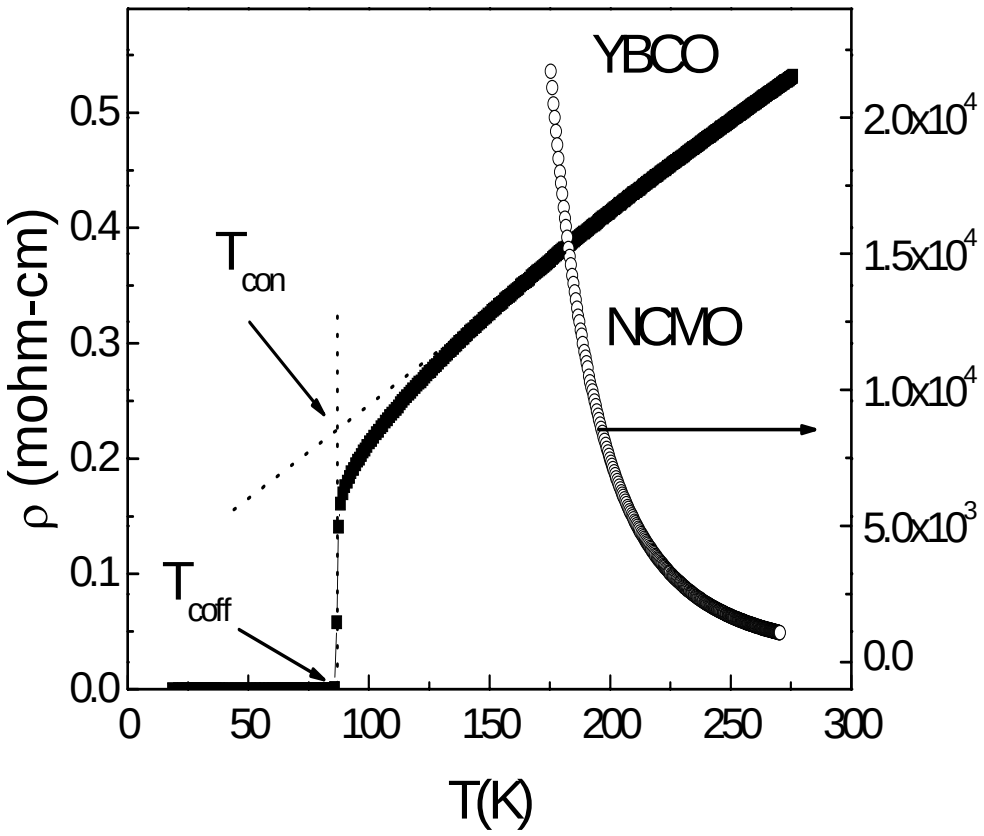

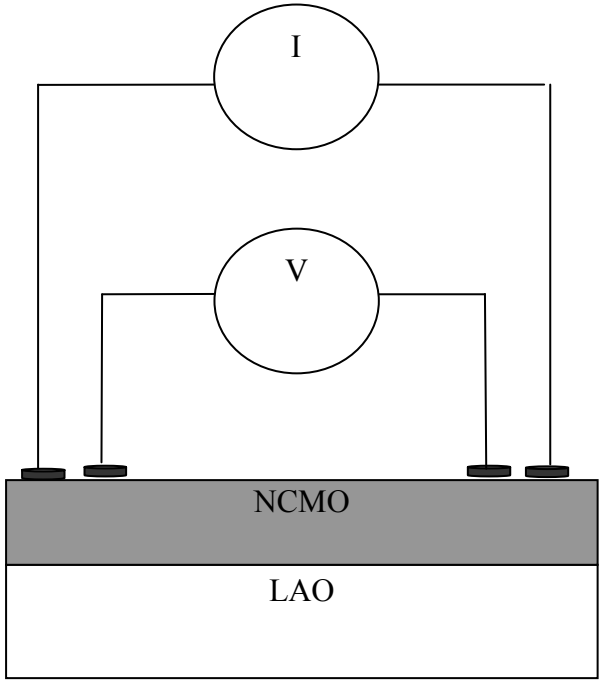

Resistivity (ρ) vs. Temperature (T)

- For I_a = 1 – 90 mA, normal state increases & T_c drops with a rate 0.1K/mA.
- open a gap at 230 K ?

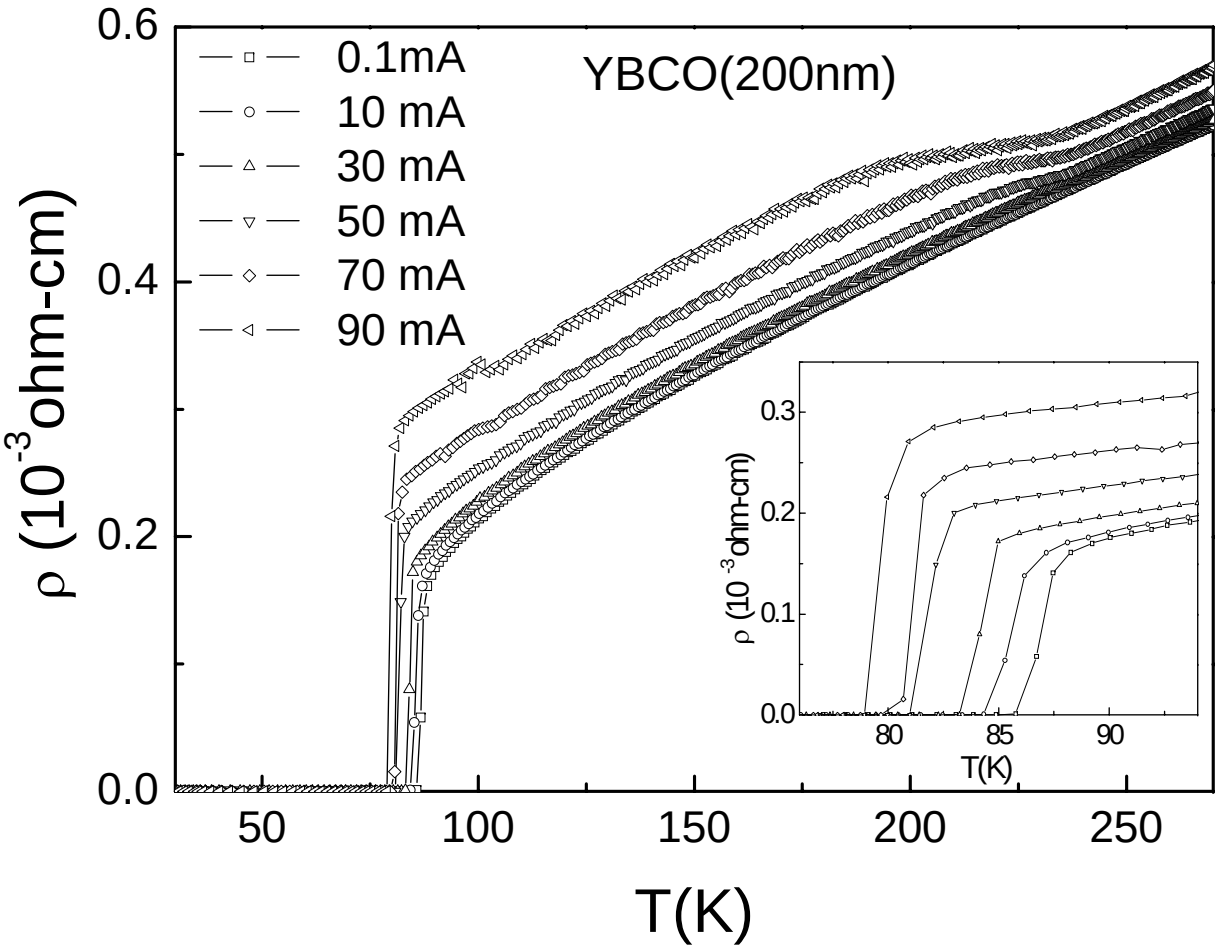

Resistivity (ρ) vs. Temperature (T)

- For I_a = 5 – 30 mA, resistivity decreases.

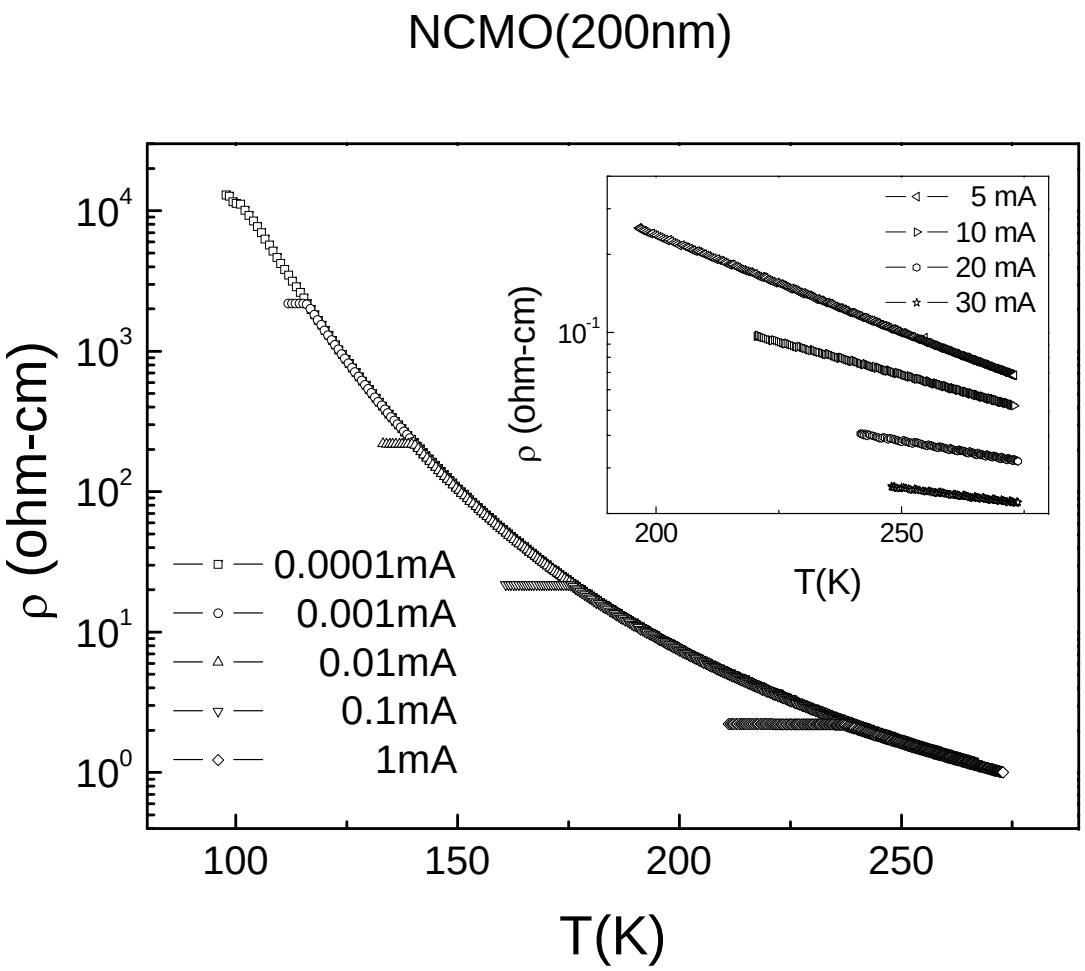

Resistivity (ρ) vs. Temperature (T)

NCMO(200nm)/YBCO(200nm)

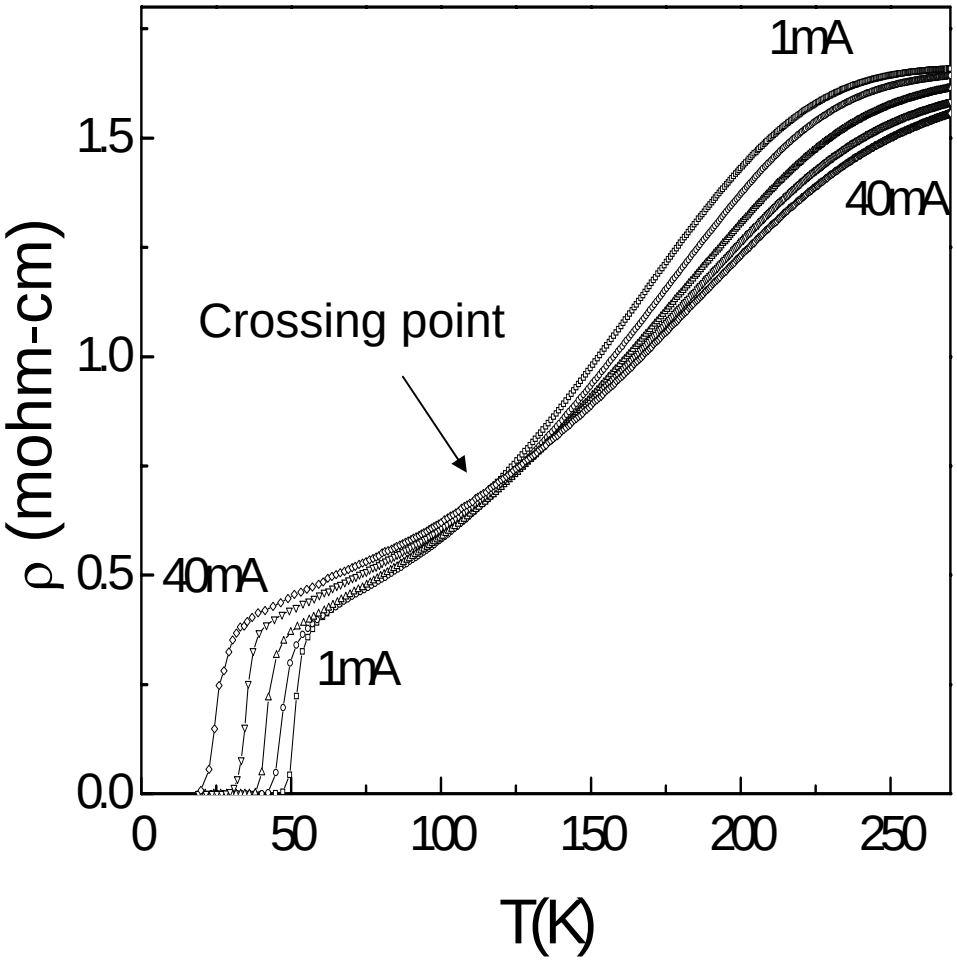

- For I_a = 1 – 40 mA, normal state increases & T_c drops with a rate of 1.0 K/mA.

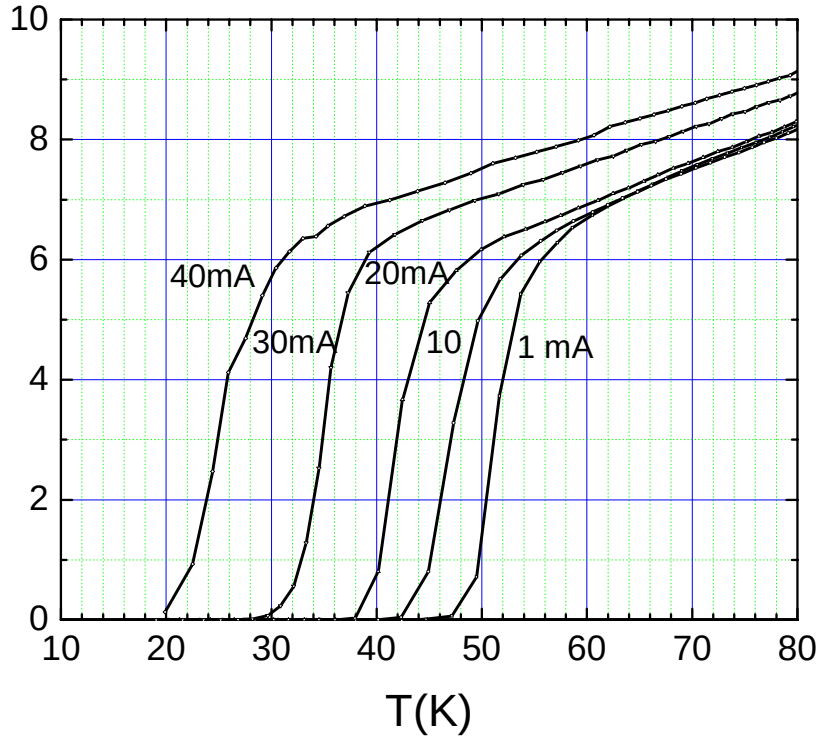

Resistivity (ρ) vs. Temperature (T)

- For I_a = 1 – 40 mA, normal state decreases 30% & T_c drops with a rate of 1.4 K/mA.

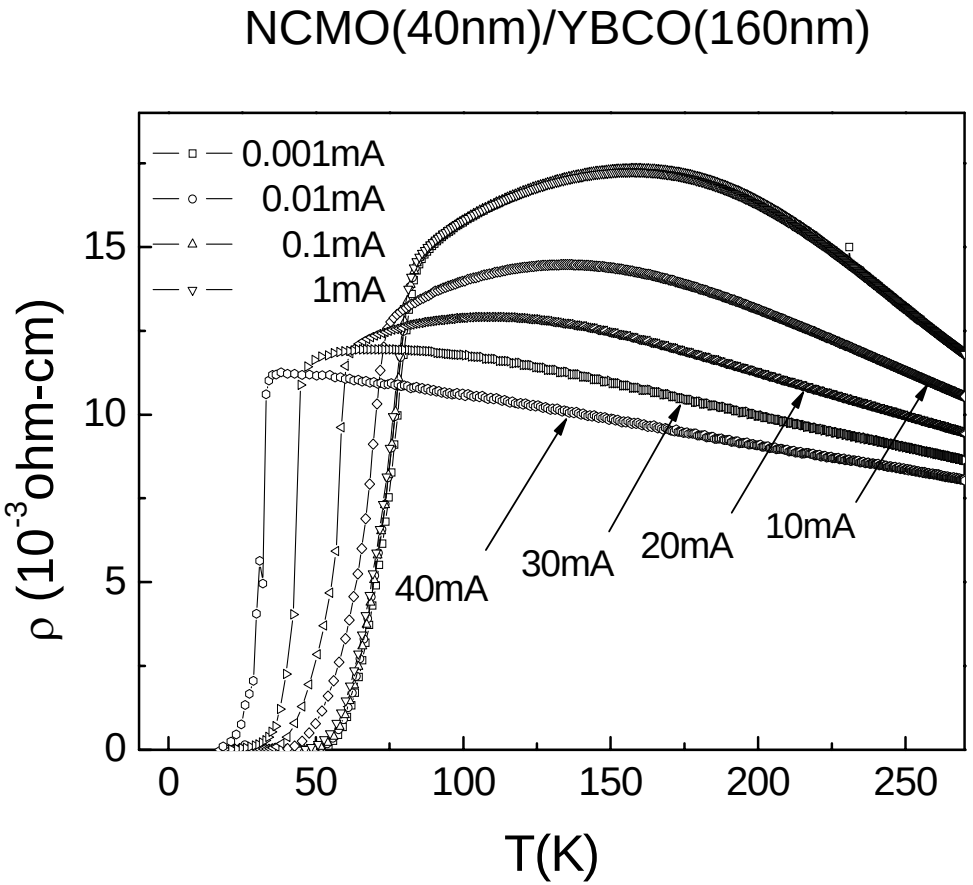

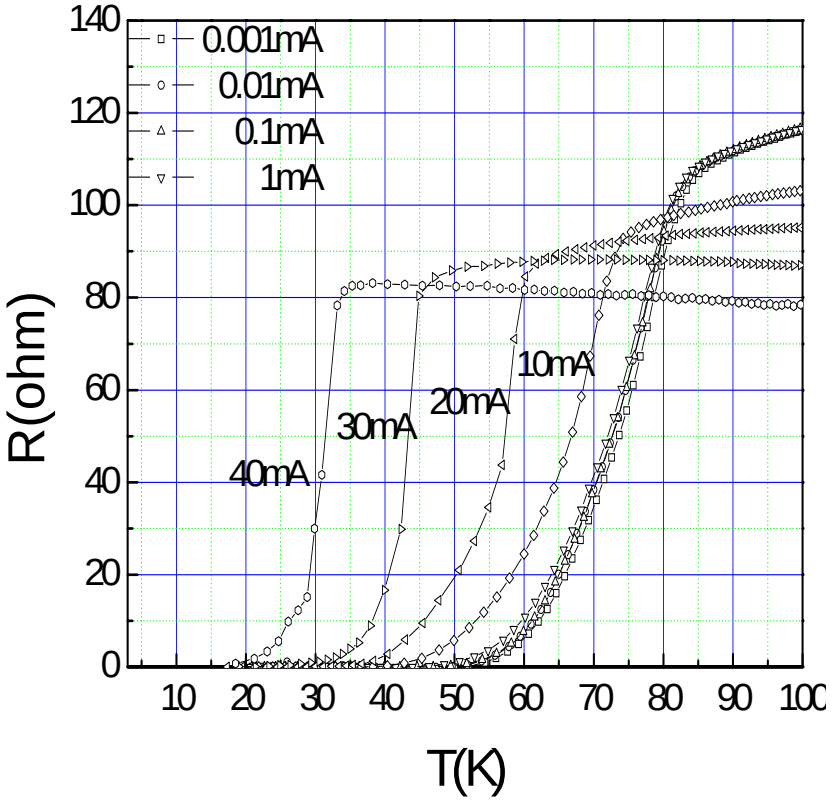

Superconducting temperature vs. applying current

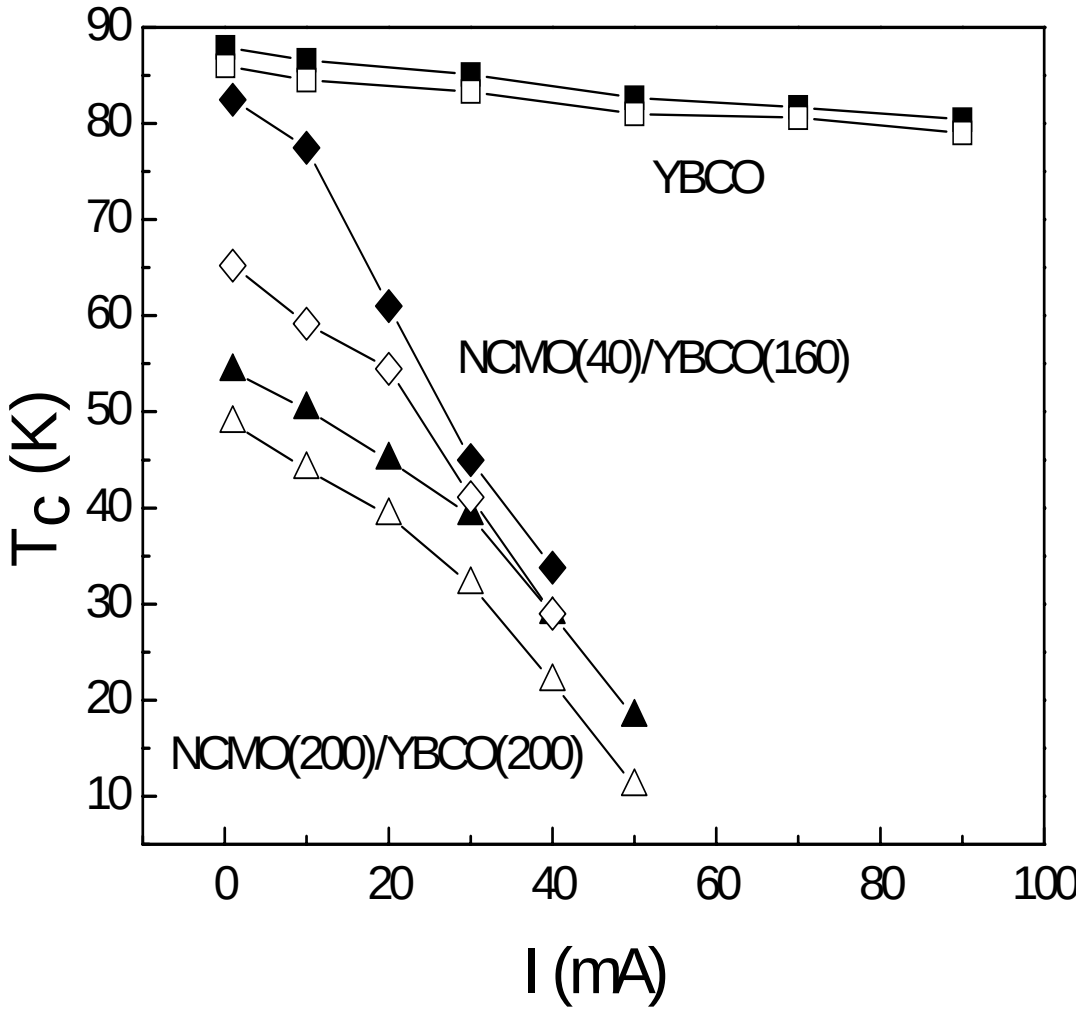

- T_c is suppressed by proximity in NCMO/YBCO at I < 1 mA.
- T_c-suppresion rate at I > 1 mA is one order higher in bilayer due to the spin-injection.

- **Proximity effect**

$H_{eff\text{-}ex} = H_{ex} \{d_F/(dS + d_F)\}$

$0.5H_{ex}$ for NCMO(200nm)/YBCO(200nm)
$0.2H_{ex}$ for NCMO(40nm)/YBCO(160nm)

ΔT_c ~ 34K / 16K

- **Current induces spin-injection effect**

Observe a threshold of effective current I > 1 mA
Large T_c-suppresion in a rate of 1.4 K/mA.

JOURNAL OF APPLIED PHYSICS 101, 09G106 (2007)

Proximity effect of superconductivity and magnetism in the $Nd_{0.7}Ca_{0.3}MnO_3/YBa_2Cu_3O_7$ bilayer

J. G. Lin[a)]
Center for Condensed Matter Sciences, National Taiwan University, Taipei, 106 Taiwan, Republic of China and Center for Nanostorage Research, National Taiwan University, Taipei, 106 Taiwan, Republic of China

Daniel Hsu
Center for Condensed Matter Sciences, National Taiwan University, Taipei, 106 Taiwan, Republic of China; Center for Nanostorage Research, and Department of Mechanical Engineering, National Taiwan University, Taipei, 106 Taiwan, Republic of China

W. F. Wu
Department of Mechanical Engineering, National Taiwan University, Taipei, 106 Taiwan, Republic of China

C. H. Chiang and W. C. Chan
Department of Physics, Tamkang University, Tamsui, Taipei, 251 Taiwan, Republic of China

APPLIED PHYSICS LETTERS 90, 162504 (2007)

Current enhanced magnetic proximity in $Nd_{0.7}Ca_{0.3}MnO_3/YBa_2Cu_3O_7$ bilayer

Daniel Hsu
Center for Condensed Matter Sciences, Center for Nanostorage Research, and Department of Mechanical Engineering, National Taiwan University, Taipei, Taiwan 106, Republic of China

J. G. Lin[a)]
Center for Condensed Matter Sciences and Center for Nanostorage Research, National Taiwan University, Taipei, Taiwan 106, Republic of China

C. P. Chang and C. H. Chen
Center for Condensed Matter Sciences, National Taiwan University, Taipei, Taiwan 106, Republic of China

W. F. Wu
Department of Mechanical Engineering, National Taiwan University, Taipei, Taiwan 106, Republic of China

C. H. Chiang and W. C. Chan
Department of Physics, Tamkang University, Taipei, Taiwan 251, Republic of China

JOURNAL OF APPLIED PHYSICS **103**, 07C710 (2008)

Thickness dependent spin-injection effects in $Nd_{0.7}Ca_{0.3}MnO_3/YBa_2Cu_3O_7$ bilayers

Daniel Hsu,[1,2] J. G. Lin,[1,2,a)] C. P. Chang,[1] C. H. Chen,[1] C. H. Chiang,[3] W. C. Chan,[3] and W. F. Wu[4]
[1]*Center for Condensed Matter Sciences, National Taiwan University, Taipei 106, Taiwan, Republic of China*
[2]*Center for Nanostorage Research, National Taiwan University, Taipei 106, Taiwan, Republic of China*
[3]*Department of Physics, Tamkang University, Tamsui, Taipei 251, Taiwan, Republic of China*
[4]*Department of Mechanical Engineering, National Taiwan University, Taipei 106, Taiwan, Republic of China*

(Presented on 9 November 2007; received 10 September 2007; accepted 26 October 2007; published online 8 February 2008)

Two $Nd_{0.7}Ca_{0.3}MnO_3/YBa_2Cu_3O_7$ (NCMO/YBCO) bilayers with different thickness ratios are fabricated and the spin-injection effects are investigated. The NCMO/YBCO samples have thicknesses of 100 nm/200 nm and 200 nm/200 nm, which are denoted as N/Y(1) and N/Y(2), respectively. It is shown that the current-induced suppression rate of superconducting transition temperature (dT_c/dI) in YBCO is enhanced by four to six times of magnitude in N/Y(1) and N/Y(2) compared with that in pure YBCO. Furthermore, dT_c/dI in N/Y(2) is larger than that in N/Y(1), which suggests that the thickness of NCMO has influence on the pair breaking in YBCO.
 [DOI: 10.1063/1.2833819]

JOURNAL OF APPLIED PHYSICS **104**, 053910 (2008)

Strain enhanced spin polarization in $Nd_{0.43}Sr_{0.57}MnO_3/YBa_2Cu_3O_7$ bilayers

Awadhesh Mani,[1,2] T. Geetha Kumary,[2] Daniel Hsu,[1] and J. G. Lin[1,a)]
[1]*Center for Condensed Matter Sciences/Center for Nanostorage Research, National Taiwan University, Taipei 106, Taiwan*
[2]*Materials Science Division, Indira Gandhi Centre for Atomic Research, Kalpakkam 603102, India*

(Received 24 June 2008; accepted 8 July 2008; published online 12 September 2008)

Electrical and magnetic properties of antiferromagnetic/superconducting bilayers $Nd_{0.43}Sr_{0.57}MnO_3/YBa_2Cu_3O_7$ (NSMO/YBCO) are investigated as functions of NSMO thickness (d) and current density (J). The superconducting transition temperatures (T_c) of bilayers decrease monotonically with decreasing d, and the suppression rate of T_c with J (dT_c/dJ) is enhanced by three orders of magnitude in NSMO(d)/YBCO compared with that in pure YBCO. Based on the analysis on the d dependencies of T_c and dT_c/dJ, it is suggested that the strain enhanced spin polarization is responsible for the great suppression of superconductivity in NSMO(d)/YBCO with d=40 and 80 nm. [DOI: 10.1063/1.2976365]

Modulation of superconductivity by spin canting in a hybrid antiferromagnet/superconductor oxide

Awadhesh Mani,[1,2] T. Geetha Kumary,[2] Daniel Hsu,[1] J. G. Lin,[1,a)] and Chyh-Hong Chern[3]
[1]*Center for Condensed Matter Sciences, National Taiwan University, Taipei 106, Taiwan*
[2]*Materials Science Division, Indira Gandhi Centre for Atomic Research, Kalpakkam 603102, India*
[3]*Department of Physics, National Taiwan University, Taipei 106, Taiwan*

(Received 4 December 2008; accepted 4 February 2009; published online 20 February 2009)

The proximity effect of a *C*-type antiferromagnet with the spin canting at low temperature is investigated in the hybrid $Nd_{0.35}Sr_{0.65}MnO_3/YBa_2Cu_3O_7$ oxide system through magnetic and transport measurements. It is found that the onset of a spin-canted state destroys partially the superconducting order parameter. Interestingly, due to the instability of this spin-canted state, zero resistivity recovers at the offset of spin canting. Our result demonstrates clearly the high sensitivity of superconducting order parameter to a modulation of internal field. © *2009 American Institute of Physics*. [DOI: 10.1063/1.3087000]

Electrically driven spin polarization in $Pr_{0.7}Ca_{0.3}MnO_3/YBa_2Cu_3O_7$ heterostructures

J. G. Lin,[1,a)] Daniel Hsu,[1] C. H. Chiang,[2] and W. C. Chan[2]
[1]*Center for Condensed Matter Sciences, National Taiwan University, Taipei, 106 Taiwan, Republic of China*
[2]*Department of Physics, Tamkang University, Tamsui, Taipei, 251 Taiwan, Republic of China*

(Presented 13 November 2008; received 4 September 2008; accepted 2 October 2008; published online 29 January 2009)

The current and temperature dependent electrical transport is investigated in $Pr_{0.7}Ca_{0.3}MnO_3/YBa_2Cu_3O_7$ (PCMO/YBCO) heterostructures which are fabricated by pulsed laser deposition. Two PCMO/YBCO heterostructures are made with the thicknesses of PCMO varied. It is shown that the superconducting transition temperature significantly decreases with increasing thickness of PCMO and with increasing applied current, which are related to the pair breaking via the polarized electrons. However, the current-dependent normal-state resistivity shows two crossing points, indicating the competition of various phases. According to our analysis, the melting of charge ordering state by the electrical current may be the major cause for the electrically driven enhancement of spin polarization in PCMO/YBCO. © *2009 American Institute of Physics*. [DOI: 10.1063/1.3055269]

Conclusion Remark

Half metal is the promising material for various kinds of future spintronic devices